

NASA Contractor Report CR-2004-211526

Tower Mesonetwork Climatology and Interactive Display Tool

Prepared By:
The Applied Meteorology Unit

Prepared for:
Kennedy Space Center
Under Contract NAS10-01052

NASA
National Aeronautics and
Space Administration

Office of Management
Scientific and Technical
Information Program

2004

Attributes and Acknowledgments

NASA/KSC POC:

Dr. Francis J. Merceret

YA-D

Applied Meteorology Unit (AMU) / ENSCO Inc.

Jonathan L. Case

William H. Bauman III

Executive Summary

Forecasters at the 45th Weather Squadron (45 WS) use the wind and temperature data from the tower network over the Kennedy Space Center (KSC) and Cape Canaveral Air Force Station (CCAFS) to evaluate Launch Commit Criteria and to issue and verify temperature and wind advisories, watches, and warnings for ground operations. The Spaceflight Meteorology Group also uses these data when issuing forecasts for shuttle landings at the KSC Shuttle Landing Facility. The National Weather Service at Melbourne, FL uses tower data to monitor sea/river breeze boundary interactions and verify marine/thunderstorm warnings, and also assimilates these data into their local analysis system. Systematic biases in these parameters at any of the towers could adversely affect an analysis, forecast, or verification for all of these operations. In addition, substantial geographical variations in temperature and wind speed can occur under specific wind directions. Therefore, the Applied Meteorology Unit (AMU) was tasked to develop a monthly and hourly climatology of temperatures and winds from the tower network, and identify the geographical variation, tower biases, and the magnitude of those biases.

Nine years of archived high-resolution wind and temperature data from instrumented towers at KSC, CCAFS, and surrounding locations of east-central Florida were used to generate a monthly mesoclimatology of temperatures and winds at heights of 6 ft and 54 ft. Data were analyzed at 33 selected towers, four of which are located near launch complexes and have two sensors at opposite sides of the towers at the same height. All 33 selected towers provided 6-ft temperature and 54-ft wind data archived at 5 minute intervals, while 19 of the towers also provided 54-ft temperature data every 5 minutes. The period of record for the analysis is February 1995 to January 2004.

The monthly mesoclimatology was developed by computing hourly means, standard deviations, biases, and data availability percentages of temperatures and winds at all selected towers and sensors. Only towers with at least 70% data availability were used in any given month. Prior to calculations, several automated quality control algorithms were applied to the data, as well as a manual quality control process for temperatures. The data were categorized into separate wind direction bins every 45°, and statistics were computed to determine the climatological variations across KSC/CCAFS under different wind directions.

The mesoclimate of KSC/CCAFS is largely driven by the complex land-water interfaces of the Atlantic Ocean, Mosquito Lagoon, Indian River, and Banana River. Towers with close proximity to water typically had much warmer nocturnal temperatures and higher wind speeds throughout the year. A 7–10°F difference occurred in the mean 6-ft temperature across the network during all months, most notable in the pre-dawn hours. The variations in 54-ft temperatures were much smaller, so near-surface stability disparities were generally caused by variations in 6-ft temperatures.

Mean domain-wide wind speeds were generally 4–6 kt during the nocturnal hours and 7–9 kt during the day. The strongest mean nocturnal wind speeds of 6–7 kt occurred from October to March when large-scale weather systems drive much of central Florida's weather. Meanwhile, the strongest mean daytime wind speeds of 8.5–9.5 kt occurred from February to May, probably due to a combination of large-scale weather systems and strengthening sea-breeze circulations during this latter portion of the Florida dry season. Coastal and causeway towers had mean wind speeds 2–4 kt stronger than the overall network mean. Mainland towers had mean speeds weaker than the network average by about the same magnitude. The resulting gradient in the mean wind speed across the network was typically 5–8 kt over a distance of 15–20 nm, with the strongest speeds found at towers along the Atlantic coast.

The AMU developed an interactive, web-based graphical user interface (GUI) for displaying and overlaying information from the 9-year climatology. The web-based interface includes graphical displays of mean, standard deviation, bias, and data availability for any combination of towers, variables, months, hours, and wind direction bins. These graphical displays employ the Microsoft® Excel® pivot chart capability to provide the user with this flexibility. In addition, geographical plots and contours of the various statistical quantities provide the user with images of the spatial variability in temperatures and winds across the tower network. The GUI includes an online help section to aid users in navigating through the GUI tool, manipulating graphs using the pivot chart capabilities, and displaying and animating geographical contour plots. All AMU customers will receive a copy of the interactive GUI tool as part of the task deliverables.

Table of Contents

Executive Summary.....	iii
Table of Contents	iv
List of Figures	v
List of Tables.....	ix
1. Introduction	1
1.1 Motivation.....	1
1.2 Task background.....	1
2. Tower Data Description	2
2.1 Brief History of Tower Network.....	2
2.2 Current Mesonetwork.....	2
2.3 Instrumentation and Measurement	3
2.4 Tower Exposure at Sites Presented in Climatology	7
2.5 Data Archive Comprising Climatology.....	14
2.6 Range Standardization and Automation (RSA) Changes	15
3. Methodology	18
3.1 Data Quality Control	18
3.2 Data Processing.....	21
3.3 Analysis and Display Tools.....	22
4. Climatology Results.....	24
4.1 Overview of results	24
4.2 Data Requirement and Availability	24
4.3 Climatological Probabilities of Wind Directions	27
4.4 Temperatures.....	29
4.5 Wind Speeds	42
4.6 Monthly and Diurnal Variations in Wind Direction Deviation	52
5. Training for Interactive Analysis and Display Tool	53
5.1 Overview and Layout of Interactive Web Tool.....	53
5.2 Excel Pivot Chart Tutorial	63
6. Summary.....	75
7. References	77
List of Abbreviations and Acronyms.....	78

List of Figures

Figure 2.1.	(a) Locations of all towers within the KSC/CCAFS mesonetwork, and (b) Locations of only those towers used in the nine-year climatology.....	2
Figure 2.2	Distance to the nearest tower, contoured every 1.6 nm (3 km), from CSR (2000).	3
Figure 2.3.	Photographs of coastal tower 0006 (a) from a distance, and (b) two sensors at 6 ft and 12 ft on opposite sides of the tower.	8
Figure 2.4.	Photographs of coastal tower 0022 (a) looking northwest, and (b) looking northeast.	8
Figure 2.5.	Photographs of causeway tower 0300 (a) looking south, and (b) looking east.	9
Figure 2.6.	Photographs of causeway tower 1007 (a) looking east, and (b) close-up of 6-ft temperature sensor and solar radiation shield for natural aspiration system.	9
Figure 2.7.	Photograph of CCAFS tower 0303.	10
Figure 2.8.	Photographs of CCAFS tower 0403 (a) looking south, and (b) close-up of 6-ft temperature sensor with mechanical aspiration system.	11
Figure 2.9.	Photograph of Merritt Island tower 0509.....	11
Figure 2.10.	Photograph of 492-ft tall Merritt Island tower 0313.....	12
Figure 2.11.	Photograph of mainland tower 0819 (a) looking south, and (b) looking north.	13
Figure 2.12.	Photograph of mainland tower 1204 (a) looking up with pine tree limbs shrouding tower, and (b) looking east with sun shining on 6-ft temperature sensor.	13
Figure 2.13.	Photograph of mainland tower 1612 within swamp/meadow lands, depending on wet or dry season. This photograph was taken in late May at the end of the Florida dry season.	14
Figure 2.14.	The modified tower network with the RSA program.	16
Figure 3.1.	The percent availability of archived 5-minute, 6-ft temperature observations for all towers during March for the years 1995 – 2003. Towers with percentages less than 70% were excluded due to insufficient data availability.....	19
Figure 3.2.	The frequency distribution of the number of 6-ft temperature observations during March (1995–2003) at towers 0001, 0003, 0019, 0020, 0021, and 0022. Note the outliers at tower 0001 with temperatures above 90°F.....	20
Figure 3.3.	A contour diagram showing the 2D frequency distribution of 6-ft temperatures at tower 0001 during March (1995–2003) as a function of UTC hour. Note that the high-temperature outliers of Figure 3.2 occurred between 1500 and 1700 UTC. Frequencies are contoured every 50 units beginning at 0.5, in order to depict one or more occurrences with shading.	20
Figure 3.4.	A contour diagram showing the 2D frequency distribution of 6-ft temperatures at tower 0001 during March (1995–2003) as a function of year. Note that the high-temperature outliers of Figure 3.3 occurred in 1995. Frequencies are contoured every 100 units beginning at -99.5, to depict one or more occurrences with shading.	21

Figure 3.5.	Three-panel geographical contour plot of mean (left panel) bias (middle), and standard deviation of 54-ft wind speed (right), valid for all tower observations during the 1800 UTC hour of April for the period of record 1995–2003.	23
Figure 4.1.	The percentage of temperature data availability at towers used in the climatology as a function of UTC hour for (a) each individual tower at 54 ft and 6 ft, and (b) all towers combined (ALL), forecast critical towers combined (Fcst), and launch / safety critical towers combined (Launch).....	26
Figure 4.2.	The climatological probability of the wind direction falling into eight different bins for all towers combined during the nine-year period of record. Twenty-four hourly climatological probabilities are given in each month of the year along the x-axis. The wind direction bin labeling convention is given in Table 4.1.....	28
Figure 4.3.	The climatological probability of the wind direction falling into eight different bins for all towers combined during the nine-year period of record, valid for July only. Twenty-four hourly climatological probabilities are given along the x-axis. The wind direction bin labeling convention is given in Table 4.1.....	28
Figure 4.4.	The diurnal range in mean 6-ft temperatures during all months of the year for (a) all tower locations, and (b) coastal tower 0022, causeway tower 0300, Merritt Island tower 0509, and mainland tower 0819, and all towers averaged together (ALL). The x-axis contains 24 hours embedded within each month of the year.	30
Figure 4.5.	The hourly mean 6-ft and 54-ft temperatures at selected coastal/causeway, Merritt Island, and mainland Florida towers during (a) January, and (b) July.	31
Figure 4.6.	(a) The diurnal range in the mean 54-ft minus 6-ft temperatures at all towers and for all months of the year. (b) The 1-hour changes in the mean temperature at tower 0303 for all months of the year.	33
Figure 4.7.	Hourly mean wind speeds at tower 0303 for all months of the year.....	34
Figure 4.8.	The hourly mean 6-ft temperatures versus wind direction bin, averaged over all towers in the KSC/CCAFS network, valid for (a) the cool-season months (November–April), and (b) the warm-season months (May–October).....	35
Figure 4.9.	Diurnal distribution of 6-ft temperature biases at all towers in the KSC/CCAFS network and for all months of the year.....	36
Figure 4.10.	Diurnal distribution of the 54-ft and 6-ft temperature biases at all towers in the climatology during the months of (a) January, and (b) July.	37
Figure 4.11.	Bias of the differences in the 54-ft and 6-ft temperatures during the months of January and July.....	38
Figure 4.12.	The hourly mean 6-ft temperature biases during the Florida cool season months of November through April at (a) coastal tower 0394 (SLC 39A), (b) causeway tower 0300, (c) Merritt Island tower 0509, (d) mainland tower 1612, (e) CCAFS tower 0403 adjacent to the Banana River, and (f) causeway tower 1007 adjacent to the Indian River.	39
Figure 4.13.	Bias of 6-ft temperature at the northwest (0061) and southeast (0062) sensors of tower 0006.	42
Figure 4.14.	Hourly mean wind speeds for all months of the year at (a) all towers, and (b) towers 0022, 0300, 0509, 0819, and all towers averaged together (ALL).....	44

Figure 4.15. Plot of the hourly differences between the buoy and tower network mean 6-ft temperatures ($T_b - T_n$), and the hourly mean wind speed normalized by the monthly mean wind speed (all-mean), valid for the months of (a) October to March, and (b) April to September. Solid lines represent the time of minimum $T_b - T_n$ and dashed lines represent the time of the maximum mean wind speed.	45
Figure 4.16. The hourly standard deviations of the 54-ft wind speeds during all months of the year at coastal tower 0022, causeway tower 0300, Merritt Island tower 0509, and mainland tower 0819.	46
Figure 4.17. Hourly mean wind speeds stratified by wind direction bin for all towers used in the climatology averaged together during (a) the cool-season months, and (b) the warm-season months.	47
Figure 4.18. Hourly mean wind speeds stratified by wind direction bin during the cool-season months at (a) coastal tower 0022, (b) causeway tower 0300, (c) Merritt Island tower 0509, and (d) mainland tower 0819.	48
Figure 4.19. Hourly and monthly biases of 54-ft wind speeds at coastal tower 0022, causeway tower 0300, Merritt Island tower 0509, and mainland tower 0819.	50
Figure 4.20. The hourly bias of 54-ft wind speeds as a function of wind direction bin at coastal towers 0022 and 0394 (SLC 39A), causeway towers 0300 and 1007, CCAFS tower 0303, Merritt Island towers 0509 and 3131, and mainland tower 0819, valid for (a) the cool-season months, and (b) the warm season months.	51
Figure 4.21. The mean hourly and monthly standard deviation of wind direction at coastal towers 0022 and 0394 (SLC 39A), causeway tower 0300, Merritt Island towers 0509 and 3131, and mainland tower 0819.	52
Figure 5.1. Main menu of the GUI provides navigation to the pivot charts, maps, or help files.	53
Figure 5.2. The pivot chart selection page provides two navigation choices.	54
Figure 5.3. Pivot chart parameter selection page for pivot charts displaying all months and all wind directions.	54
Figure 5.4. Pivot chart data set type selection page for pivot charts displaying all months and all wind directions using a parameter of 54-ft temperature minus 6-ft temperature.	55
Figure 5.5. Display of a sample pivot chart showing the parameters and data sets chosen by the user.	55
Figure 5.6. Display of a pivot chart with corresponding pivot table.	56
Figure 5.7. Pivot chart parameter selection page for pivot charts stratified by season and wind direction.	56
Figure 5.8. Pivot chart season selection page for pivot charts displaying data stratified by season and wind direction using the 6-ft temperature parameter.	57
Figure 5.9. Pivot chart data set type selection page for pivot charts displaying data stratified by season and wind direction using the 6-ft temperature parameter during the cool season.	57
Figure 5.10. Display of a pivot chart stratified by season and wind direction, showing the parameters and data sets selected by the user.	58

Figure 5.11. The main maps selection page provides navigation to all 12 months.....	59
Figure 5.12. Maps hour selection page for maps displaying data from July.....	59
Figure 5.13. Maps level and parameter selection page for maps displaying data from July at 10Z.	60
Figure 5.14. Maps wind direction bin selection page for maps displaying data from July at 10Z for 54-ft wind speed.	60
Figure 5.15. Maps page showing data from July at 10Z for 54-ft wind speed with a wind direction bin of 091°-135°.....	61
Figure 5.16. Maps page displaying hourly data from June with the JavaScript animation tool, looping through all hours for 6-ft temperature with a wind direction bin of 316°-360°.....	62
Figure 5.17. Pivot chart demonstrating the locations of the <i>Filter</i> , <i>Series</i> , <i>Category</i> , and <i>Data</i> fields as described in the text. The drop-down list for the <i>Filter</i> field 'Dirn' is also shown.	64
Figure 5.18. Pivot table associated with the pivot chart in Figure 5.17.....	65
Figure 5.19. Pivot chart as in Figure 5.17, but with the drop-down list for the <i>Series</i> field 'TwrID' shown with check boxes next to each <i>Item</i>	65
Figure 5.20. Warning pop-up window when first accessing pivot chart data if the GUI tool is run from a server.....	67
Figure 5.21. Default pivot chart displayed when selecting all months and all wind direction, temperature by height, and mean from the Mesonet Wind and Temperature Climatology Tool.....	67
Figure 5.22. Display of all monthly mean 6-ft temperatures at tower 0303 as a function of UTC hour. The value from the corresponding pivot table shows up in a small pop-up window if the mouse is moved over any individual plotted element.....	68
Figure 5.23. Display of hourly mean 6-ft temperatures at tower 0303 for all months, with the x-axis containing both 'Month' and 'Hour' as the <i>Category</i> fields.	69
Figure 5.24. Default pivot chart displayed when selecting all months and all wind directions, temperature by height, and bias from the Mesonet Wind and Temperature Climatology Tool.....	70
Figure 5.25. Display of the 54-ft and 6-ft hourly temperature biases during January for towers 0061, 0300, 0303, 1101, and 3131.....	71
Figure 5.26. Display of the 6-ft hourly temperature biases for all months at towers 0061, 0300, 0303, 1101, and 3131.....	71
Figure 5.27. Display of hourly mean 54-ft wind speeds at all towers during the month of January, stratified by wind direction bin.	73
Figure 5.28. Display of hourly mean 54-ft wind speeds at towers 0398 (SLC 39B), 0412, and 1012 during January, stratified by wind direction bin.....	73
Figure 5.29. Display of hourly mean 54-ft wind speeds at tower 0398 (SLC 39B) for all cool-season months, stratified by wind-direction bin.....	74

List of Tables

Table 2.1.	List of the tower identifiers, flag as to whether the data were used in the climatology (blank = yes), the tower requirements group, and the heights (in ft) of variables measured by each tower.	5
Table 2.2.	Air temperature and relative humidity sensor suites for the launch, safety, and forecast critical towers.	6
Table 2.3.	Air temperature and relative humidity sensor specifications for the launch, safety, and forecast critical towers.	6
Table 2.4.	WINDS legacy wind speed and direction sensor specifications.	7
Table 2.5.	RSA replacement specifications for sonic anemometers, temperature, and humidity sensors.....	17
Table 4.1.	Wind direction bin labeling convention.	27

1. Introduction

The Kennedy Space Center (KSC), Cape Canaveral Air Force Station (CCAFS), and surrounding areas in east-central Florida have a high-resolution network of over 40 instrumented meteorological towers. With measurements every 1 to 5 minutes at an average station spacing of ~ 2.7 nm (5 km), the network provides timely weather observations for ground, space launch, and Space Shuttle landing operations.

1.1 Motivation

Forecasters at the 45th Weather Squadron (45 WS) use the wind and temperature data from the tower network to evaluate Launch Commit Criteria and to issue and verify temperature and wind advisories, watches, and warnings for ground operations. The Spaceflight Meteorology Group also uses these data when issuing forecasts for shuttle landings at the KSC Shuttle Landing Facility. The National Weather Service (NWS) at Melbourne, FL uses tower data to monitor and predict sea- and river-breeze boundary interactions, verify marine and thunderstorm warnings. The NWS Melbourne also assimilates these data into their locally configured ARPS Data Analysis System (Case et al. 2002). Systematic biases in these parameters at any of the towers could adversely affect an analysis, forecast, or verification for all of these operations. In addition, substantial geographical variations in temperature and wind speed can occur under specific wind directions. Therefore, forecasters need to know if any towers exhibit a consistent bias in temperature and/or wind speed, and what the typical geographical and diurnal variations of temperature and wind speed are throughout the tower network.

1.2 Task background

The Applied Meteorology Unit (AMU) was tasked to develop a monthly and hourly climatology of temperatures and winds from the towers in the KSC/CCAFS network, and identify towers with biases and the magnitude of those biases. The biases could be a combination of instrument bias, site/location problems, and/or natural geographical variations within the tower network. It was also requested that the AMU develop a display tool that can summarize the climatology results in both a tabular and geographical format.

Capabilities for computing climatologies from archived KSC/CCAFS tower data were developed under the Statistical Short-Range Guidance for Peak Wind Speed Forecasts on KSC/CCAFS Phase I task (Lambert 2002). These capabilities include automated quality control (QC) of tower observations on a monthly basis, calculations of monthly peak-wind climatologies as a function of month and hour, and the development of conditional climatologies based on wind direction bins. These capabilities were expanded in this task to compute climatologies for sustained wind speed, temperature at 6 ft and 54 ft, the difference between the 54-ft and 6-ft temperature, and wind direction standard deviation.

Climatologies were developed on a monthly and hourly basis, and by wind direction bins. The database in this task was expanded to include additional variables and most towers within the KSC/CCAFS network, compared to the specific subset of towers used in Lambert (2002). Extensive manual QC of temperature data was required above and beyond the automated QC algorithm. Both the automated and manual QC methodologies are described in Section 3.1.

This report presents a nine-year climatology of the KSC/CCAFS tower network, highlighting the sensor and geographical biases based on location, month, times of day, and specific wind direction regime. Section 2 provides a description of the tower mesonetwork and instrumentation characteristics. Section 3 presents the methodology used to construct the tower climatology including QC methods, data processing, and the development of an interactive display tool. The results of the tower climatology are presented in Section 4. Section 5 provides training documentation on how to use the interactive display tool. Finally, Section 6 summarizes the report.

2. Tower Data Description

2.1 Brief History of Tower Network

In 1961 and 1962, a research project called the Ocean Breeze and Dry Gulch Diffusion program was conducted at Cape Canaveral, FL and Vandenberg Air Force Base, CA, respectively, by the Air Force Cambridge Research Laboratories (Haugen and Fuquay 1963; Haugen and Taylor 1963). The program was designed to address air pollution hazards associated with planned launches of the Titan II missile at both ranges. Another goal of the program was to provide range safety personnel and staff meteorologists with an operationally useful system for observing the state of the atmospheric boundary layer. Such a system was required for staff meteorologists to interpret the fine-scale meteorological conditions during launch operations for evaluating safety considerations, pad conditions of winds and wind gusts, and to generate precise short-range forecasts at the launch pads.

As a result of the program, the Weather Information Network Display System (WINDS) was developed and implemented at Cape Canaveral, FL consisting of eight towers in the original operational system in 1964. WINDS was expanded in 1966 and 1984, reaching a total of 29 towers covering an area of 230 nm² (790 km²). WINDS was again expanded to 49 towers in 1987 to cover an area of approximately 467 nm² (1600 km², Harms et al. 2001), and to accommodate forecasting techniques recommended by Watson et al. (1989). The network was then reduced in the early 1990s to its current number of 44 towers.

2.2 Current Mesonetwork

The current tower network (Figure 2.1a, CSR 2000) consists of 44 towers that measure temperature, humidity, and winds at various locations and heights. Due to poor data availability in the archive or measurement heights inconsistent with the majority of the towers in the network, several towers were excluded from the climatology. Figure 2.1b shows only the tower locations used for the climatology. It is important to note that several of the forecast critical towers over mainland Florida suffered from poor data availability.

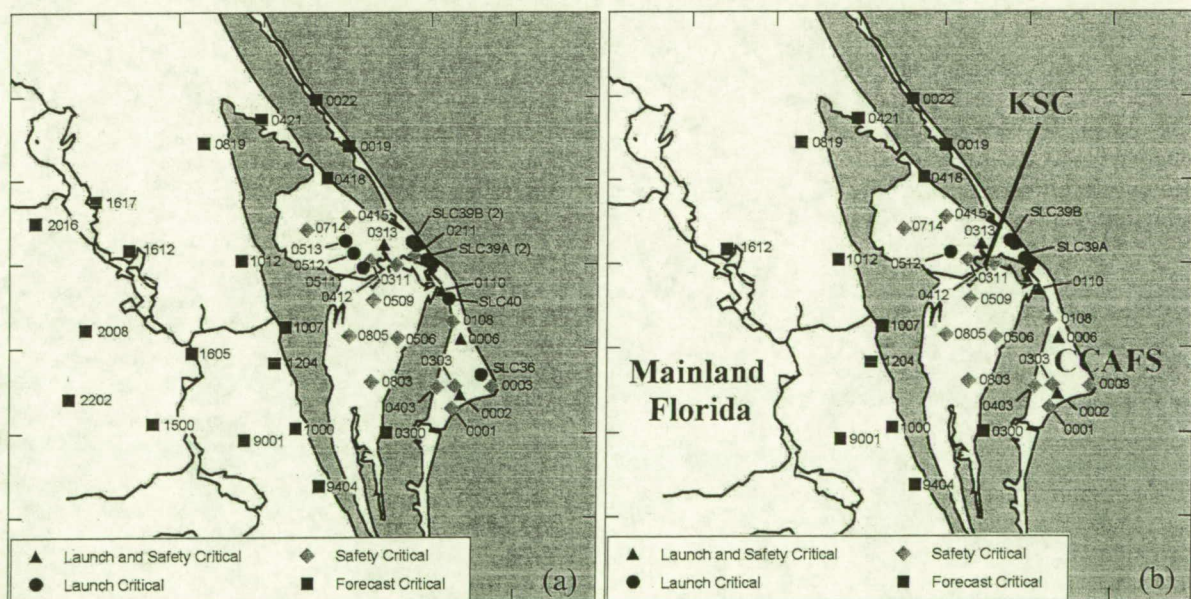


Figure 2.1. (a) Locations of all towers within the KSC/CCAFS mesonetwork, and (b) Locations of only those towers used in the nine-year climatology.

2.2.1 Tower identifier naming convention

The tower identifier (ID) naming convention for all towers is based on the number of nautical miles (nm) inland from the Atlantic coast and north/south of Port Canaveral (CSR 2000). The first two digits represent the nautical miles inland and perpendicular to the coast while the last 2 digits represent the nautical miles north of Port Canaveral. As an example, tower 0003 is zero nm from the coast and three nm north of the Port, whereas tower 1012 is 10 nm from the coast and 12 nm north of the Port (refer to Figure 2.1). As part of RSA changes (see Section 2.6), towers south of the port will be renamed by subtracting the number of nautical miles south of the port from 100 for the last 2 digits of the ID.

2.2.2 Tower station spacing and temporal frequency

According to Figure 2.2, the nearest-neighbor spacing between towers generally ranges from 1.6 nm (3 km) to 3.2 nm (6 km), with the smallest spacing over KSC and CCAFS. Station spacing increases markedly over mainland Florida west of KSC/CCAFS. The average tower spacing for the whole network is about 2.7 nm (5 km).

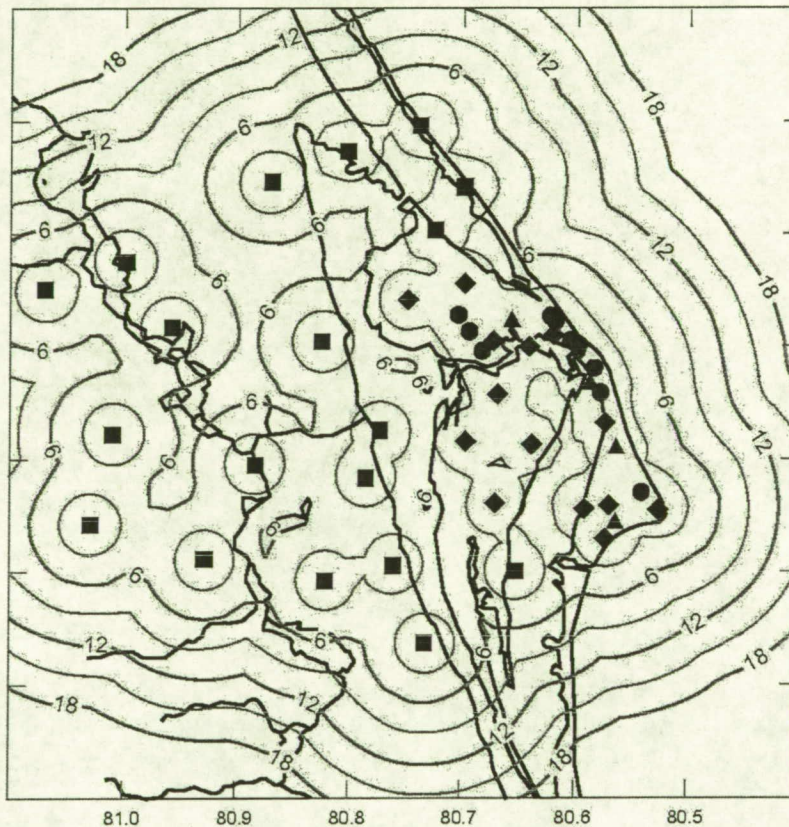


Figure 2.2 Distance to the nearest tower, contoured every 1.6 nm (3 km), from CSR (2000).

2.3 Instrumentation and Measurement

This section summarizes the variables and heights that each sensor within the tower mesonetwork measures. The towers are grouped into three categories based on user requirements (refer to Figure 2.1 for locations):

- **Launch critical towers.** These towers are used in the direct evaluation of launch constraints, have the greatest vertical measurement extent, and have sensors on opposite sides of the towers at various heights. Only data from the windward side of each tower are displayed to the forecasters, but data from both sensors at each tower were collected and archived. The data from both sensors were processed and analyzed as separate tower IDs.

- **Safety critical towers.** These towers are located at or near areas where propellants and other hazardous chemicals are stored or handled, supporting emergency response activities.
- **Forecast critical towers.** These towers surround the KSC/CCAFS area and support the 45 WS in routine weather forecast and warning operations.

2.3.1 Measurement heights/variables

Table 2.1 provides a summary of the heights and variables measured at each tower location. Forecast towers have the simplest sensor suite, consisting of 6-ft temperature and humidity measurements, and 54-ft wind readings. Safety towers measure temperature at 6 ft and 54 ft, winds at 12 ft and 54ft, and do not provide any humidity measurements. The launch critical towers provide measurements of temperature and winds at multiple heights and on two or more sides of the towers.

The tallest launch critical tower, 0313, has wind, temperature, and humidity sensors at multiple levels up to 492 ft on the southwest (ID#3131) and northeast sides (ID#3132). Launch critical towers 0002, 0006, and 0110 have sensors up to 204 ft on the northwest and southeast sides (IDs given in Table 2.1). The only other launch critical towers used in the climatology are those at space launch complex (SLC) 39A and SLC 39B (tower IDs 0394 and 0398), which measure temperatures at 6 ft and 60 ft, and winds and humidity at 60 ft for the Space Shuttle launch pads. In order to simplify the climatology, the 60-ft temperatures and winds at towers 0394 and 0398 are grouped together with all the 54-ft winds and temperatures. It is important to note, however, that the 6-ft temperature sensors at SLC 39A and 39B are positioned on a mound elevated several feet around the surrounding ground. Therefore, the 6-ft temperatures at 0394 and 0398 may not necessarily be representative of the true 6-ft temperatures.

Table 2.1. List of the tower identifiers, flag as to whether the data were used in the climatology (blank = yes), the tower requirements group, and the heights (in ft) of variables measured by each tower.

Sensor Complement (heights in ft)					
Tower ID	Data Used?	Group	Wind	Temperature	Humidity
0001		Safety	12, 54	6, 54	N/A
0002					
(0020, NW)		Launch	12, 54, 204 (NW)	6, 54, 204 (NW)	6, 54, 204 (NW)
(0021, SE)			12, 54, 204 (SE)	6, 54, 204 (SE)	6, 54, 204 (SE)
0003		Safety	12, 54	6, 54	N/A
0006			12, 54, 162, 204		
(0061, NW)		Launch	(NW)	6, 54, 204 (NW)	6, 54, 204 (NW)
(0062, SE)			12, 54, 162, 204 (SE)	6, 54, 204 (SE)	6, 54, 204 (SE)
0019		Forecast	54	6	6
0022		Forecast	54	6	6
0108		Safety	12, 54	6, 54	N/A
0110			12, 54, 162, 204		
(1101, NW)		Launch	(NW)	6, 54, 204 (NW)	6, 54, 204 (NW)
(1102, SE)			12, 54, 162, 204 (SE)	6, 54, 204 (SE)	6, 54, 204 (SE)
0211	No	Safety	12, 54	6, 54	N/A
0300		Forecast	54	6	6
0303		Safety	12, 54	6, 54	N/A
0311		Safety	12, 54	6, 54	N/A
0313					
(3131, SW)		Launch	12, 54, 162, 204, 295,	6, 54, 204, 492	6, 54, 204, 492
(3132, NE)			394, 492 (SW & NE)	(SW & NE)	(SW & NE)
0403		Safety	12, 54	6, 54	N/A
0412		Safety	12, 54	6, 54	N/A
0415		Safety	12, 54	6, 54	N/A
0418		Forecast	54	6	6
0421		Forecast	54	6	6
0506		Safety	12, 54	6, 54	N/A
0509		Safety	12, 54	6, 54	N/A
0511	No	Launch	30	N/A	N/A
0512	6-ft T only	Launch	30	6	6
0513	No	Launch	30	N/A	N/A
0714		Safety	12, 54	6, 54	N/A
0803		Safety	12, 54	6, 54	N/A
0805		Safety	12, 54	6, 54	N/A
0819		Forecast	54	6	6
1000		Forecast	54	6	6
1007		Forecast	54	6	6
1012		Forecast	54	6	6
1204		Forecast	54	6	6
1500	No	Forecast	54	6	6
1605	No	Forecast	54	6	6
1612		Forecast	54	6	6
1617	No	Forecast	54	6	6
2008	No	Forecast	54	6	6
2016	No	Forecast	54	6	6
2202	No	Forecast	54	6	6
9001		Forecast	54	6	6
9404		Forecast	54	6	6
SLC 36	No	Launch	90	N/A	N/A
SLC 39A (0394)		Launch	60	6, 60	60
SLC 39B (0398)		Launch	60	6, 60	60
SLC 40	No	Launch	54	N/A	N/A

2.3.2 Temperature/humidity sensor description

The launch and safety critical towers are instrumented with sensors that use a current loop to communicate measurements whereas the forecast critical sensors use a voltage level (Table 2.2). Also, the forecast critical temperature sensors are naturally aspirated whereas the launch/safety towers are equipped with mechanical aspirators. These contrasting sensor configurations could present a source of difference between the launch/safety and forecast critical temperature sensors, particularly in situations when the naturally aspirated sensors are not adequately ventilated. It should be noted that the Range Technical Services Contractor (currently Computer Science Raytheon, Inc.) routinely maintains and re-calibrates the sensors every 3 months, so corrosion or major wear should not be a problem with any of the sensors. The specifications of the sensors are given in Table 2.3.

Table 2.2. Air temperature and relative humidity sensor suites for the launch, safety, and forecast critical towers (CSR 2000).

Sensor Group	Sensor Type	Aspirator Type	Dual Sensors at each Level
Launch Critical	Air temperature and relative humidity Rotronic TM12R-SCC 4-20 mA input	Mechanical R.M. Young 43408	Yes
Safety Critical	Air temperature only JMS 3ESBK4 4-20 mA input	Mechanical R.M. Young 43408	No
Forecast Critical	Air temperature and relative humidity Rotronic TM12R-SCV 12 volts dc input	Natural R.M. Young 41002	No

Table 2.3. Air temperature and relative humidity sensor specifications for the launch, safety, and forecast critical towers (CSR 2000).

Variable & Characteristic	Launch Critical Towers (Rotronic TM12R-SCC)	Safety Critical Towers (JMS 3ESBK4)	Forecast Critical Towers (Rotronic TM12RSCV)
Air Temperature			
Operating range	0 to 120°F (-17.8 to 48.9 C)	0 to 120°F (-17.8 to 48.9 C)	0 to 120°F (-17.8 to 48.9 C)
Accuracy	0.4°F (0.2 C) RMS error	0.4°F (0.2 C) RMS error	0.4°F (0.2 C) RMS error
Time Constant	~ 30 s	Unknown	~ 30 s
Stability	0.2°F (0.1 C)/month	< 0.1°F (0.05 C)/12 months at 32°F (0 C)	0.2°F (0.1 C)/month
Excitation voltage	+12 V	+12 V	+12 V
Relative Humidity			
Operating range	0-100 %	N/A	0-100 %
Accuracy	2% RMS error	N/A	2% RMS error
Time Constant	~ 30 s	N/A	~ 30 s
Stability	2% / year	N/A	2% / year
Excitation voltage	+12 V	N/A	+12 V

2.3.3 Wind sensor specifications

The specifications for the wind speed and direction sensors is provided in Table 2.4. The accuracy and thresholds for the launch/safety versus forecast critical towers are generally quite similar.

Table 2.4. WINDS legacy wind speed and direction sensor specifications (CSR 2000).		
Variable & Characteristic	Launch and Safety Critical Towers (R.M. Young 05305-18)	Forecast Critical Towers (R.M. Young 05103)
Wind Speed		
Operating range	0.64–105 kt (0.33–54 m s ⁻¹)	1.7–116 kt (0.9–60 m s ⁻¹)
Survival range	116 kt (60 m s ⁻¹)	155 kt (80 m s ⁻¹)
Sensor	0.66 ft (20 cm) diameter 4-blade helicoids carbon fiber propeller	0.59 ft (18 cm) diameter 4-blade helicoids polypropylene propeller
Accuracy	±0.6 kt (± 0.3 m s ⁻¹)	±0.6 kt (± 0.3 m s ⁻¹)
Starting threshold	0.64 kt (0.33 m s ⁻¹)	1.9 kt (1.0 m s ⁻¹)
Distance constant	≤ 17 ft (≤ 5.2 m)	8.9 ft (2.7 m)
Wind Direction		
Operating range	0-360° mechanical 0-355° electrical	0-360° mechanical 0-355° electrical
Sensor	Balanced vane, 1.2 ft (38 cm) turning radius	Balanced vane, 1.2 ft (38 cm) turning radius
Accuracy	± 3°	± 3°
Damping ratio	≤ 0.4	0.25
Delay distance	4.3 ft (1.3 m)	4.3 ft (1.3 m)
Starting threshold	≤ 0.64 kt (0.33 m s ⁻¹) for 10° displacement	1.7 kt (0.9 m s ⁻¹) for 10° displacement

2.4 Tower Exposure at Sites Presented in Climatology

This sub-section describes the locations and site exposure of many of the towers highlighted in the climatology results section of this report (Section 4). The proximity to water bodies is also noted and photographs are provided when possible. The towers highlighted in this sub-section include coastal/causeway sites 0006, 0022, 0300, and 1007, CCAFS sites 0303 and 0403, Merritt Island sites 0509 and 0313, and mainland sites 0819, 1204, and 1612 (see Figure 2.1a).

The coastal and causeway towers generally have little surrounding vegetation and are well-exposed to the elements. The 204-ft tower 0006 is just inland of the Atlantic Ocean and immediately south of the Delta launch complex. This tower has some fairly tall vegetation around its perimeter (Figure 2.3a) which could impact the wind speeds at 54 ft and especially 12 ft. Tower 0006 is one of the launch critical towers and thus has two sensors at the same height on the northwest and southeast parts of the tower (Figure 2.3b). Tower 0022, the windiest overall tower according to the climatology, is situated just over the sand dunes on the north end of Mosquito Lagoon (Figure 2.4). This tower has very little surrounding vegetation and has a high exposure to winds off both the Atlantic Ocean to its north and east and the Mosquito Lagoon to its west.

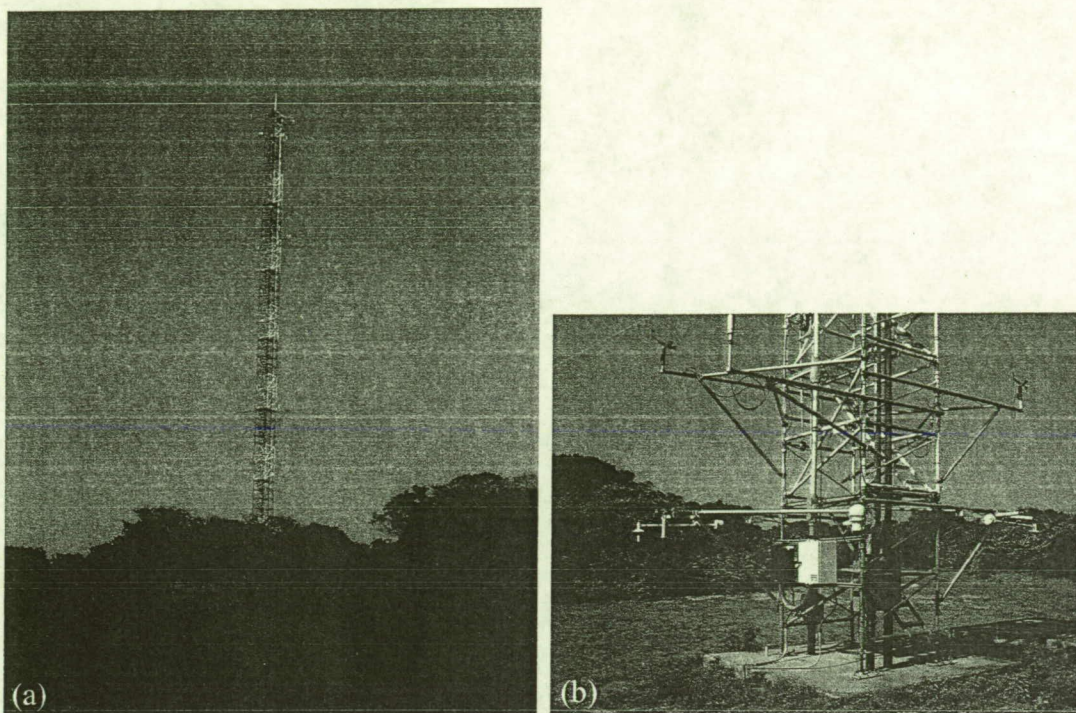


Figure 2.3. Photographs of coastal tower 0006 (a) from a distance, and (b) two sensors at 6 ft and 12 ft on opposite sides of the tower.

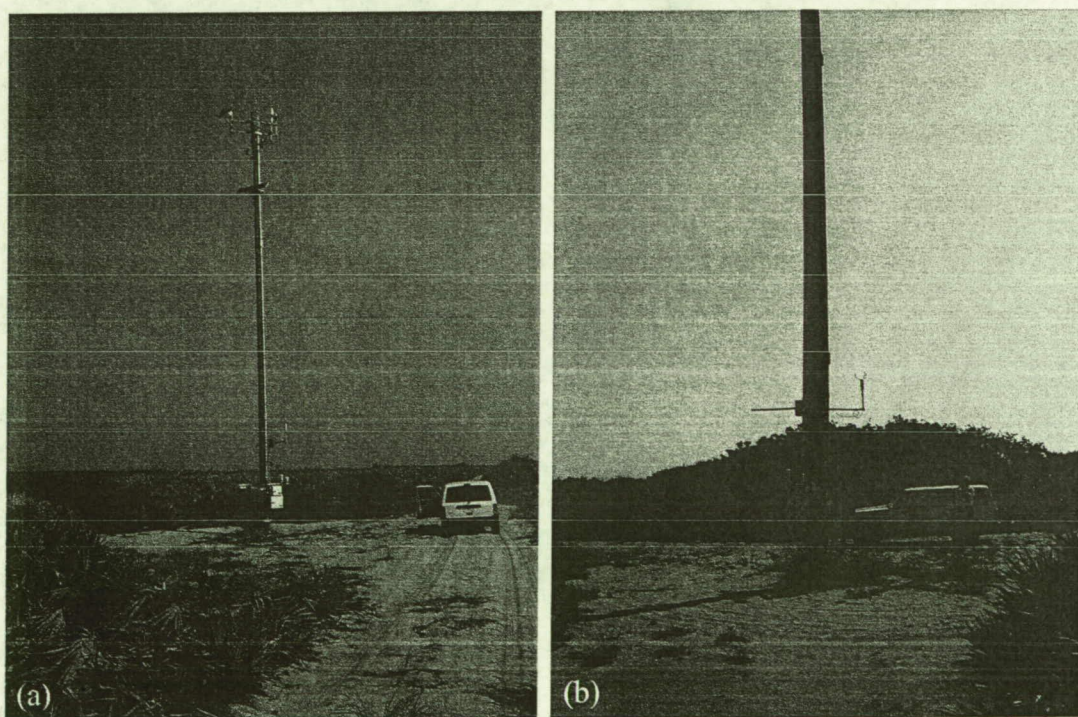


Figure 2.4. Photographs of coastal tower 0022 (a) looking northwest, and (b) looking northeast.

The causeway towers 0300 and 1007 along state route 528 and the NASA causeway, respectively, are both located on the western portions of the causeway (Figure 2.1a). Tower 0300 has full exposure to the Banana River (Figure 2.5). Highway 528 is just to its north and no significant vegetation or obstructions are found to the north of the tower (not shown). These site characteristics help make tower 0300 another one of the windiest towers in the network. Tower 1007 has some vegetation to its south (Figure 2.6a), which may impede some of the wind speeds compared to tower 0300. Figure 2.6b shows an example of a naturally aspirated temperature sensor with a solar shield at forecast critical tower 1007.

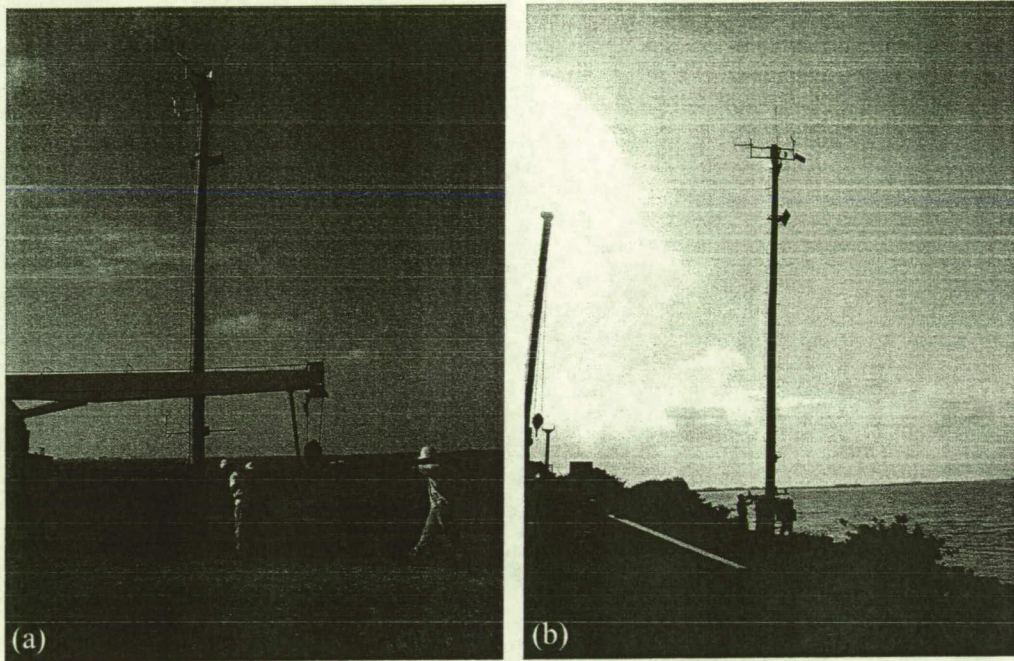


Figure 2.5. Photographs of causeway tower 0300 (a) looking south, and (b) looking east.

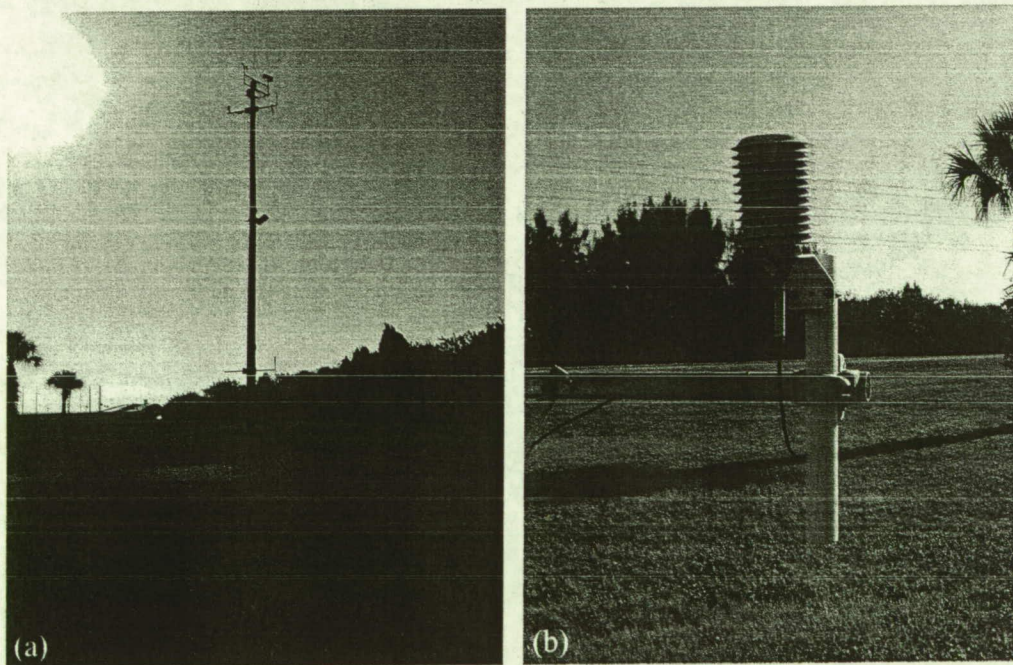


Figure 2.6. Photographs of causeway tower 1007 (a) looking east, and (b) close-up of 6-ft temperature sensor and solar radiation shield for natural aspiration system.

Tower 0303 is a safety critical tower in a land-locked location in the middle of CCAFS and typically has one of the coolest 6-ft temperature readings within the tower network. The tower is surrounded by vegetation about 20 ft tall (Figure 2.7). Tower 0403 is located on the western portion of CCAFS a few tenths of a nautical mile east of the Banana River. This tower is well-exposed with little surrounding vegetation (Figure 2.8). Both of these CCAFS towers have temperature sensors with a mechanical aspirator, an example of which is shown in Figure 2.8b at tower 0403. Tower 0509 is another safety critical tower, land-locked in central Merritt Island. It was built up on a mound, giving it full exposure to all directions (Figure 2.9).

Tower 0313 is the tallest tower in the network, reaching a height of 492 ft. It was built with an elevator to help with maintenance at the numerous observing levels (Table 2.1). Located in the northeast portion of Merritt Island and KSC, it has very little vegetation or obstructions on all sides of the tower. Data from this tower proved valuable in a previous AMU study on land breezes (Case and Wheeler 2002) since the depth of land breezes is often confined to under 492 ft. A photograph of tower 0313 with its numerous supporting cables is provided in Figure 2.10.

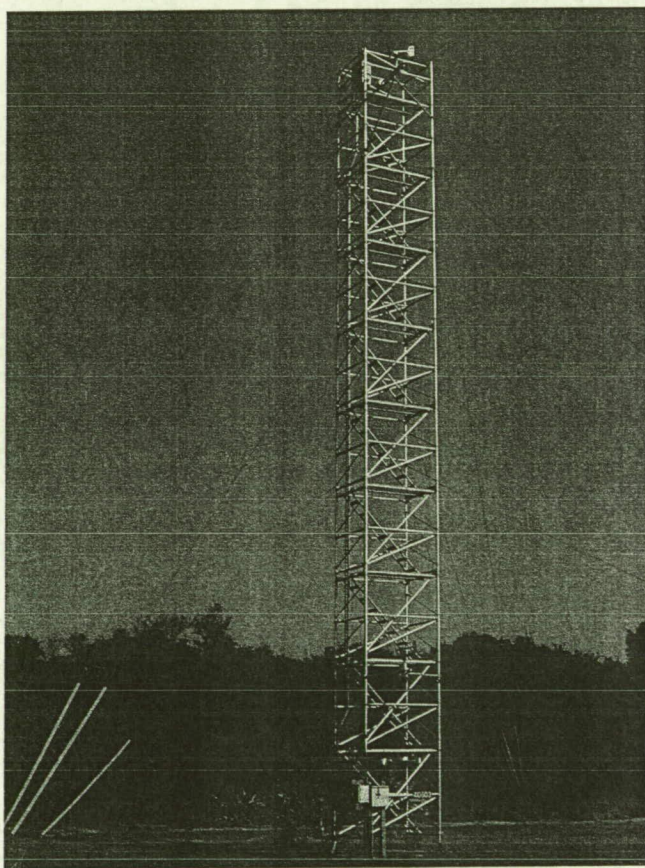


Figure 2.7. Photograph of CCAFS tower 0303.

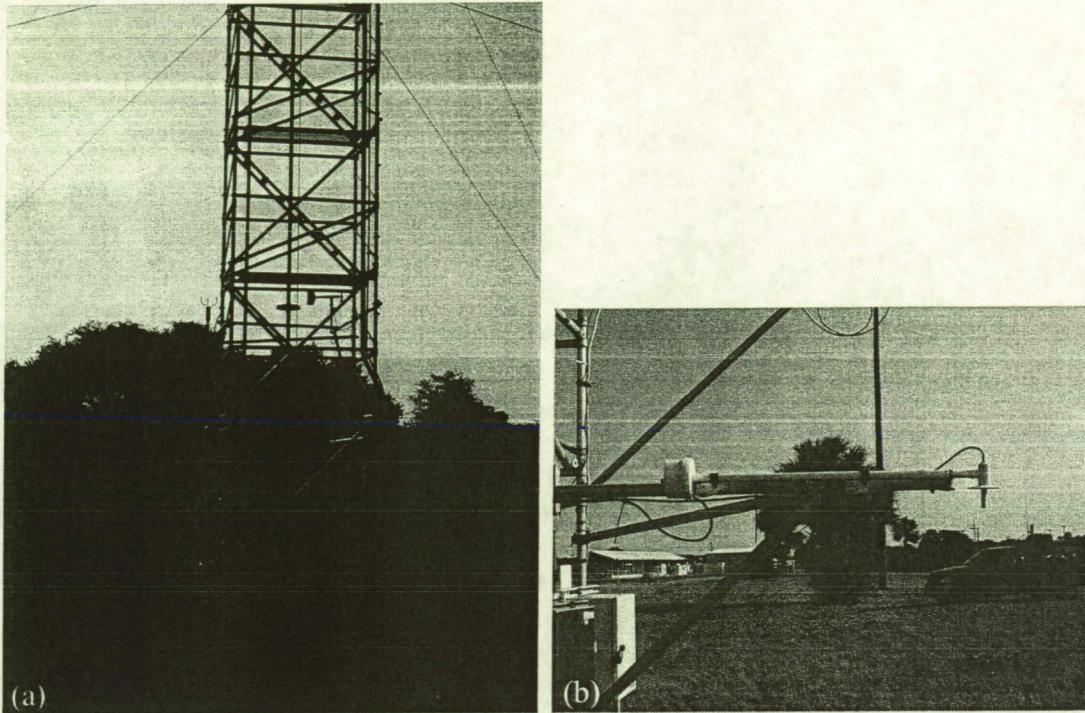


Figure 2.8. Photographs of CCAFS tower 0403 (a) looking south, and (b) close-up of 6-ft temperature sensor with mechanical aspiration system.

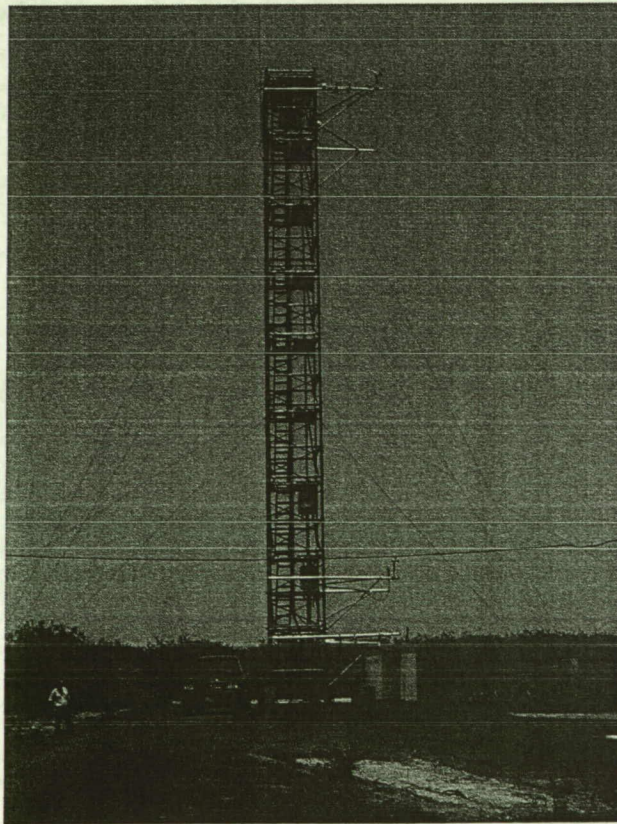


Figure 2.9. Photograph of Merritt Island tower 0509.

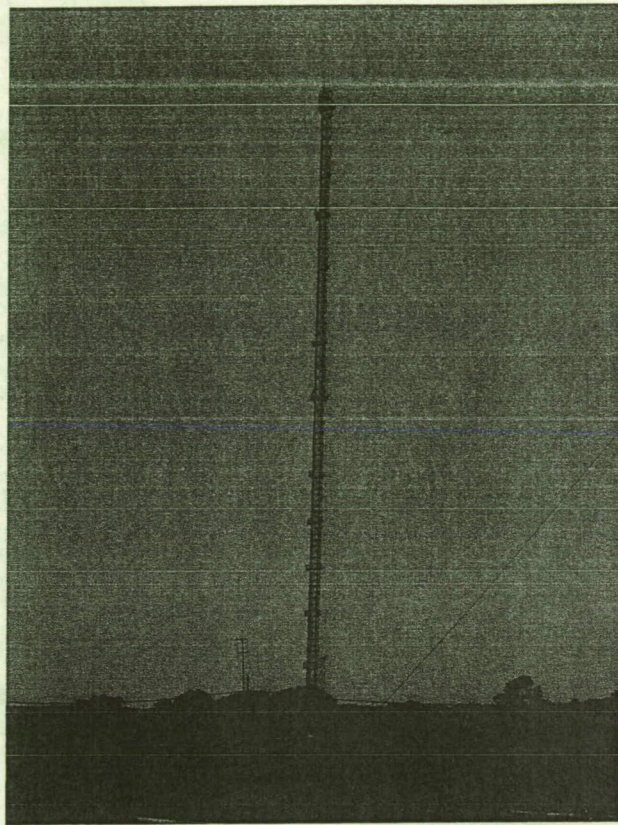


Figure 2.10. Photograph of 492-ft tall Merritt Island tower 0313.

Three of the forecast critical towers on mainland Florida that are discussed in the climatology results section are towers 0819, 1204, and 1612. Tower 0819 is in one of the farthest northern locations among the mainland towers. The tower is adjacent to relatively substantial vegetation about 30 ft tall, immediately to the south of the pole (Figure 2.11a). To the north of 0819, there is a campsite with fairly open, unobstructed land (Figure 2.11b). Notice that the instruments are missing at 0819 because the Range Technical Services Contractor was in the process of replacing the wooden pole with a concrete pole.

Tower 1204 is located in the town of Port St. John, near the backyard of a new house. This tower has serious exposure problems, since large pine trees obstruct the pole (Figure 2.12a). Due to these obstructions, the wind ventilation for the naturally aspirated temperature sensor is inhibited. The result of late morning sun exposure during the spring and summer months (Figure 2.12b) and inhibited natural aspiration at this tower will be discussed in Section 4.4.3. Mainland tower 1612 is the farthest west among the towers used in this climatology (Figure 2.1b). This tower can be very difficult to reach for maintenance at times, since the Savanna environment at the end of the dry season (Figure 2.13) turns into a marsh with standing water and mud during the wet season. Water depths exceeding 2 feet have been known to occur in and around tower 1612 in the past.

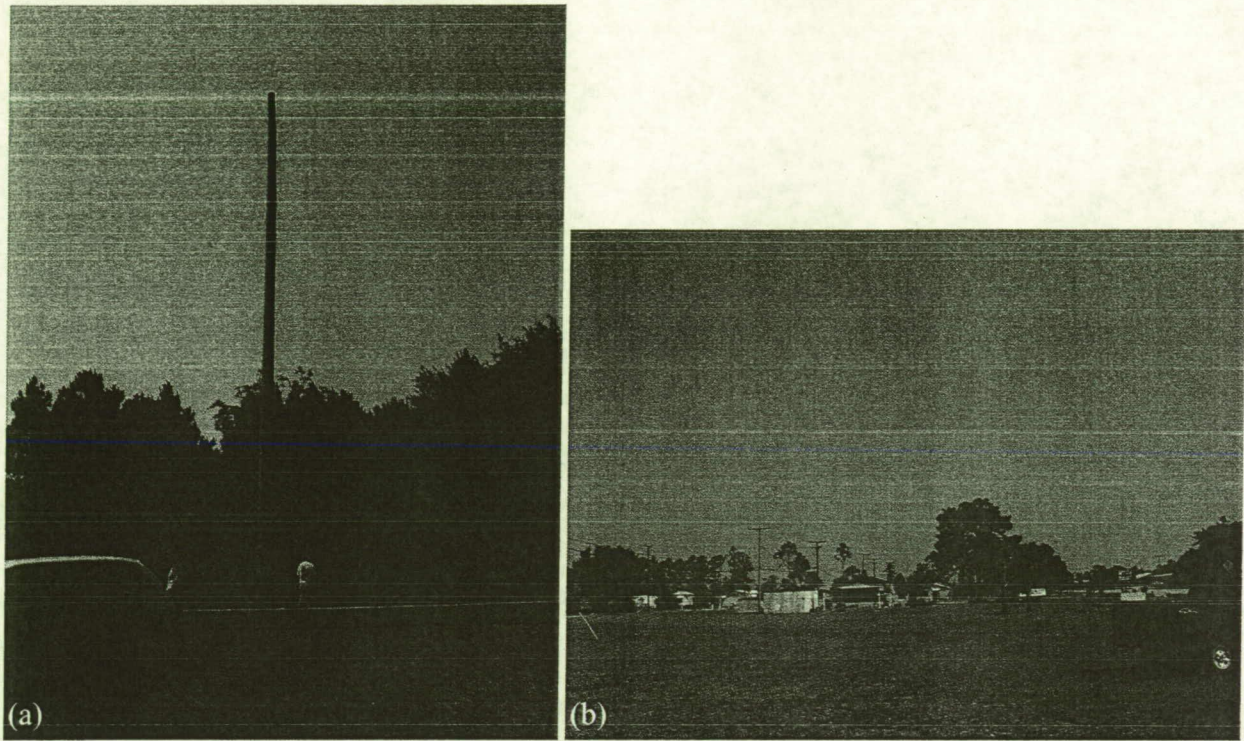


Figure 2.11. Photograph of mainland tower 0819 (a) looking south, and (b) looking north.

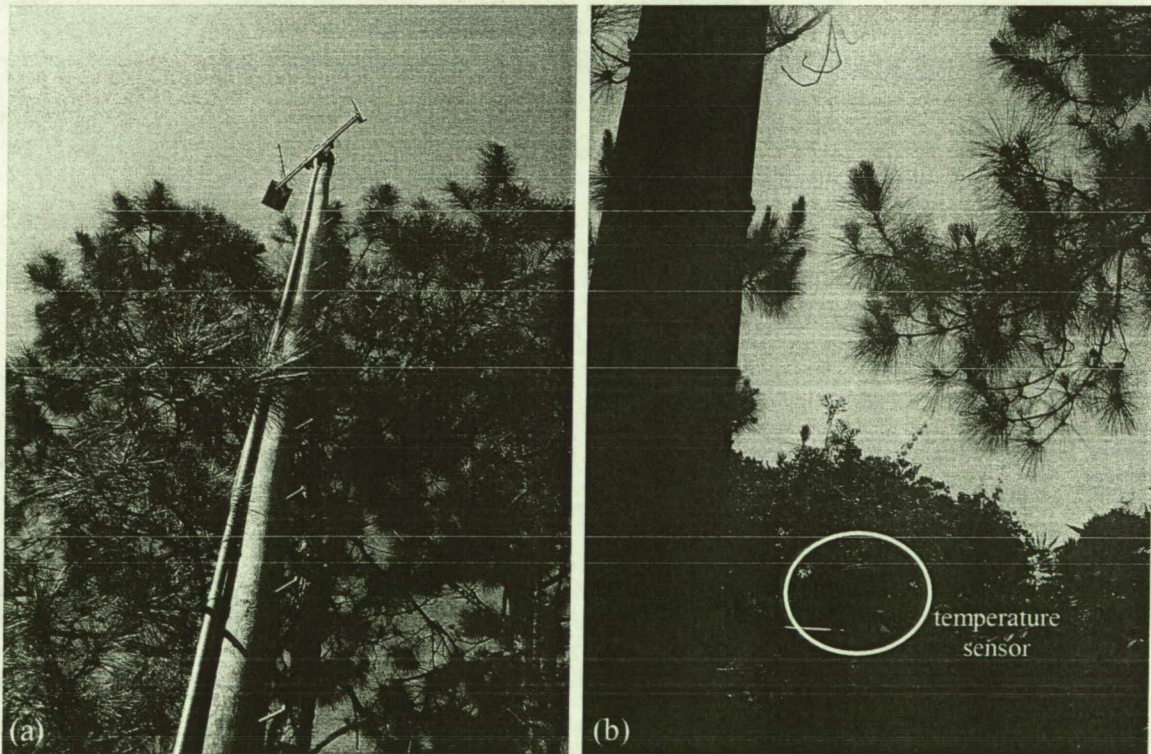


Figure 2.12. Photograph of mainland tower 1204 (a) looking up with pine tree limbs shrouding tower, and (b) looking east with sun shining on 6-ft temperature sensor.



Figure 2.13. Photograph of mainland tower 1612 within swamp/meadow lands, depending on wet or dry season. This photograph was taken in late May at the end of the Florida dry season.

2.5 Data Archive Comprising Climatology

Archived data were collected from all towers in the network over the period from February 1995 to January 2004 (nine years total for each month). Data were not used prior to February 1995 due to unreliable data quality, availability, and differences in numerical precision compared to post-January 1995 archives. The data set consists of the year/month/day/hour/minute and height of the observations. The time resolution of the data is 5 minutes. The meteorological variables in the data set include

- Temperature and dew point temperature (derived from temperature and relative humidity measurements) in degrees Celsius,
- 5-minute average and 5-minute peak wind speeds in meters per second,
- 5-minute average and 5-minute peak wind direction in degrees,
- Deviation of the 5-minute average wind direction in degrees, and
- Relative humidity in percent.

The wind speed and direction data were sampled every second. The 5-minute average is the mean of all 300 1-second observations in the 5-minute period. The peak wind is the maximum 1-second speed in the 5-minute period and its associated direction. Before processing, the temperatures were converted to degrees Fahrenheit with the equation

$$^{\circ}\text{F} = 1.8 * \text{C} + 32, \quad (2.1)$$

and the wind speeds were converted to knots (kt) with the equation

$$\text{Knots} = 1.9424 * \text{m s}^{-1}. \quad (2.2)$$

Several towers were not included in the nine-year climatology due to excessive missing data or inconsistent measuring heights. Towers that were excluded due to too much missing data are IDs 1500, 1605, 1617, 2008, 2016, and 2202, all forecast critical towers. Towers that had measuring heights inconsistent with most of the network include IDs 0511, 0512, 0513, and SLC 36. The SLC 40 tower only measures winds at 54 ft, so this tower was not used either. Finally, tower 0211 was not included in the climatology because this tower changed location in September 2000 from the original tower 0112.

2.6 Range Standardization and Automation (RSA) Changes

Through the RSA program, several towers will be deleted, moved (with new IDs), or added to the network. Among the towers used in the current climatology, the following towers will be deleted or moved (Figure 2.14):

- 0019, 0303, 0418, 0805, and 1204. Among these towers, only 0805 will retain the original ID since the distance moved will be very small. Additional towers to be deleted that were not included in this climatology due to insufficient data are 1617 and 2008.

The following new towers will be implemented through RSA:

- 0011 (False Cape), 0015 (Playalinda), 0095 (Lori Wilson Park), 0103 (Weather Station A), 0316 (0418 replacement at Mosquito Lagoon), 0496 (Merritt Island Beacon), 0805 (replacement of current 0805), 0889 (Viera), and 1305 (replacement of 1204).

Note that towers 9001 and 9404 will be renamed to 1299 and 0795, respectively, to adhere to the tower ID naming convention described in Section 2.2.1.

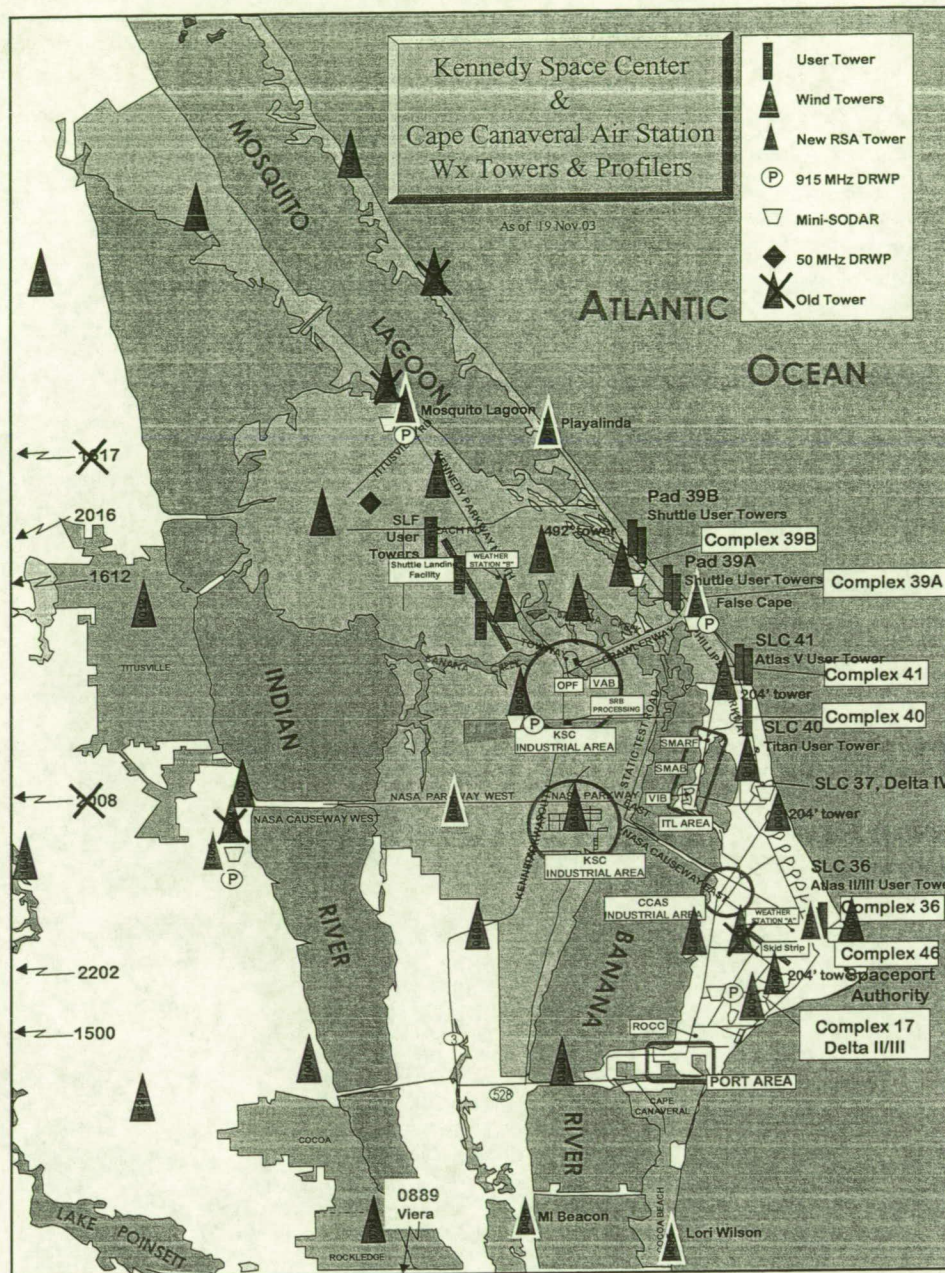


Figure 2.14. The modified tower network with the RSA program.

Table 2.5 summarizes the characteristics, accuracy, and thresholds for the RSA replacement sensors. All sensors except for the user towers at the launch pads (e.g. SLC 39A and 39B) will be replaced with this new suite of sensors by no earlier than 2006. The most significant difference is the use of sonic anemometers with RSA compared to the traditional cup anemometers and wind vanes on the legacy sensors comprising the climatology. The advantages of the sonic anemometers are a lower starting speed threshold and higher accuracy. The primary performance differences in the specifications of the temperature and humidity sensors are slightly better relative humidity accuracy and larger operating range for temperature in the RSA sensors.

Table 2.5. RSA replacement specifications for sonic anemometers, temperature, and humidity sensors.

Variable & Characteristic	RSA sensor and specifications
Wind Speed	
Sensor	Vaisala Ultrasonic Wind Sensor WS425
Operating range	0–126 kt (0–65 m s ⁻¹ , serial output); 0–109 kt (0–56 m s ⁻¹ , analog output)
Accuracy	± 0.26 kt (± 0.135 m s ⁻¹)
Starting threshold	Virtually zero
Resolution	0.2 kt (0.1 m s ⁻¹)
Wind Direction	
Sensor	Vaisala Ultrasonic Wind Sensor WS425
Operating range	0–360°
Delay distance	Virtually zero
Accuracy	± 2°
Starting threshold	Virtually zero
Resolution	1°
Air Temperature	
Sensor	Rotronic Hygroclip S3 humidity temperature probe MP400H Pt100 1/3 DIN (standard) 118 x 3 mm
Operating range	-40 to 140°F (-40 to 60 C)
Accuracy	±0.4°F (at 73°F) [±0.2 C (at 23 C)]
Voltage supply	5 V
Current consumption	Max. 45 mA
Relative Humidity	
Sensor	Rotronic Hygroclip S3 humidity temperature probe MP400H HYGROMER™ C94 capacitive humidity sensor
Operating range	0–100%
Accuracy	±1.5%
Voltage supply	5 V
Current consumption	Max. 45 mA

3. Methodology

The development of a nine-year climatology involved both automated and manual QC of tower data. Once the data were quality controlled, several scripts were written to re-format data and calculate statistics on a monthly and hourly basis using the S-PLUS® software (Insightful Corporation 2000). Data processed in S-PLUS were then exported to Microsoft® Excel® and the General Meteorological Package (GEMPAK) software formats for post-analysis and the creation of a graphics tool. This section describes the procedures used to generate the climatological statistics and develop a graphical tool for analyzing the tower climatology results.

3.1 Data Quality Control

A large portion of this task involved running an automated QC algorithm on the wind and temperature data, and then performing manual QC on the temperature data. Manual QC was needed to supplement the automated QC for temperatures since some bad data survived the automated QC checks.

3.1.1 Automated quality control

Five QC routines from Lambert (2002) were used remove bad data:

- An unrealistic value check (e.g. wind speed < 0),
- A standard deviation (σ) check (e.g. temperature not within 5σ of mean),
- A peak-to-average wind speed ratio check in which the peak wind must be within a specified factor of the average wind speed (factor value dependent on average speed),
- A vertical consistency check between sensor levels at each individual tower, and
- A temporal consistency check for each individual sensor.

Only a small percentage of the data were flagged as erroneous by these QC routines: from 0.6 to 2.1% per tower and month, which resulted in a large set of good quality data for analysis and forecast-tool development. There was one known instance when good data were eliminated by the automated QC. In early May 1999, exceptionally cool temperatures occurred compared to all other months of May in the period of record. These temperatures were so unusually cool that the 5σ standard deviation check removed large portions of the data from the first couple days of May 1999. To alleviate this problem, the standard deviation check was modified to 10σ , but only for May data. Refer to Lambert (2002) for more specific details of the automated QC algorithm.

3.1.2 Manual quality control

An initial examination of the quality-controlled data indicated that manual QC was also required for the temperature observations. This section describes the methodology developed for manual QC of the 5-minute temperature observations at 6 ft and 54 ft prior to analysis for systematic biases and geographical variability.

The methodology for manual QC of the 6-ft and 54-ft temperatures contains the following steps:

1. Determine the percentage availability of data at each individual tower location,
2. Generate frequency distributions of temperatures at towers with at least 70% data availability,
3. Identify the towers that have data outliers, then generate two-dimensional (2D) frequency diagrams of the temperature distributions versus UTC hour and year to determine if these outliers are bad data, and
4. Using the combined information in the 2D frequency diagrams, along with climate data, and adjacent tower information (as necessary), identify the exact times and years with bad data, and set these data to missing in the database.

This manual QC process is illustrated in an example for tower 0001 data from March, as shown in Figure 3.1 through Figure 3.4. About 90% of the 5-minute data at tower 0001 were available from the March 1995 to 2003 period of record (Figure 3.1). Several towers inland of KSC (i.e. towers 1500 to 2202) had poor data availability at only 40 to 70%. Towers with such low data availability were excluded from the climatology in order to obtain representative means and standard deviations of temperatures and wind speeds when categorizing the data into UTC hour and wind-direction bins.

Since tower 0001 showed an adequate amount of data during March, the frequency distribution was plotted to determine if any outliers were present in the database (Figure 3.2). By comparing the frequency distributions of several different towers from the same month on one chart, it was easier to identify anomalies. According to Figure 3.2, tower 0001 measured anomalously high temperatures above 90°F, compared to the other towers plotted on the chart.

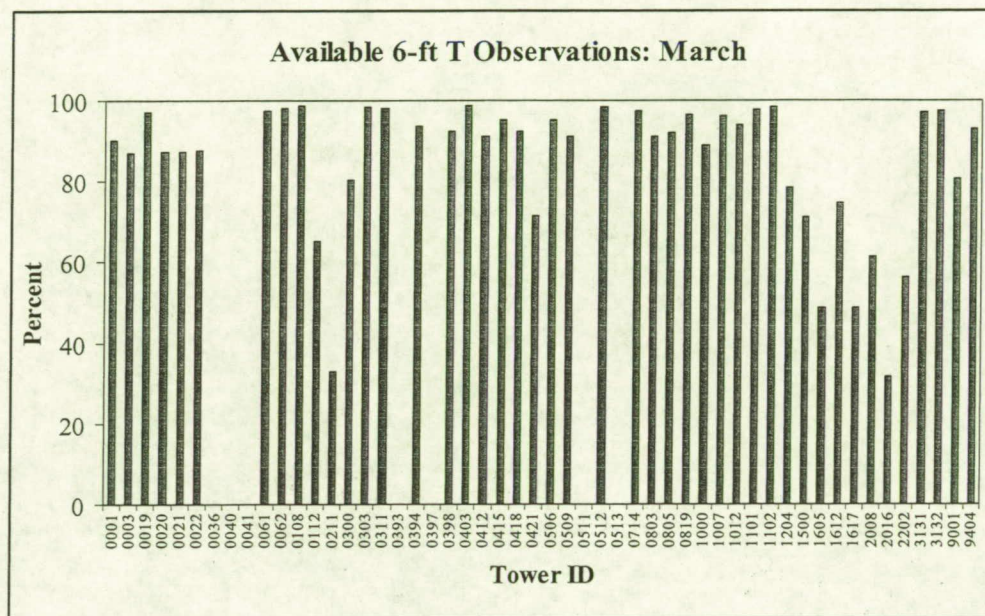


Figure 3.1. The percent availability of archived 5-minute, 6-ft temperature observations for all towers during March for the years 1995 – 2003. Towers with percentages less than 70% were excluded due to insufficient data availability.

With the probable outliers identified, the next step was to isolate the UTC time(s) and year(s) during which the potentially bad data occurred. Figure 3.3 and Figure 3.4 depict the 2D frequency distribution of temperatures versus UTC hour and year, respectively, at tower 0001. Similar diagrams were prepared for all other towers and months exhibiting questionable frequency distributions. According to Figure 3.3, the anomalously high temperatures were observed between 1500 and 1700 UTC, since this cluster of occurrences are clearly separate from the smoother diurnal ranges in temperatures. Based on Figure 3.4, the anomalous data occurred in 1995 since a portion of the distribution is separated from the remainder of the frequency diagram, suggesting that these data are erroneous. These temperature data were determined to be erroneous or valid by examining Melbourne, FL climate data (~ 20 nm south of tower network) for the day in question, as well as the temporal variations of the 5-minute data, tower winds, and adjacent tower data (as necessary). If the readings were highly unrealistic relative to other meteorological data, then the measurements were determined to be erroneous.

These erroneous data were identified in the database using commands available in the S-PLUS software that quickly isolate the locations in the spreadsheet based on the information obtained from Figure 3.3 and Figure 3.4. The bad data were set to a missing flag to indicate that the data have been manually quality controlled. This manual QC process was repeated for each month in the period of record spanning February 1995 – January 2004.

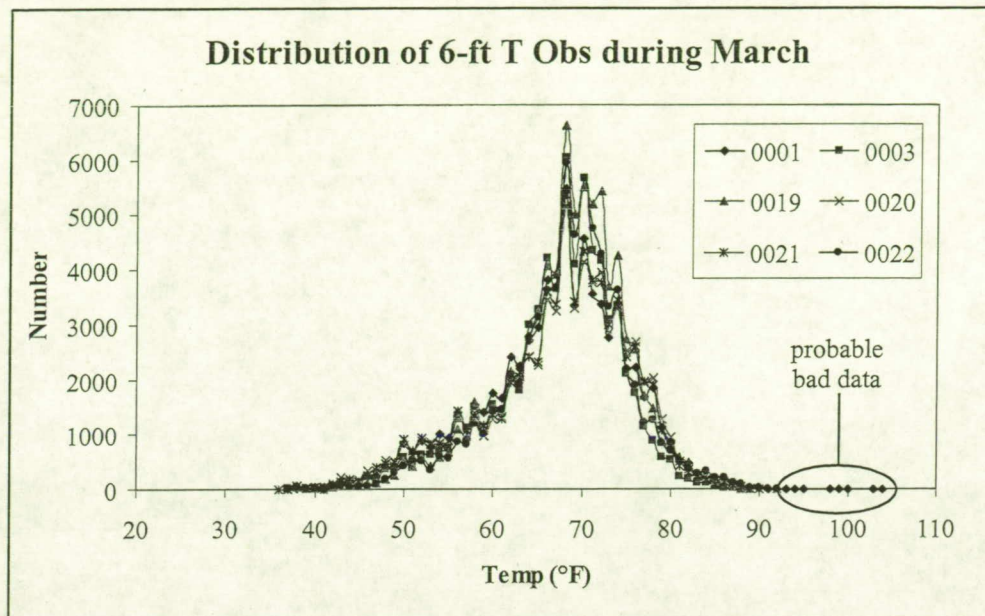


Figure 3.2. The frequency distribution of the number of 6-ft temperature observations during March (1995–2003) at towers 0001, 0003, 0019, 0020, 0021, and 0022. Note the outliers at tower 0001 with temperatures above 90°F.

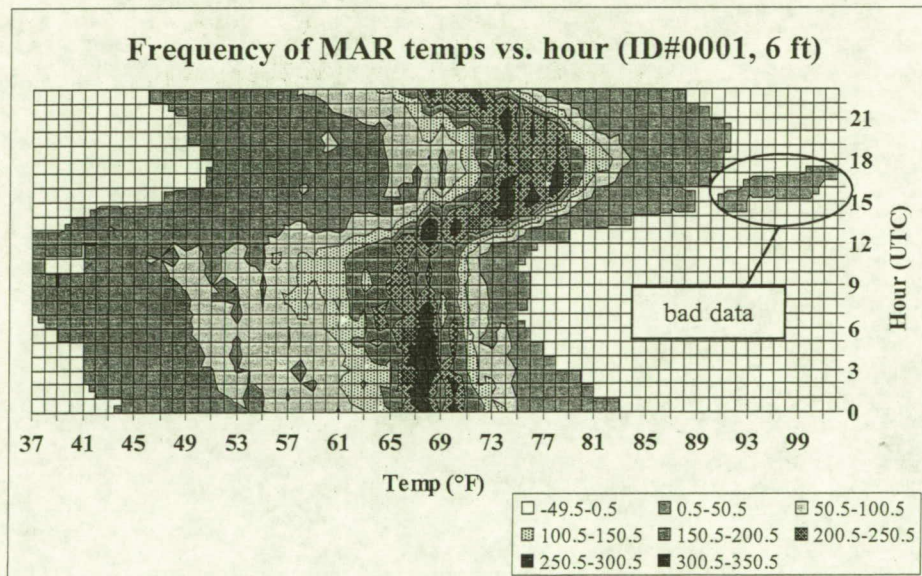


Figure 3.3. A contour diagram showing the 2D frequency distribution of 6-ft temperatures at tower 0001 during March (1995–2003) as a function of UTC hour. Note that the high-temperature outliers of Figure 3.2 occurred between 1500 and 1700 UTC. Frequencies are contoured every 50 units beginning at 0.5, in order to depict one or more occurrences with shading.

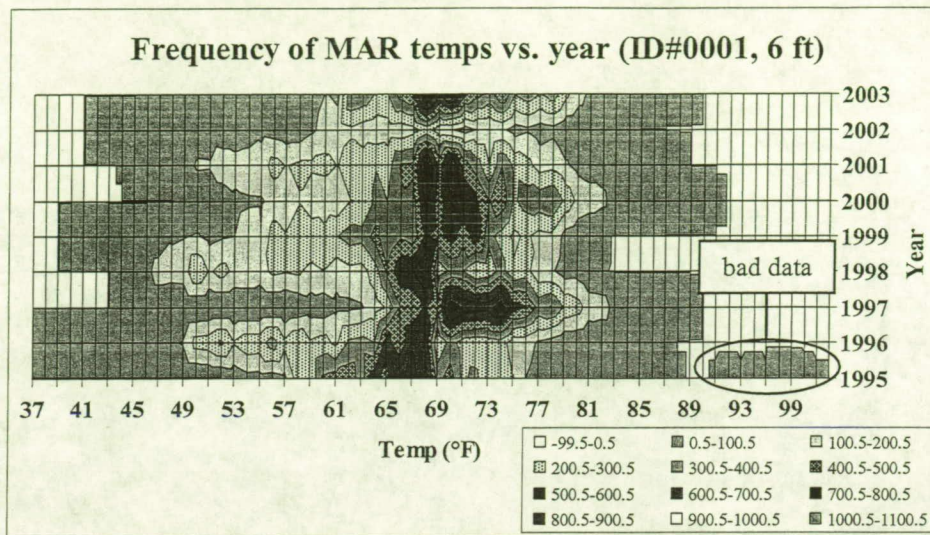


Figure 3.4. A contour diagram showing the 2D frequency distribution of 6-ft temperatures at tower 0001 during March (1995–2003) as a function of year. Note that the high-temperature outliers of Figure 3.3 occurred in 1995. Frequencies are contoured every 100 units beginning at -99.5, to depict one or more occurrences with shading.

3.2 Data Processing

All processing, calculations, and data stratification were conducted using the S-PLUS software. Even though Excel also has spreadsheet and batch capabilities, S-PLUS was selected because of the very large data files. A limitation of Excel that continues in current versions is a maximum row dimension of 65,536, whereas S-PLUS has no such limitation. This Excel limit makes it quite difficult to work with the large tower data files on a monthly basis. For nine years of data in any particular month, a single tower and height archive will contain more than 70,000 5-minute entries. Therefore, all quality controlled data were first imported into S-PLUS files prior to statistical calculations.

3.2.1 Brief description of S-PLUS

The S-PLUS software is a statistical and graphics software designed to be able to process large data sets. It has numerous features for modeling statistical processes, determining statistical distributions, displaying graphical data, and running batch scripts. Only a small sub-set of its capabilities were used for this task. One of the most helpful features of S-PLUS used for this project is its ability to calculate statistics based on categorical data stratification. For example, the mean temperature could be computed for each category of hour (ranging from 00 to 23 UTC) or pre-defined wind direction bin.

3.2.2 Variables/heights processed

The following variables and heights were processed for the climatology:

- Temperature at 6 ft,
- Temperature at 54 ft,
- Temperature at 54 ft minus temperature at 6 ft, representing near-surface stability,
- Wind speed at 54 ft, and
- Wind direction standard deviation at 54 ft.

Dew point temperature or relative humidity data were not examined for this climatology.

3.2.3 Calculations and categorizations

The following statistics were computed for each of the variables and heights listed in Section 3.2.2:

- Mean,
- Standard Deviation,
- Bias,
- Percent data availability, and
- Data count and climatological probability for wind direction bins.

All of the above quantities were calculated on an hourly basis for all years collectively in each individual month, so as to develop a monthly climatology of the diurnal variations of each variable and height. Data were also stratified by wind direction bins, every 45° from 0° to 360°.

The climatological probabilities of wind direction bins were computed by simply dividing the number of observations in a particular wind direction bin by the total count of observations for all wind directions. These probabilities were calculated for each tower individually as well as all towers used in the climatology combined.

Those towers labeled as not used in column 2 of Table 2.1 had insufficient data availability year-round, and were therefore excluded from all portions of the climatology in all months. Among the towers used in the climatology (see columns 1 and 2 in Table 2.1), only towers with at least 70% overall data availability in a given month were included in the climatology for that month. The wind direction stratification statistics were conducted using all towers except those listed as not used in column 2 of Table 2.1.

3.3 Analysis and Display Tools

After all statistics were processed using S-PLUS, the resulting data were exported into Excel and GEMPAK files for analysis, display, and the development of a graphical user interface (GUI) tool. The S-PLUS statistics were formatted for Excel pivot charts and tables, which served as the primary mechanism for displaying the tower climatology results graphically. The GEMPAK software was used to develop geographical plots and contours of the climatological statistics so that users could examine the geographical variability across the KSC/CCAFS tower network. Finally, the Excel pivot charts, tables, and GEMPAK geographical plots were integrated into a single web-based GUI tool for analysis and display by users.

3.3.1 Microsoft Excel pivot charts

Pivot charts and tables are parts of a feature that is exclusive to Excel, created as a means to summarize information in a large database quickly and in a way that is understandable to the user. These charts and tables are very flexible, allowing the user to make changes with point-click-drag-drop techniques. Axes can be switched, multiple variables can be represented on one axis, and specific fields can be temporarily removed from the display to facilitate closer examination of other fields.

The S-PLUS results for each parameter, height, and statistic were output in the format required for Excel pivot charts and tables, and exported into Excel spreadsheets. Pivot charts and tables were then created and configured for all statistics and parameters. The Excel pivot charts and tables were then saved as HyperText Markup Language (HTML) files for incorporation into the web-based GUI tool.

3.3.2 GEMPAK three-panel spatial/contour plots

After the S-PLUS statistics were exported into Excel spreadsheet files, the pivot-chart formatted data were again reformatted for exporting into GEMPAK files. First, GEMPAK surface station files were created for the mean, bias, and standard deviation of all five parameters (6-ft temperature, 54-ft temperature, 54 minus 6-ft temperature difference, 54-ft wind speed, and 54-ft wind direction deviation) and nine wind direction bins (all directions, 1–45°, 46–90°, 91–135°, 136–180°, 181–225°, 226–270°, 271–335°, 336–360°), for a total of 135 surface files. The statistics for each month were then added to the GEMPAK surface files by tower ID and UTC hour of the day.

The tower data were then analyzed onto a grid with 0.68-nm (1.25-km) horizontal grid spacing using the two-pass Barnes (1973) objective analysis technique within GEMPAK, as described in Koch et al. (1983). The resulting surface and grid GEMPAK files allowed for generating geographical plots and contours of each statistic.

Three-panel images in Graphical Interchange Format (GIF) format were created using GEMPAK surface plotting and grid contouring programs. The mean quantity is plotted in the left panel, bias in the middle panel, and standard deviation in the right panel (see sample plot in Figure 3.5). A total of 12,960 geographical plots were generated for all combinations of parameters, months, hours, and wind direction bins (5 parameters x 12 months x 24 hours x 9 wind direction bins).

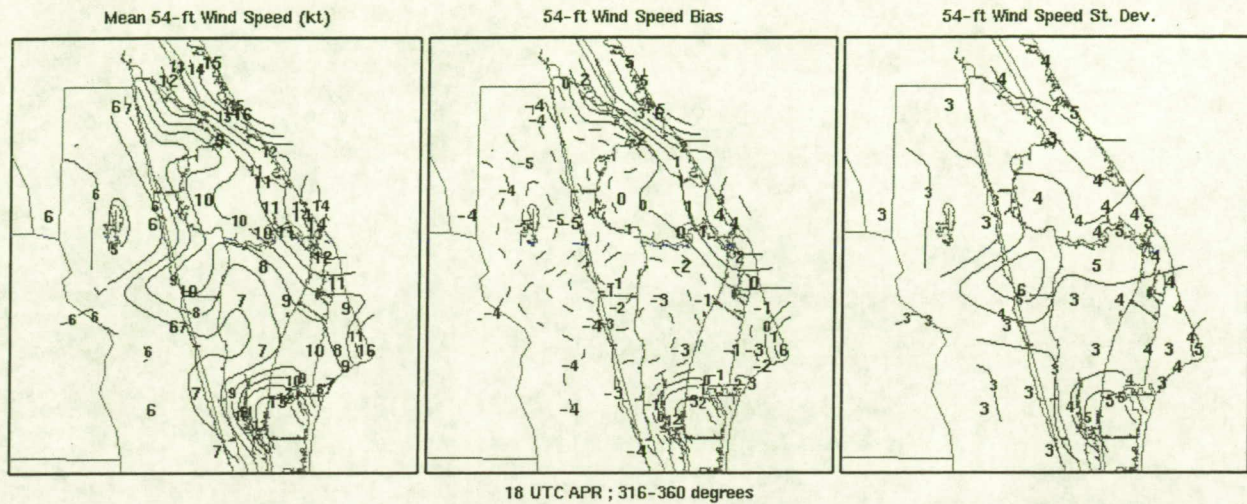


Figure 3.5. Three-panel geographical contour plot of mean (left panel) bias (middle), and standard deviation of 54-ft wind speed (right), valid for all tower observations during the 1800 UTC hour of April for the period of record 1995–2003.

3.3.3 Web-based interactive tool

The pivot charts, pivot tables, and geographical plots were all integrated into a web-based tool written in HTML using Microsoft® FrontPage®. The tool was designed to allow the user to link to any parameter, statistic, wind direction bin, and month. The training document in Section 5 has a complete description of the web-based tool's capabilities and instructions on how to navigate through and use the pivot charts and geographical maps.

4. Climatology Results

4.1 Overview of results

The climate of KSC/CCAFS is largely driven by the complex land-water interfaces of the Atlantic Ocean, Mosquito Lagoon, Indian River, and Banana River with Cape Canaveral, Merritt Island, and the Florida mainland (Figure 2.14). Towers with close proximity to water typically have much warmer nocturnal temperatures and substantially higher wind speeds throughout the year. A 7–10°F difference occurred in the mean 6-ft temperature across the network throughout the year, most notable in the pre-dawn hours. Even larger 6-ft temperature variations were found within specific wind direction ranges. The variations in 54-ft temperatures were much smaller across KSC/CCAFS, so the near-surface stability (54-ft minus 6-ft temperature) was primarily a function of the 6-ft temperatures.

Mean domain-wide wind speeds were generally 4–6 kt during the nocturnal hours and 7–9 kt during the day. The strongest mean nocturnal wind speeds of 6–7 kt occurred from October to March (the synoptic season). Meanwhile, the strongest mean daytime wind speeds of 8.5–9.5 kt occurred from February to May, probably due to a combination of synoptic systems and strengthening sea-breeze circulations during this latter portion of the Florida dry season.

Coastal and causeway towers tended to have mean wind speeds 2–4 kt stronger than the overall network mean. Meanwhile, mainland towers had mean speeds weaker than the network mean by about the same magnitude. The resulting gradient in the mean wind speed across the network was typically 5–8 kt over a distance of 15–20 nm (20–30 km), with the strongest speeds occurring along the Atlantic coastal towers.

The standard deviation of the wind direction (i.e. direction deviation) was proportional to the diurnal variation in wind speeds. Higher direction deviations and wind speeds occurred during the day compared to night. The direction deviation was highest over inland stations and Merritt Island/CCAFS towers not adjacent to any water body. Direction deviation tended to be highest during the summer months when afternoon and evening convective outflows led to large fluctuations in wind direction.

The bias statistic is given by the mean difference between the quantity at a given tower and the mean value for the whole network. The bias can be composed of any of the following causes for errors or deviations:

- Instrument / sensor error,
- Communication / processing error,
- Exposure / placement / representativeness error,
- Meteorological variability due to geography.

Most “biases” were largely a result of the geographical variability, which tended to mask the smaller instrument, processing, and exposure errors. Therefore, the bias can generally be considered a station’s tendency to deviate in a certain direction relative to the overall network mean primarily due to the local geography.

4.2 Data Requirement and Availability

For meaningful climatological statistics and comparisons among towers, an average hourly data availability of at least 70% was required at any particular tower for a given month. Towers that consistently had too much missing data in many months were excluded upfront from the climatology (refer to Section 2.4 and Table 2.1). Thirty-three towers, including four towers with sensors on opposite sides at the same height, for a total of 37 tower IDs, met the 70% minimum availability criterion (Figure 4.1).

Most of the launch/safety towers (labeled as "Launch" in Figure 4.1b) averaged over 90% data availability for both 6-ft and 54-ft temperatures while the forecast critical towers ("Fcst" in Figure 4.1b) had about 85% availability for all hours except for 00 UTC. A software deficiency occurred at the turn of the UTC day at the forecast towers, which caused a much lower data percentage for the 00 UTC hour. Because the 54-ft temperatures are measured only at the launch/safety towers, most sites had over 90% data availability except for towers 0003, 0020/0021, and 0398 (SLC 39B). Similar data availability was found with the 54-ft winds and direction deviation (not shown).

The forecast critical towers typically had a lower data availability because of the remote locations and occasional inaccessibility of these towers. During periods of heavy rainfall, the unpaved roads leading to some of these towers can be difficult or impossible to traverse, making routine maintenance and repairs impossible for weeks at a time. Furthermore, due to their remote locations, the forecast critical towers are operated by batteries that are automatically recharged by solar panels, whereas the launch/safety towers have ac power with battery backup. This also contributes to lower reliability of the forecast towers.

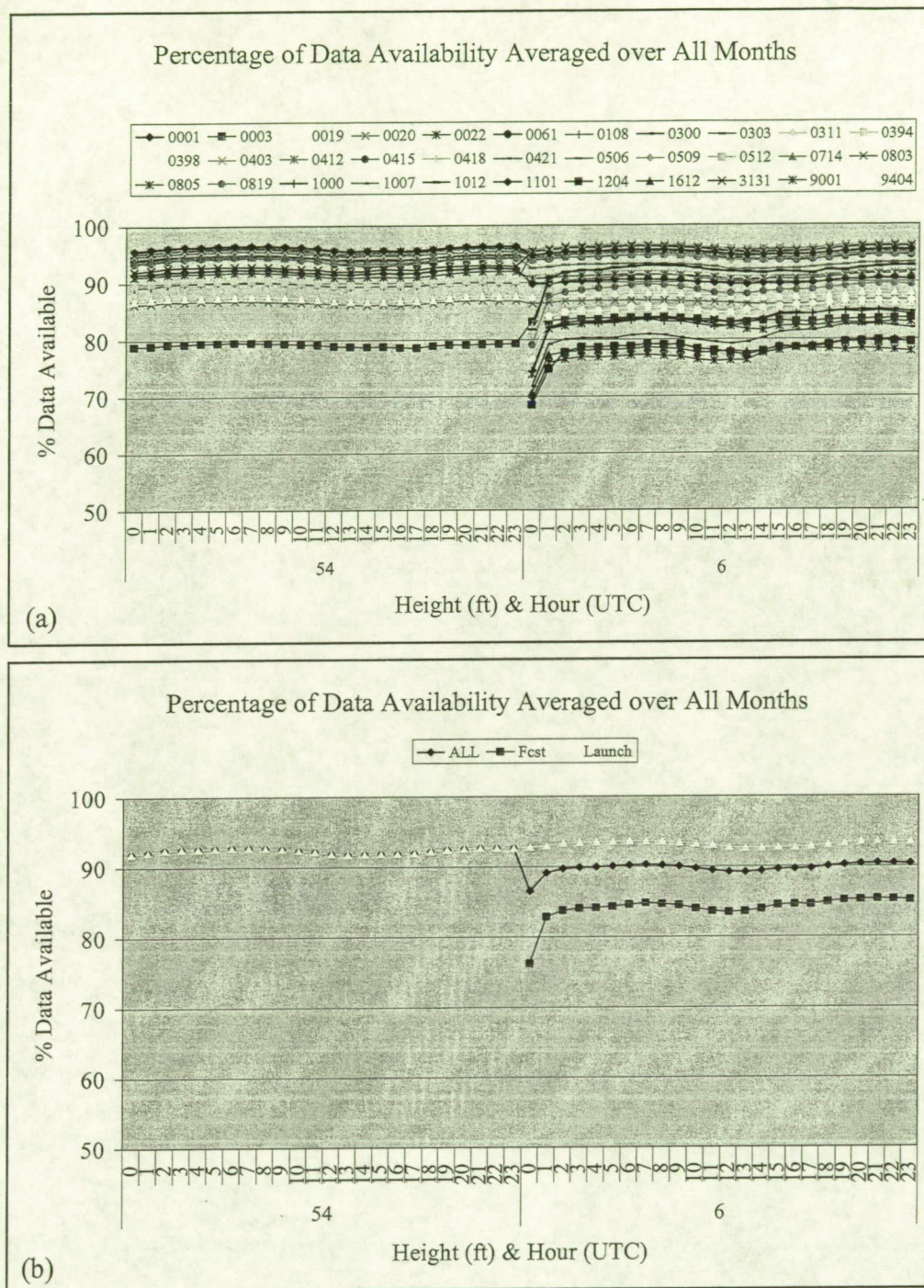


Figure 4.1. The percentage of temperature data availability at towers used in the climatology as a function of UTC hour for (a) each individual tower at 54 ft and 6 ft, and (b) all towers combined (ALL), forecast critical towers combined (Fcst), and launch / safety critical towers combined (Launch).

4.3 Climatological Probabilities of Wind Directions

The annual distribution of climatological probabilities of wind direction ranges (defined in Table 4.1) for the entire KSC/CCAFS tower network is shown in Figure 4.2. The hourly values within each month (ranging from 00 to 23 UTC) reveal the mean diurnal variation in climatological probabilities across the network.

A distinct annual trend is evident from the probabilities given in Figure 4.2. North and northwest winds (315° and 360° bins) are most prevalent from November to February ($\sim 20\text{--}30\%$), then steadily decrease in probability, reaching a minimum in June and July ($\sim 5\text{--}10\%$). Thereafter, the probabilities of north and northwest winds increase again, particularly in October. Conversely, the southeast and south wind direction bins (135° and 180°) experience a minimum in probability from November to February ($\sim 5\text{--}15\%$), steadily increase to a maximum in July ($\sim 30\text{--}40\%$), and then decrease thereafter, especially from September to October. Most of the other wind direction bins fluctuate between $5\text{--}15\%$ probabilities throughout the year, except for the southwest and west bins during the summer months. A much higher occurrence of southwest and west winds is found during the nocturnal and early morning hours from June to August.

A closer look at the climatological probabilities during July reveals the typical diurnal variations in wind directions during the Florida warm season (Figure 4.3). From the mid-morning to early afternoon hours ($\sim 1500\text{--}1800$ UTC), the east and southeast probabilities increase rapidly, representing the typical onset time of the sea breeze. After 1800 UTC, the wind directions steadily rotate clockwise, with the south-southeast bin (180°) probabilities peaking at 0000 UTC, the south-southwest bin (225°) reaching a maximum at 0600 UTC, and the west-southwest bin (270°) peaking at 1200 UTC. This steady clockwise rotation in the favored wind direction illustrates the impact of the Coriolis force on the local wind field across east-central Florida. The land-sea thermal contrast causes the initial rapid increase in onshore (easterly) winds during the midday hours, but then the Coriolis acts to rotate the winds in a clockwise sense by an average of 45° every six hours.

Table 4.1. Wind direction bin labeling convention.

Wind Direction Bin Label	Valid Wind Direction Range
45°	$0^\circ < \text{wind direction} \leq 45^\circ$
90°	$45^\circ < \text{wind direction} \leq 90^\circ$
135°	$90^\circ < \text{wind direction} \leq 135^\circ$
180°	$135^\circ < \text{wind direction} \leq 180^\circ$
225°	$180^\circ < \text{wind direction} \leq 225^\circ$
270°	$225^\circ < \text{wind direction} \leq 270^\circ$
315°	$270^\circ < \text{wind direction} \leq 315^\circ$
360°	$315^\circ < \text{wind direction} \leq 360^\circ$

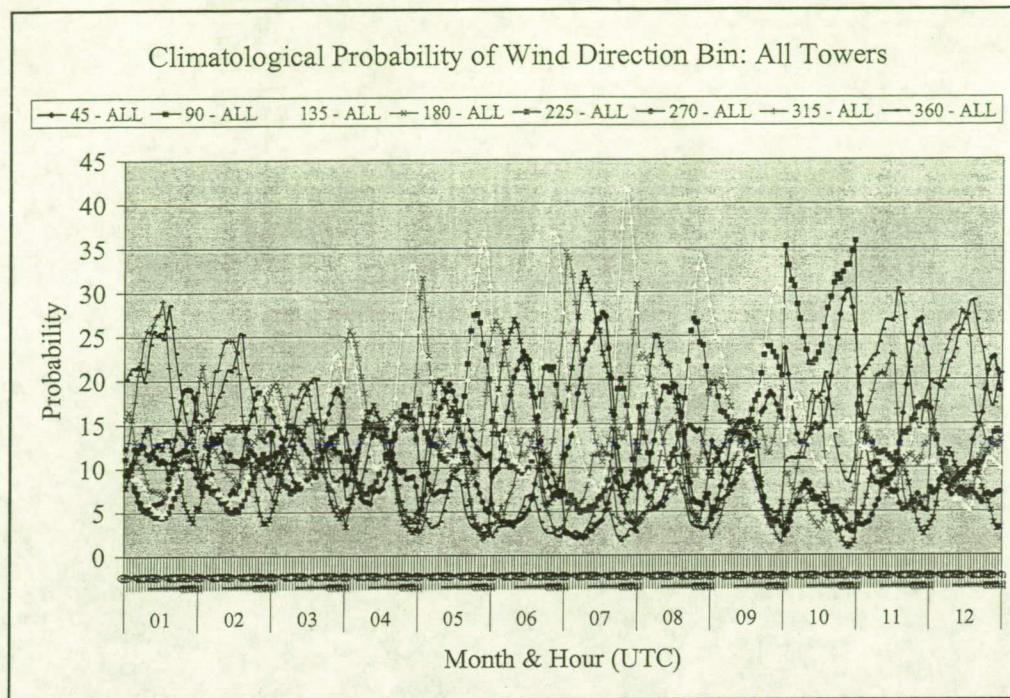


Figure 4.2. The climatological probability of the wind direction falling into eight different bins for all towers combined during the nine-year period of record. Twenty-four hourly climatological probabilities are given in each month of the year along the x-axis. The wind direction bin labeling convention is given in Table 4.1.

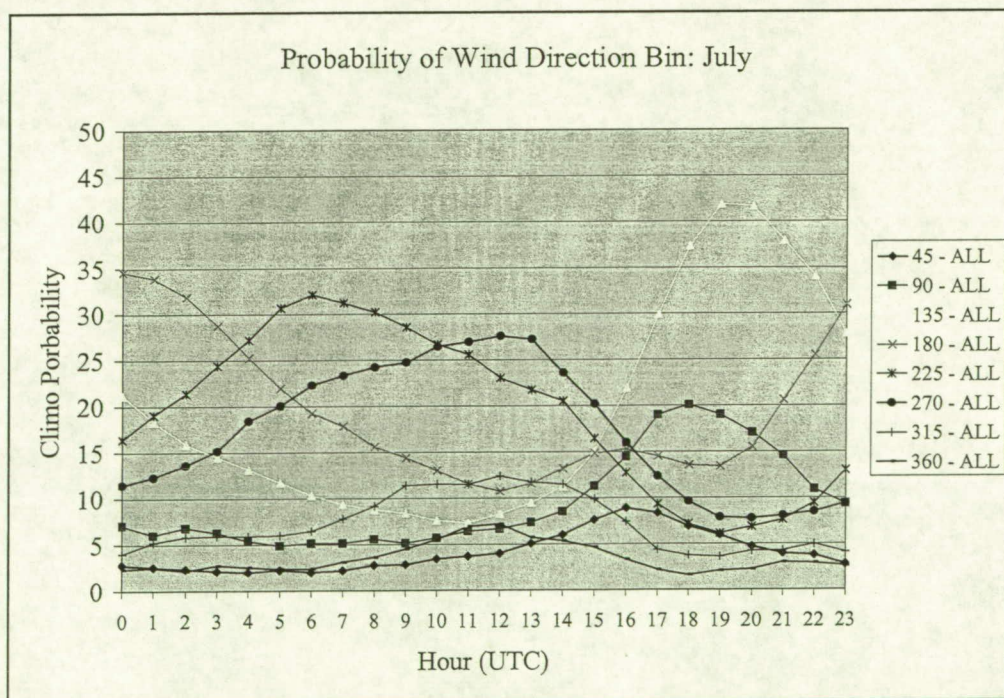


Figure 4.3. The climatological probability of the wind direction falling into eight different bins for all towers combined during the nine-year period of record, valid for July only. Twenty-four hourly climatological probabilities are given along the x-axis. The wind direction bin labeling convention is given in Table 4.1.

4.4 Temperatures

4.4.1 Monthly and diurnal variations

The variation of temperatures encountered across KSC/CCAFS is mostly linked to a station's proximity to water bodies. The diurnal range of mean 6-ft temperatures at all towers used in the climatology indicates that a 7–10°F variation typically occurs during the nocturnal hours (Figure 4.4a) throughout the entire year. The variation in mean 6-ft temperatures were not usually as large during the daytime hours, particularly in the morning hours shortly after sunrise; however, variations in the mean temperature were still often 5°F or more.

Figure 4.4b shows the mean diurnal range of temperatures at a coastal (0022), causeway (0300), Merritt Island (0509), and mainland (0819) tower, as well as the overall mean of all towers (ALL). As expected, the coastal and causeway towers had considerably higher mean temperatures than the overall network during the nocturnal hours for all months of the year. Meanwhile, tower 0819 usually had the highest mean 6-ft temperatures during the time of maximum heating and the lowest mean temperatures at night.

The mean 6-ft and 54-ft temperatures both exhibit a greater diurnal range at the Merritt Island and mainland towers compared to the coastal sites (Figure 4.5). The CCAFS, Merritt Island, and mainland towers were generally 3–5°F cooler at night and up to 3°F warmer during the daytime in January, particularly at 6 ft (Figure 4.5a). In July, similar variations were found between the coastal and land-locked towers, but with smaller differences between the 6-ft and 54-ft means (Figure 4.5b). The mainland towers (0819 and 1000) had the largest mean diurnal temperature ranges at 6 ft among the towers shown in Figure 4.5. Fifty-four-foot temperatures were not available at the forecast critical mainland towers. Figure 4.4 and Figure 4.5 should help provide a flavor for the typically mean temperature differences between coastal and land-locked tower locations.

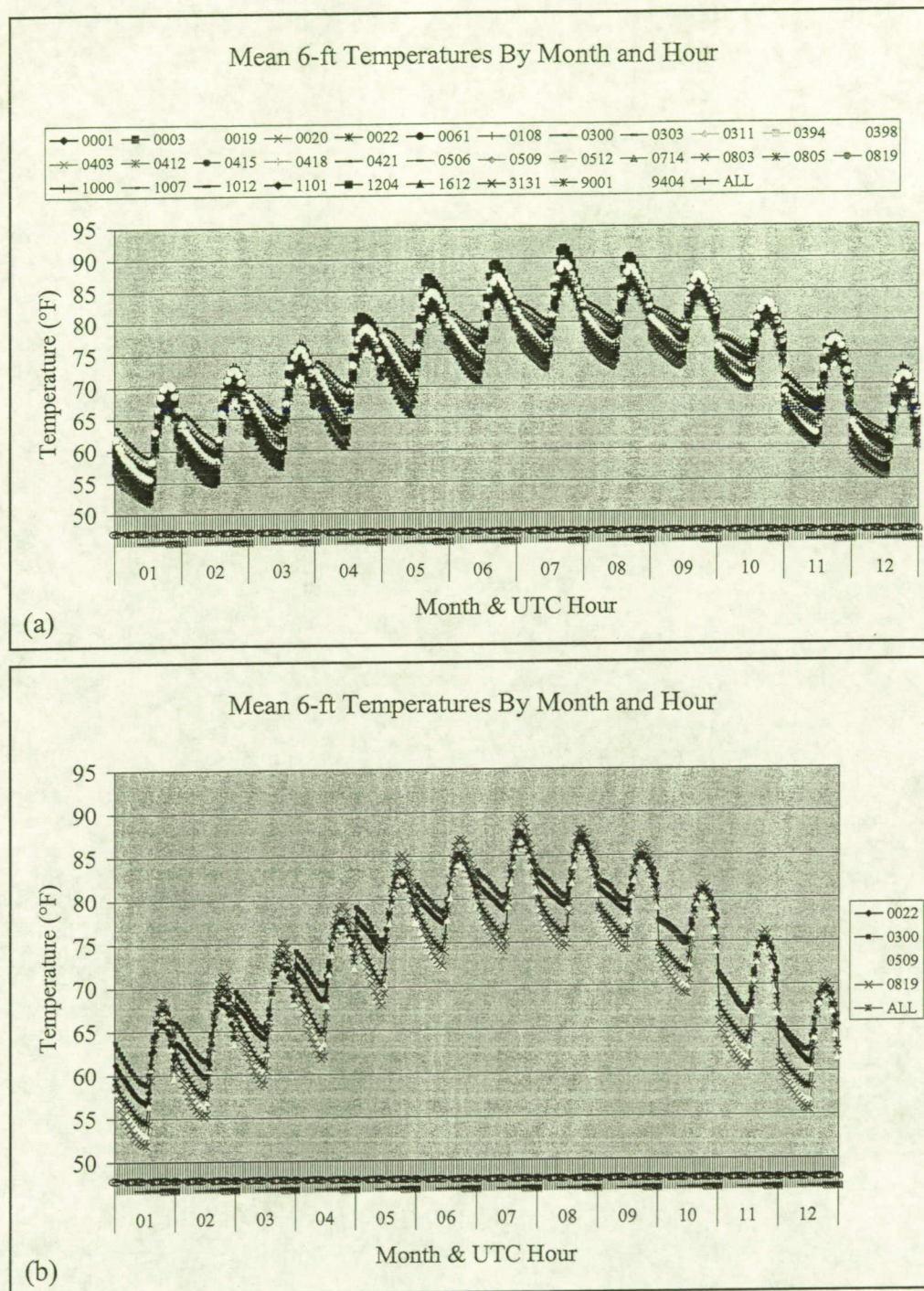


Figure 4.4. The diurnal range in mean 6-ft temperatures during all months of the year for (a) all tower locations, and (b) coastal tower 0022, causeway tower 0300, Merritt Island tower 0509, and mainland tower 0819, and all towers averaged together (ALL). The x-axis contains 24 hours embedded within each month of the year.

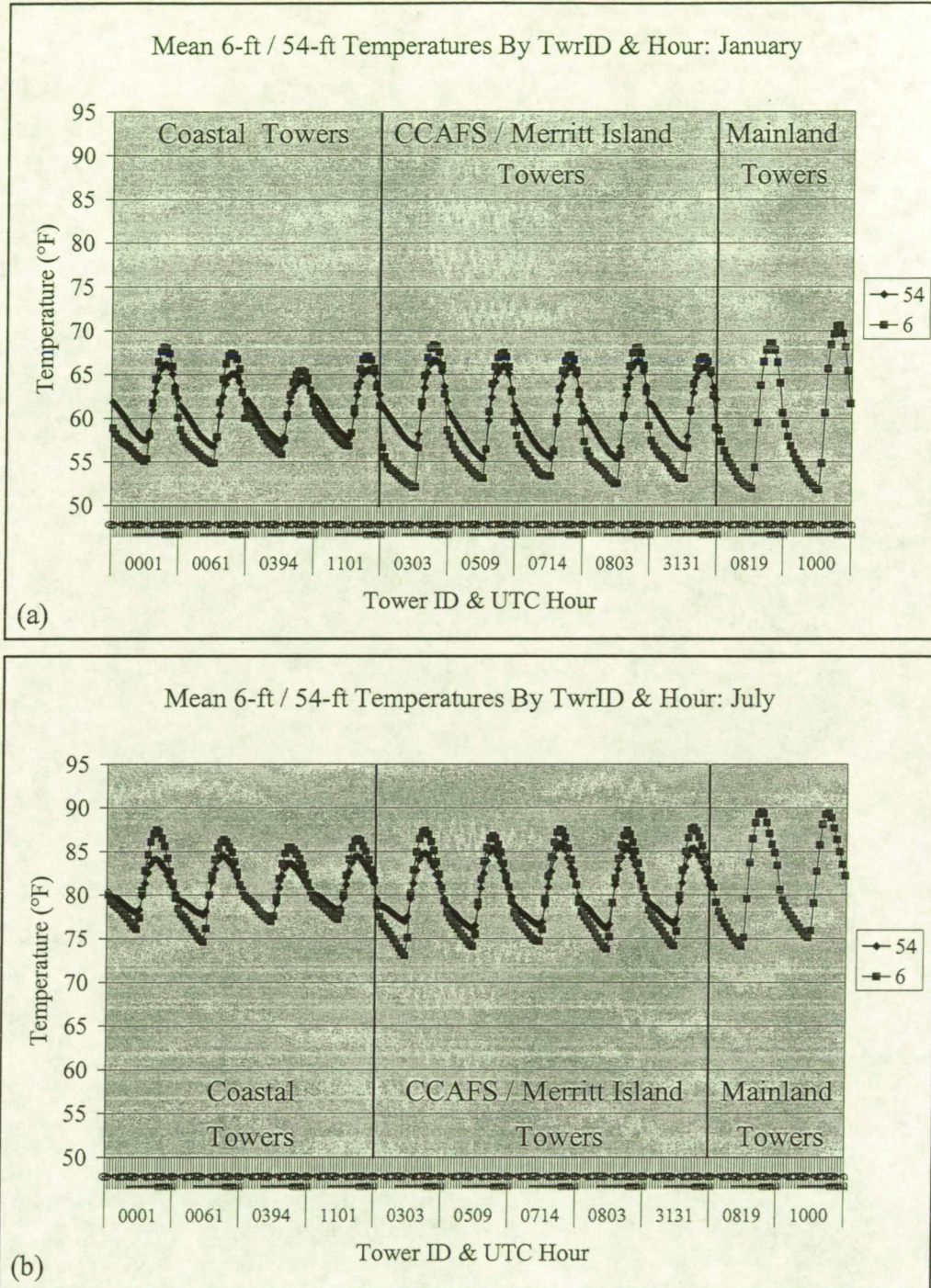


Figure 4.5. The hourly mean 6-ft and 54-ft temperatures at selected coastal/causeway, Merritt Island, and mainland Florida towers during (a) January, and (b) July.

The difference between the 54 and 6 ft temperatures (i.e. near-surface stability) shows some interesting variation throughout the year. From March to September, the mean near-surface stability tends to increase steadily during the night until sunrise, thereafter decreasing abruptly with the onset of solar heating (Figure 4.6a). From November to January, a different pattern appears in the nocturnal mean near-surface stability. The stability values peak at about 0300 UTC and then gradually decrease during the remainder of the night. The shift in the nocturnal stability pattern occurs at nearly all towers within the network. October and February appear to be transition months between these distinctly different behaviors. This climatological behavior in near-surface stability could be used as first-order guidance by the 45th Space Wing Range Safety. These data could help Range Safety assess the times of the day and year when stability poses the greatest risk for a potentially hazardous plume or shock wave adversely affecting populated areas during launch operations at CCAFS.

The 1-hour changes in mean temperature at tower 0303 (Figure 4.6b) show that the maximum increase in mean temperatures after sunrise is nearly uniform throughout the year at $4\text{--}6^{\circ}\text{F h}^{-1}$ at 6 ft, and $2\text{--}3^{\circ}\text{F h}^{-1}$ at 54 ft. However, the initial 6-ft temperature decrease after sunset exhibits a distinct trend from a maximum of $\sim -1.5^{\circ}\text{F h}^{-1}$ in July and August to a minimum of -3.5 to $-4.0^{\circ}\text{F h}^{-1}$ from November to February. Coincident with the larger temperature decrease after sunset during the winter months is a corresponding rapid increase in the temperature change immediately after the minimum, especially at 6 ft. This characteristic of the low-level temperatures in Figure 4.6b leads to the observed patterns of near-surface stability in Figure 4.6a.

The physical explanation for the different near-surface stability behaviors between the winter months and rest of the year can be found in the mean wind speed plot at tower 0303 (Figure 4.7). During the months when stability increased steadily throughout the night, the mean wind speeds at tower 0303 tended to decrease steadily during the same hours. However, during the winter months, wind speeds initially drop rapidly with sunset, but then level off for the remainder of the night instead of continuing to decrease. Similar nocturnal mean wind speed trends occurred at most other towers in the network as well (see Figure 4.14a). Therefore, the stability peak near 0300 UTC during the winter months is probably mechanical in nature, since the initial sharp decrease in wind speeds at sunset led to a rapid decrease in 1.8 m temperatures. The mean stability then levels off or slightly decreases during the remainder of the night because of the nearly constant wind speed that prevailed due to a higher frequency of synoptic-scale weather features in the Florida cool season.

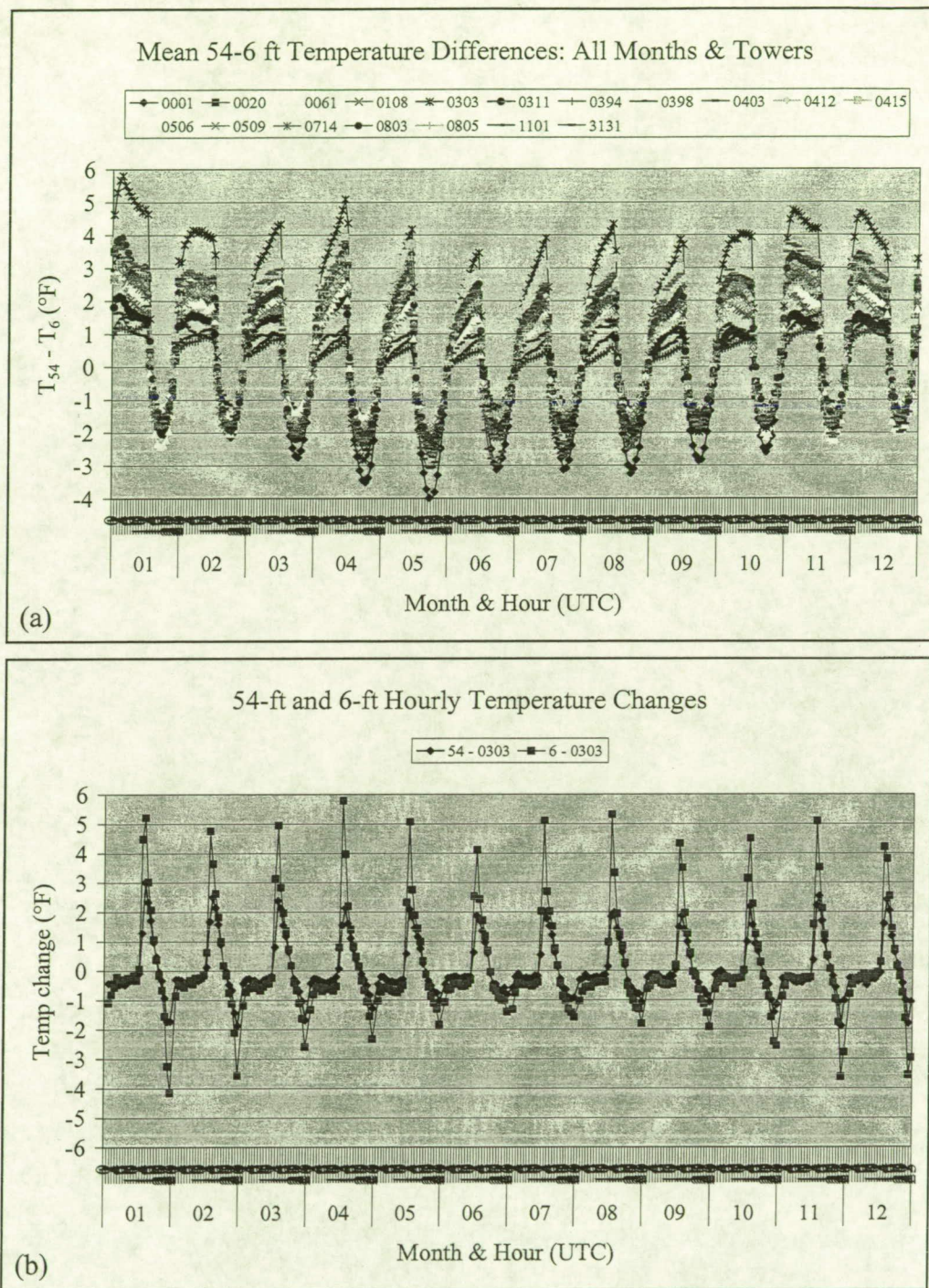


Figure 4.6. (a) The diurnal range in the mean 54-ft minus 6-ft temperatures at all towers and for all months of the year. (b) The 1-hour changes in the mean temperature at tower 0303 for all months of the year.

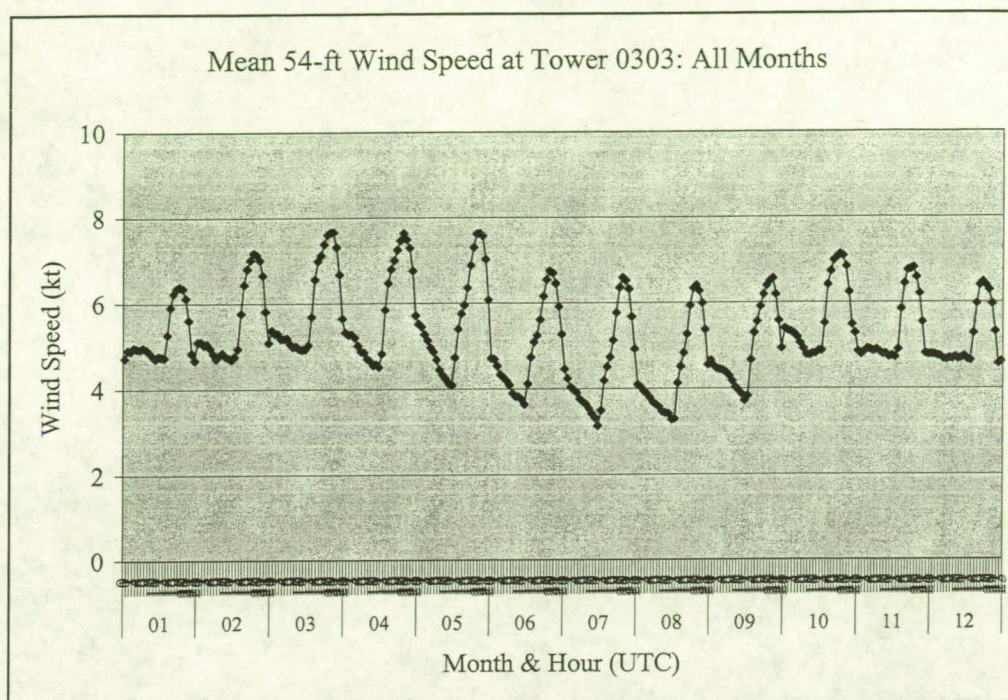


Figure 4.7. Hourly mean wind speeds at tower 0303 for all months of the year.

4.4.2 Variations by wind direction

The mean temperatures across the tower network had much more variability with wind direction during the cool-season months than during the warm season. From November to February, the mean temperatures for the northwest and north bins (315° and 360° in Figure 4.8a, or 271° – 360° wind directions) were 10 – 15°F or more cooler than the southeast and south bins (135° and 180°), which tended to be the warmest during these months. The 271° – 315° wind directions were the coolest of all, with a minimum mean temperature of 47°F in January. Any wind direction with a southerly component had the highest mean temperatures, with the southeasterly winds having the highest mean nocturnal temperatures in most cool-season months.

Unlike the cool season, the warm season months exhibited much less variation in the mean 6-ft temperatures as a function of wind direction. The mean temperatures for most wind direction bins were within 5°F of one another, particularly from July to September (Figure 4.8b). May had the largest range of mean temperatures versus wind direction during the day, and October had the largest range at night; however, October tends to be a transition month between the warm/wet and cool/dry season.

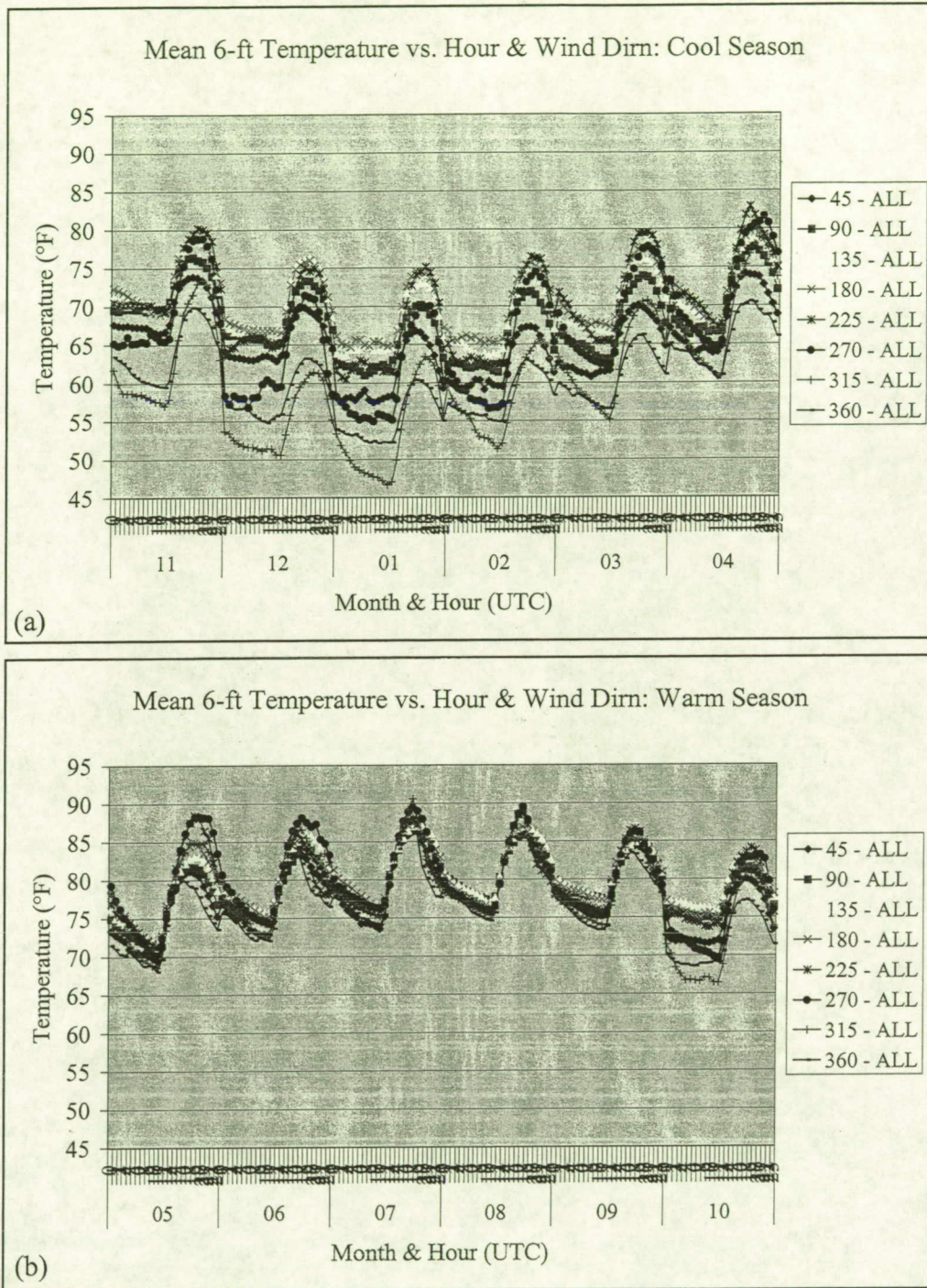


Figure 4.8. The hourly mean 6-ft temperatures versus wind direction bin, averaged over all towers in the KSC/CCAFS network, valid for (a) the cool-season months (November-April), and (b) the warm-season months (May-October).

4.4.3 Notable temperature biases

Most temperature biases in the tower network resulted from the geographical variability of KSC/CCAFS and a station's proximity to a water body. As much as 10°F or more variation occurred in the 6-ft temperatures on average in nearly every month of the year. Given the magnitude of the biases simply caused by the geography of KSC/CCAFS, any instrumentation or exposure biases could not be readily quantified at most towers.

4.4.3.1 Geographical variations and exposure biases

A 7–10°F variation in the mean 6-ft temperature was found in the KSC/CCAFS network throughout the year (Figure 4.9). The towers along the immediate Atlantic coast and in the vicinity of causeways were the warmest at night while towers in the middle of Merritt Island and over mainland Florida were the coolest at night. Nearly the opposite distribution occurred during the daytime hours.

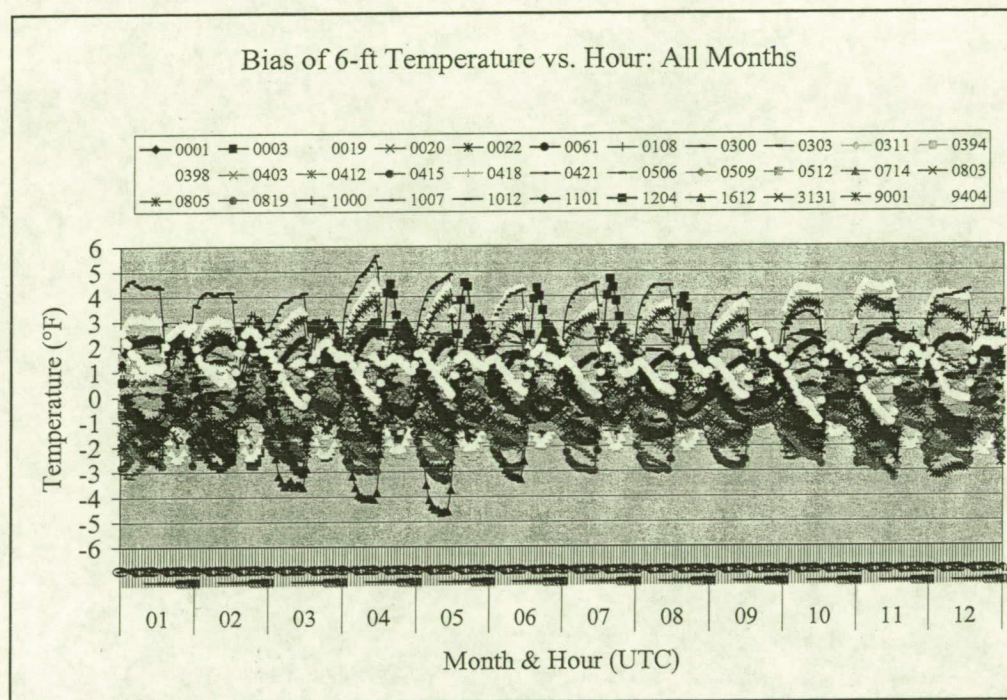


Figure 4.9. Diurnal distribution of 6-ft temperature biases at all towers in the KSC/CCAFS network and for all months of the year.

Much more variation occurred in the biases at 6 ft compared to the biases at 54 ft. At 6 ft during both January and July, nocturnal biases ranged from -3°F to 4.5°F, with tower 0300 having the largest positive bias during both months (Figure 4.10). Also in both months, towers 0394 (SLC 39A) and 0398 (SLC 39B) tended to have the most negative daytime biases, while the mainland towers generally had the most positive biases at 6 ft. At 54 ft, the biases only ranged from -1.5°F to 1.5°F during both January and July.

A notable difference between the January and July plots is the much larger positive 6-ft temperature bias between 1200–1800 UTC at tower 1204 during July. A nearly 5°F positive bias is found at tower 1204, peaking at about 1500 UTC (late morning hours). This positive bias at tower 1204 occurred most noticeably from April to August and appears to be related to sun angle and position. A photograph of the sun position relative to the 6-ft temperature sensor in late May during the late morning hours (Figure 2.12b) confirms the sun exposure during this time of year. The solar radiation exposure combined with the excessive vegetation (Figure 2.12a) that reduces natural aspiration led to this high temperature bias.

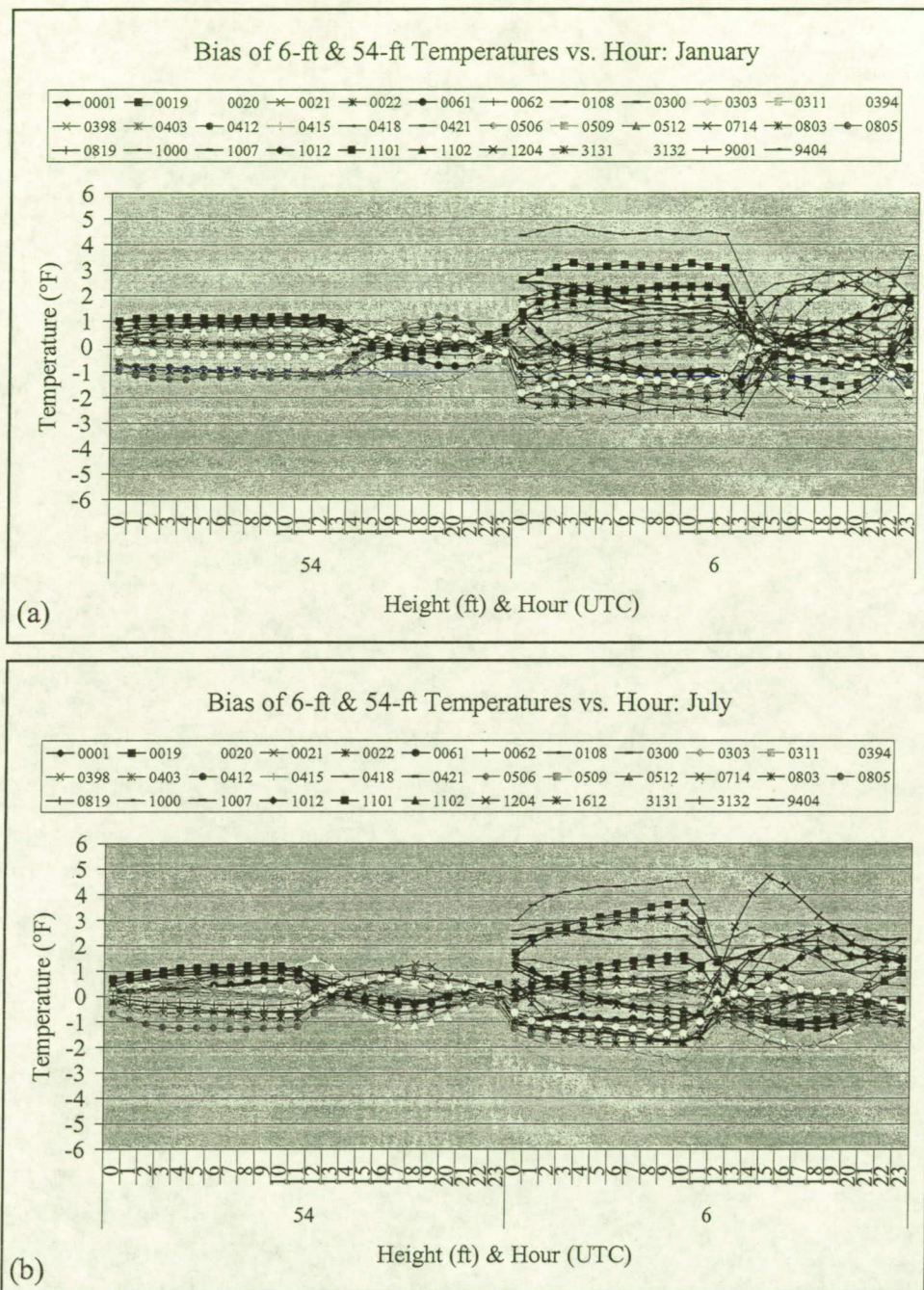


Figure 4.10. Diurnal distribution of the 54-ft and 6-ft temperature biases at all towers in the climatology during the months of (a) January, and (b) July.

The resulting biases in the 54-ft minus 6-ft temperatures (near-surface stability) are given in Figure 4.11. Tower 0303 in the middle of CCAFS had the largest nocturnal positive bias in near-surface stability during both January and July while towers 0394, 0398, and 1101 had the most negative nocturnal bias in stability for both months. During the daytime, tower 0061 had the most negative bias (most unstable) in January while tower 0001 was most unstable in July. Tower 0805 exhibited the most stable bias during the day in January whereas no towers stood out with a distinctive positive bias in July. Based on these results, the interior portions of CCAFS and Merritt Island are the most stable at night while CCAFS tends to be the most unstable during the day, particularly in July.

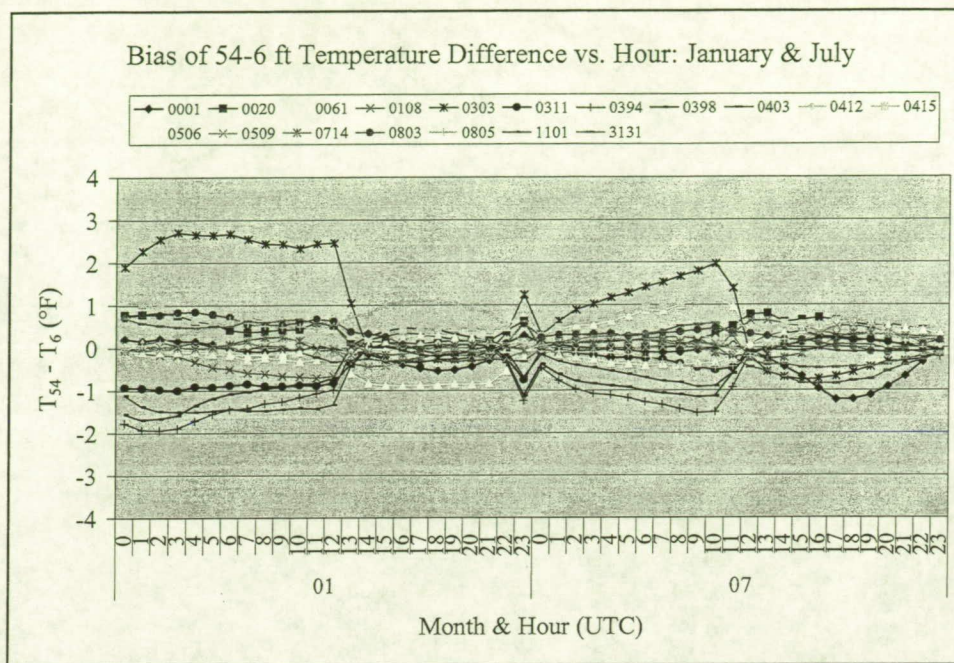


Figure 4.11. Bias of the differences in the 54-ft and 6-ft temperatures during the months of January and July.

4.4.3.2 Biases under specific wind directions

The coastal/causeway and mainland towers generally exhibited a distinct diurnal signal in the 6-ft temperature bias from nearly all wind directions, but with opposite signs. At coastal tower 0394 (SLC 39A) and causeway tower 0300 during the cool season (Figure 4.12a and b), most wind directions resulted in positive biases at night and negative biases during the day, particularly at 0300, which is nearly surrounded by water in all directions. Tower 0394 experienced the largest nocturnal positive bias with the 360° wind direction bin (316°–360° winds), since these directions result in immediate onshore flow only at 0394 and a few other towers along the coast of KSC/CCAFS.

Tower 0506 over central Merritt Island did not exhibit any noticeable trend in temperature biases by wind direction (Figure 4.12c). Overall, tower 0509 had a slight cool bias between 0° and -2°F, but this bias was found at nearly all hours and months during the cool season. Winds with an easterly component tended to yield the most substantial cool biases at night. Meanwhile at tower 1612 over mainland Florida (Figure 4.12d), a distinct diurnal trend is evident in all months, but of the opposite sense of towers 0394 and 0300. Nearly all wind directions had a negative bias at night and a positive bias during the day, with magnitudes reaching ±4 to 6°F.

Two other towers with interesting bias stratifications are towers 0403 on the western edge of CCAFS, and causeway tower 1007 on the western edge of the Indian River. Tower 0403 has water just to its west, resulting in a 2–4°F nocturnal positive bias in 6-ft temperatures with winds from 226°–315° directions (Figure 4.12e). Under easterly flow, tower 0403 generally had about a -2°F bias at night, and near zero bias during the day, due to the relatively large area of land to its east. Finally at tower 1007, winds from any easterly direction yielded the largest nocturnal warm biases of 2–6°F (particularly north-northeast winds), while the bias was slightly negative or neutral with westerly wind components (Figure 4.12f).

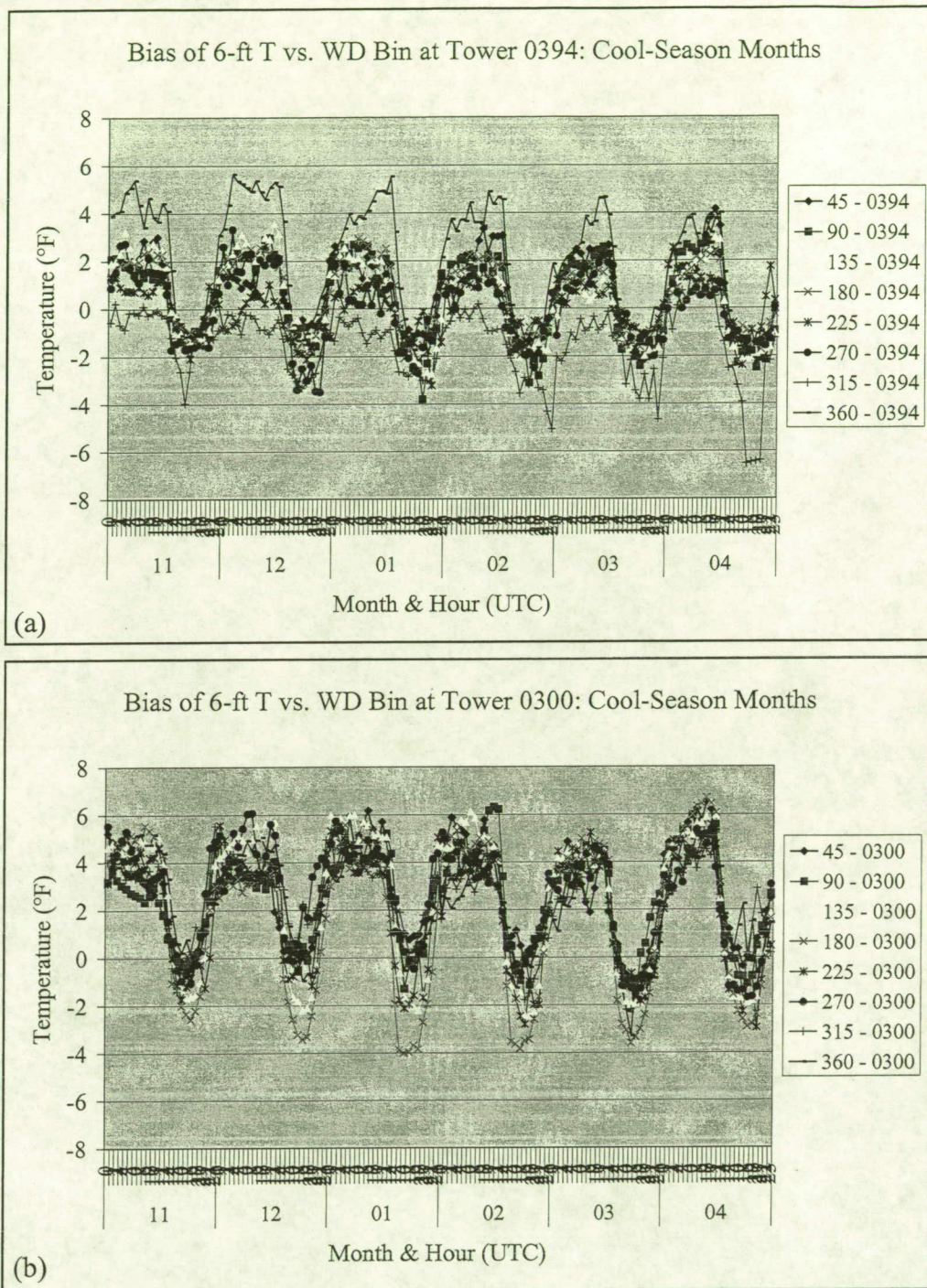


Figure 4.12. The hourly mean 6-ft temperature biases during the Florida cool season months of November through April at (a) coastal tower 0394 (SLC 39A), (b) causeway tower 0300, (c) Merritt Island tower 0509, (d) mainland tower 1612, (e) CCAFS tower 0403 adjacent to the Banana River, and (f) causeway tower 1007 adjacent to the Indian River.

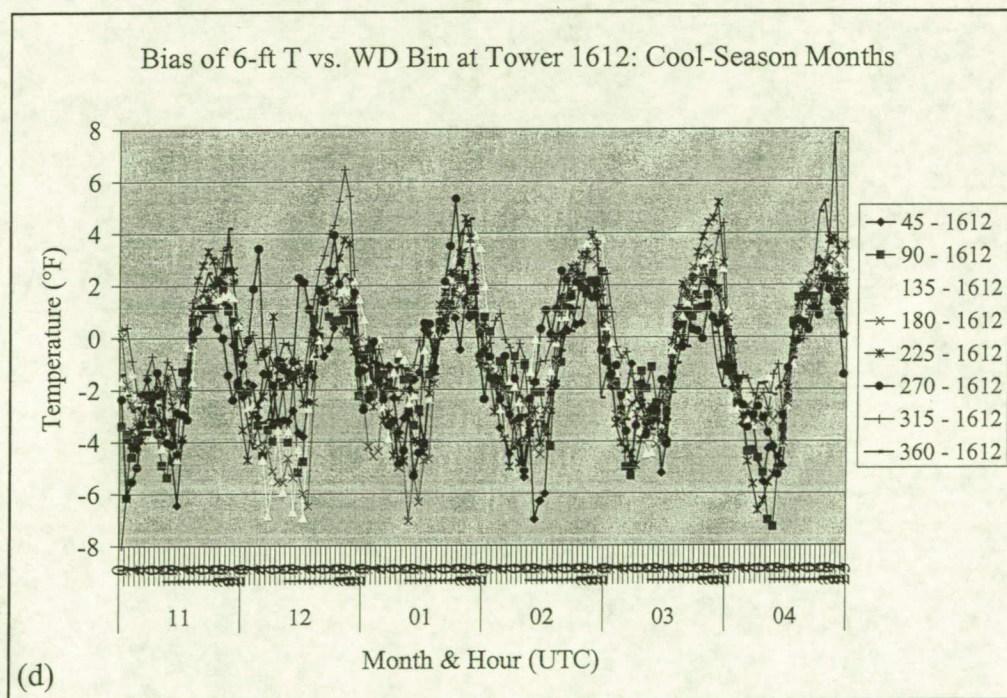
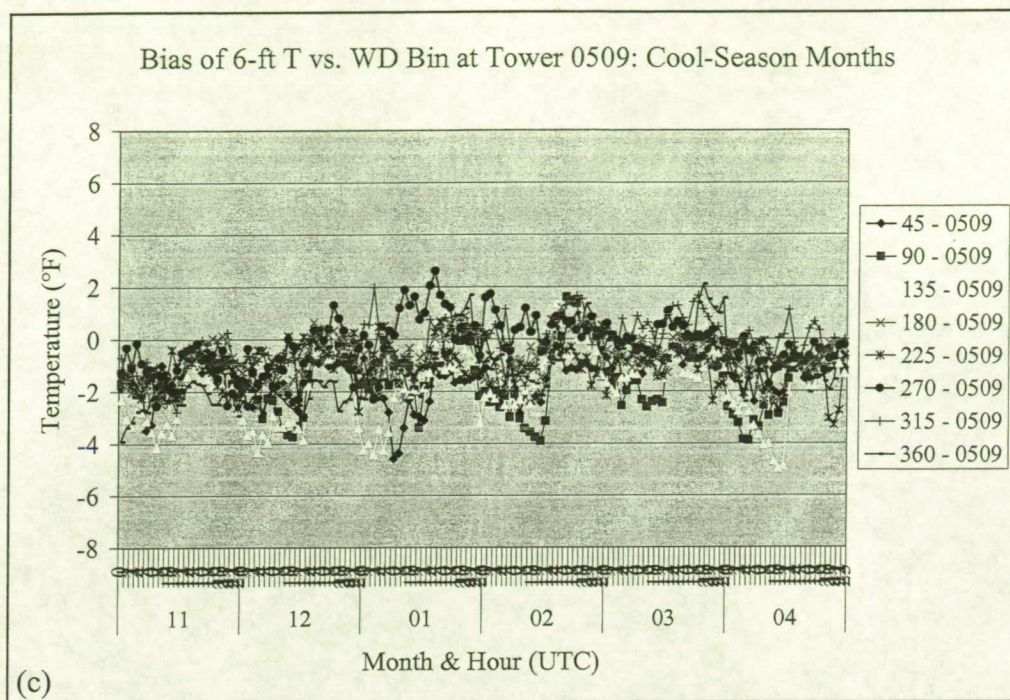


Figure 4.12, cont.

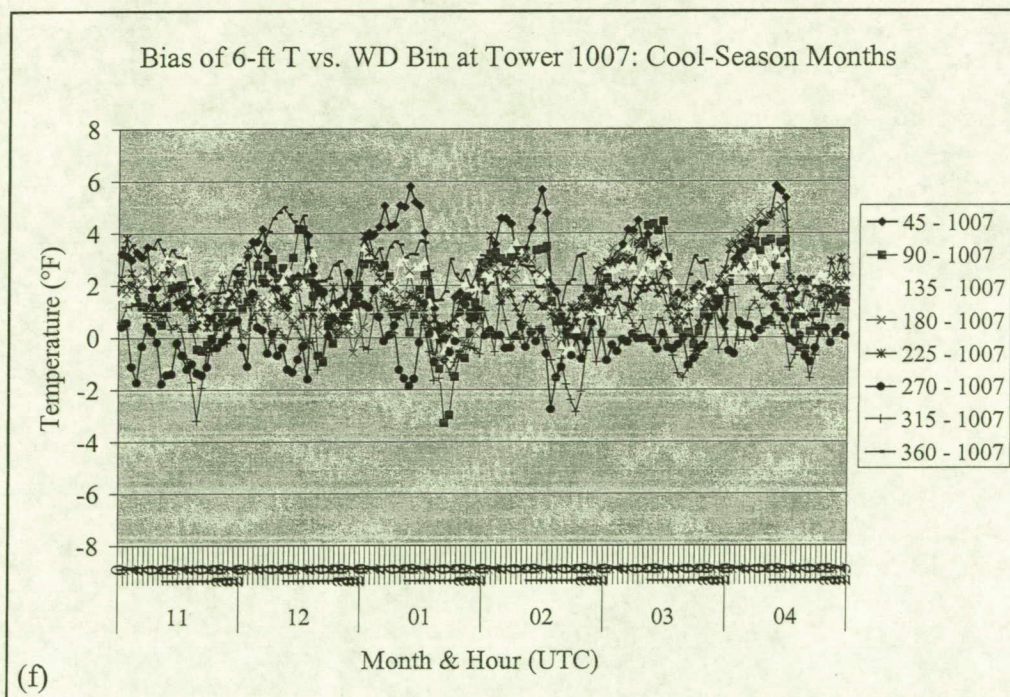
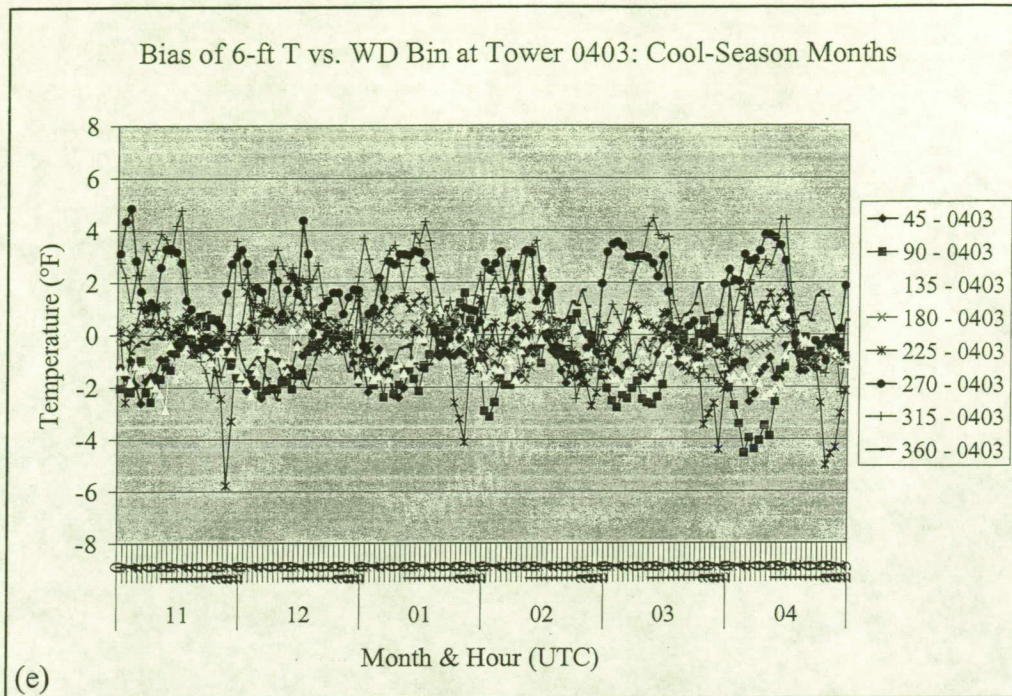


Figure 4.12, cont.

Among the launch critical towers with sensors at opposite sides, only tower 0006 exhibited some noticeable differences between the temperatures at opposite sides of the tower, mainly for certain wind directions during the cool season. For wind directions between from 180° – 315° , the southeast sensor tended to be slightly cooler by about 0.5° to 1.0°F . However, for winds coming from 316° – 360° , the upwind sensor (0061 on the northwest side of the tower) was as much as 2°F colder on average than the downwind sensor 0062. This feature could have been caused by the fact that north-northwest winds in the cool season are typically associated with cold advection patterns following cold-frontal passages. The tower could have generated sufficient heat to causes the downwind temperature sensor to read slightly warmer. In these instances, the upwind (northwest) sensor would be the most representative of the actual temperature. The warm-season months did not exhibit any such disparity between the opposite sensors, nor did any other launch critical tower behave in this manner.

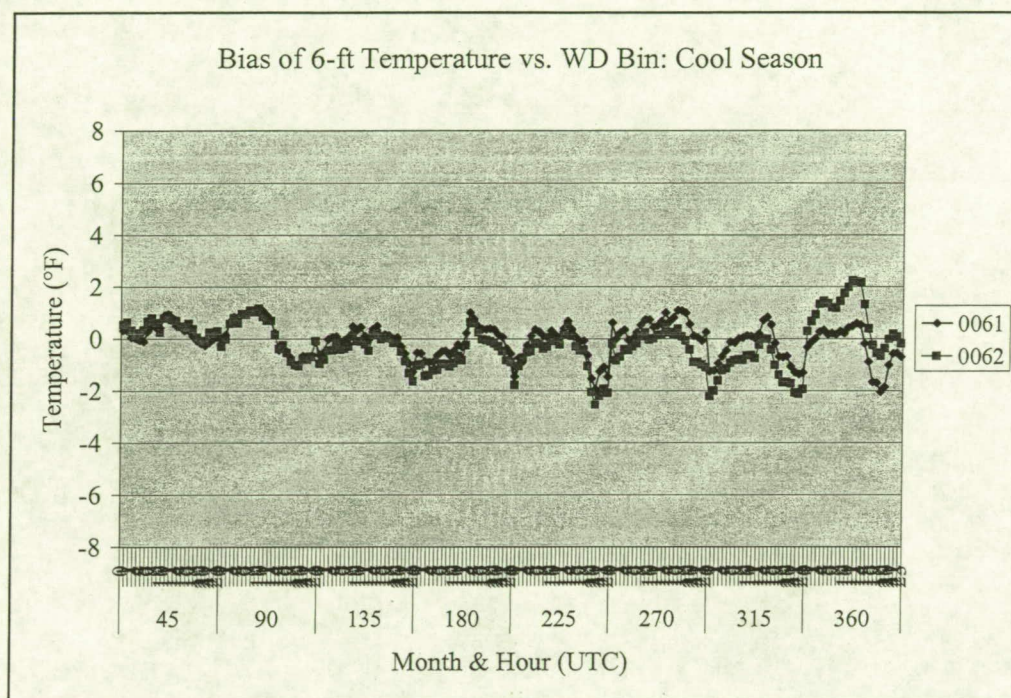


Figure 4.13. Bias of 6-ft temperature at the northwest (0061) and southeast (0062) sensors of tower 0006.

4.5 Wind Speeds

4.5.1 Monthly and diurnal variations

The mean wind speeds across the tower network exhibited a large amount of variation between the coastal and mainland towers. Coastal towers were generally more windy during all hours of the day throughout the year. The strongest mean wind speeds each month almost always occurred during the daytime hours, due to increased mechanical mixing from the surface heating.

During the cool-season months (November to April) mean speeds generally ranged from 3–10 kt at night and 6–13 kt during the day (Figure 4.14a). In the warm season (May to October), mean speeds ranged from 2–8 kt at night and 6–12 kt during the day. During the primarily synoptic-driven months of November to March, mean nocturnal speeds stayed nearly constant whereas mean speeds steadily declined throughout the night from April to September. October appears to be a hybrid month between the two nocturnal wind regimes. The months with the highest mean hourly wind speeds were February to May, and October (Figure 4.14a).

Figure 4.14b illustrates the contrast between the winds speeds at Atlantic coastal and mainland towers. The coastal tower 0022 and causeway tower 0300 generally have very similar diurnal speed distributions except for

October through January. Nighttime wind speeds were much higher at coastal tower 0022 compared to the causeway tower, particularly in October, when east and northeasterly winds tended to occur more frequently than other directions (Figure 4.2). The predominance of northeasterly wind directions led to stronger winds along the immediate coast compared to the causeway tower, because of the frictional effects as winds cross CCAFS upstream of tower 0300.

During the winter months, the time of the maximum mean wind speed corresponds well with the time of maximum heating. In the spring and summer months when daily sea breezes predominate, the time of maximum wind speeds are delayed by a few hours after peak heating. These relationships are illustrated in Figure 4.15, which shows an overlay of the hourly mean temperature differences between the near-shore buoy 41009 (20 nm east of Cape Canaveral) and the overall tower network average of 6-ft temperature ($T_b - T_n$), and the mean wind speed normalized by the monthly mean value (all-mean). This normalization is done by simply subtracting each month's overall mean speed from the individual hourly mean wind speed, in order to have similar scales along the y-axis for easier comparison. Since the mean air temperature at the buoy varies only a couple degrees on a diurnal basis, most of the variation in $T_b - T_n$ results from the diurnal heating cycle in the tower network. Minimum $T_b - T_n$ corresponds to the time of maximum heating within the tower network.

From November to January, when sea breezes seldom occur, the time of maximum heating and peak wind speed are nearly coincident (Figure 4.15a). Also, the wind speed and land-ocean temperature differential curves are symmetrically opposite in appearance, suggesting that wind speeds increase in proportion to the daytime heating across the tower network. During the spring and summer months, a 3–4 hour separation occurs between the time of maximum heating (given by the solid line in Figure 4.15b) and the time of maximum mean wind speed (given by dashed lines). These relationships suggest that synoptic gradients and vertical mixing through surface heating and destabilization drive the strength of winds during the winter months. Meanwhile, the delay in peak wind speeds during the spring and summer is consistent with the high frequency of sea breezes, caused by the temperature contrasts between the air over land and water. The sea breeze circulation strength actually peaks after the time of maximum contrast between the land-water temperatures. Convective outflows may play an additional minor role in the magnitude of the maximum mean wind speeds during the late afternoon hours in the summer months.

The standard deviations of the wind speed indicate that larger variations in the wind speed occur at the coastal sites where mean wind speeds are higher (Figure 4.16). October had the largest standard deviations at coastal tower 0022, approaching 6 kt. Relatively high standard deviations continued throughout the winter months. The standard deviations decreased steadily after March, reaching a minimum in July. These standard deviations appear to be directly proportional to the strength of the mean wind speed.

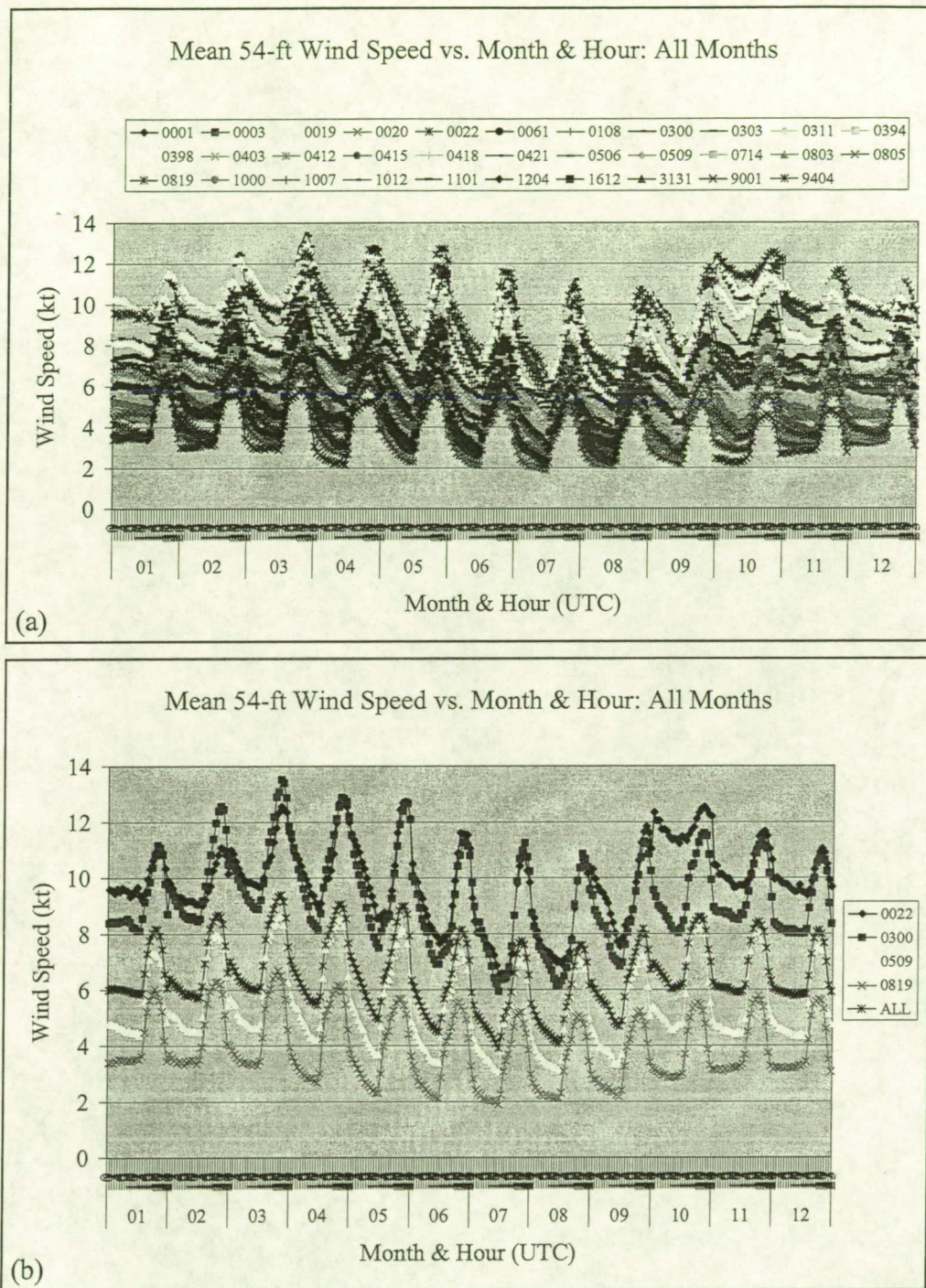


Figure 4.14. Hourly mean wind speeds for all months of the year at (a) all towers, and (b) towers 0022, 0300, 0509, 0819, and all towers averaged together (ALL).

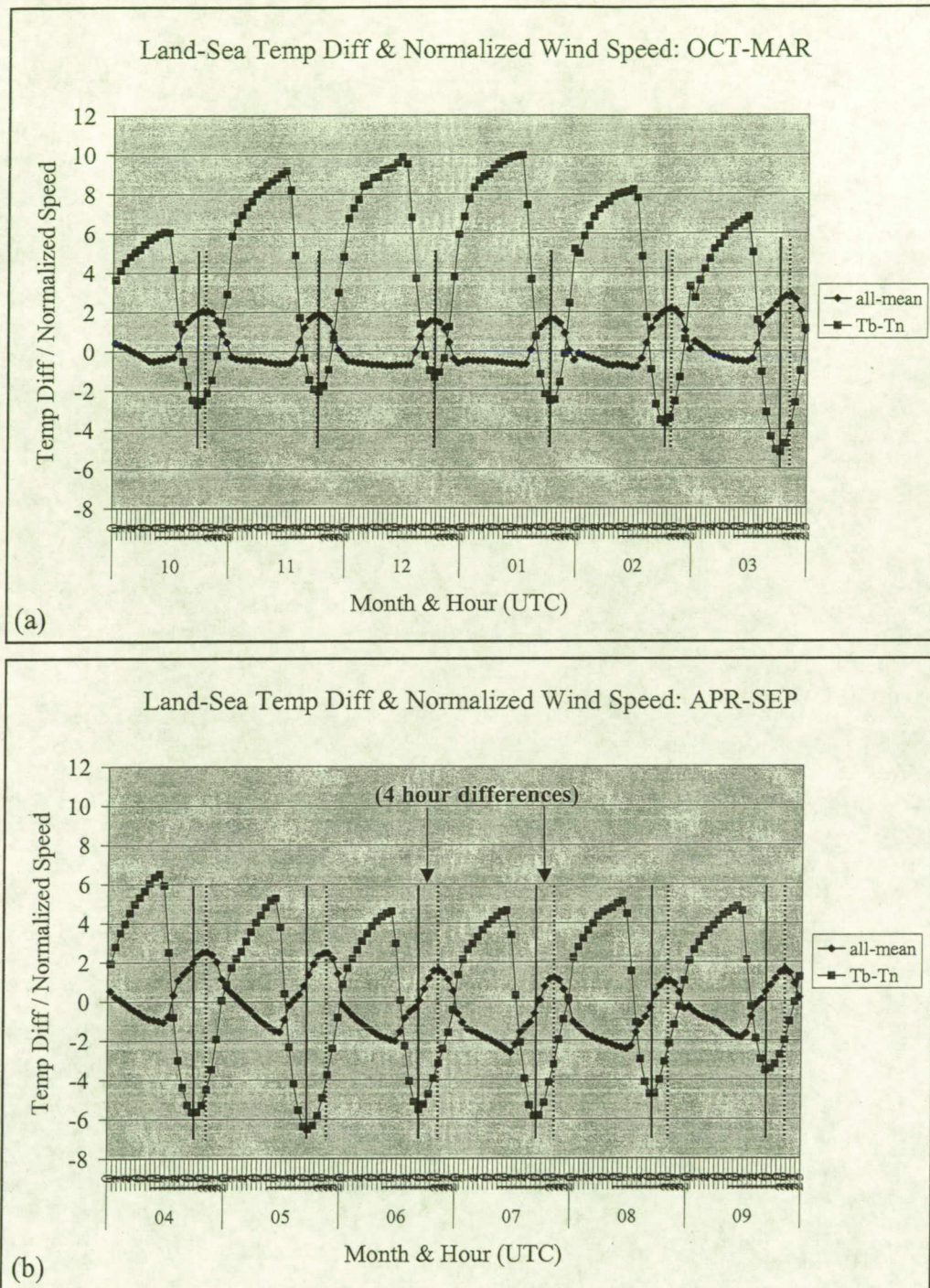


Figure 4.15. Plot of the hourly differences between the buoy 41009 (20 nm east of Cape Canaveral) and tower network mean 6-ft temperatures ($T_b - T_n$), and the hourly mean wind speed normalized by the monthly mean wind speed (all-mean), valid for the months of (a) October to March, and (b) April to September. Solid lines represent the time of minimum $T_b - T_n$ and dashed lines represent the time of the maximum mean wind speed.

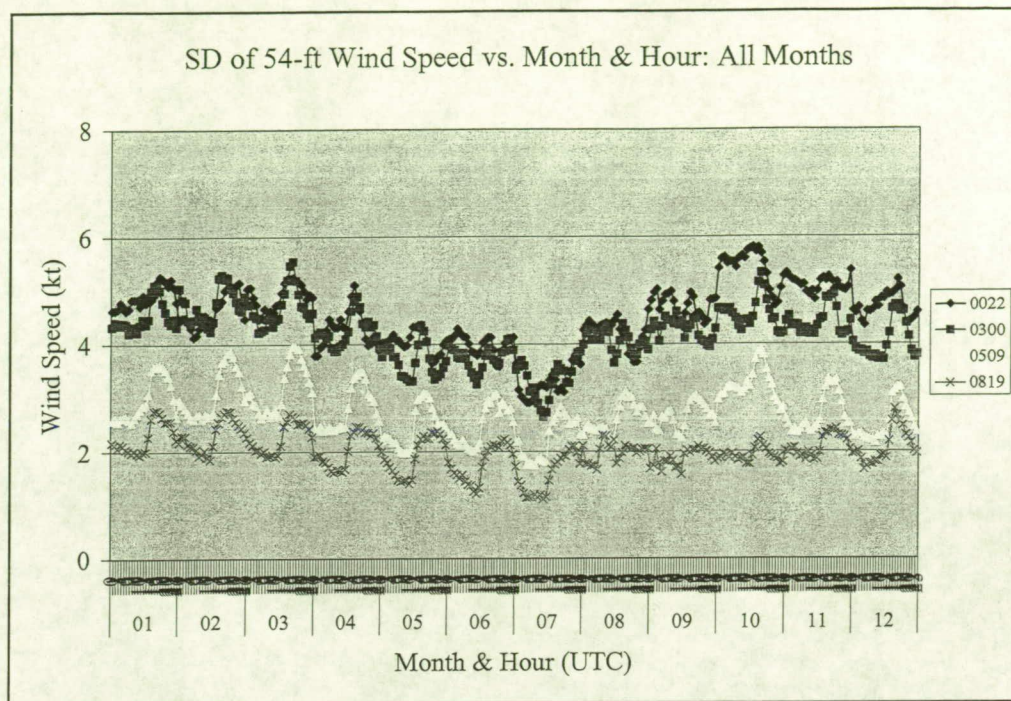


Figure 4.16. The hourly standard deviations of the 54-ft wind speeds during all months of the year at coastal tower 0022, causeway tower 0300, Merritt Island tower 0509, and mainland tower 0819.

4.5.2 Variations by wind direction

During the cool-season months, the north-northwest wind directions had the strongest mean wind speeds during the day (bin 360 - ALL in Figure 4.17a). These directions were also strongest in May and October of the warm season (Figure 4.17b). During the night, a less than 2 kt variation generally occurred among the mean wind speeds from different directions during most cool-season months. However, a much larger amount of spread in the nocturnal wind speeds occurred in November and during most warm-season months. East-northeast winds tended to be the strongest of all directions during the night from May through November with the exception of July. Offshore wind directions often had the lightest wind speeds at night, especially in the warm-season months (Figure 4.17b).

At coastal tower 0022 and causeway tower 0300 during the cool season, both locations experienced a gradual increase in the overall mean wind speeds from November through March (Figure 4.18). The windiest directions at tower 0022 were east/northeast at night and north/northeast during the day from November to February. The south/southeast direction (136–180° bin) was the strongest of all combinations during the afternoon hours in March, with mean wind speeds greater than 16 kt (Figure 4.18a). Other directions with relatively strong wind speeds during March and April included 270 (226–270°) and 360 (316–360°).

Tower 0300 had a more distinctive diurnal trend among all wind direction bins compared to tower 0022. The highest mean wind speeds occurred exclusively during the day in all cool-season months (Figure 4.18b). The highest mean speeds came from south-southeast and north-northwest directions during March and April, with maximum mean speeds greater than 16 kt from these directions. Towers 0022 and 0300 were the windiest of all towers because of the large amount of water located on all sides of these stations.

The landlocked towers 0509 and 0819 had considerably weaker wind speeds than 0022 and 0300, especially mainland tower 0819 (Figure 4.18c and d). These towers also experienced less variation among wind directions during the cool season, with generally 2–3 kt spread among the mean wind speeds from each wind direction bin. Tower 0509 had the highest mean speeds from the south or southwest directions during most cool-season months except November, when east and north/northwest tended to be strongest (Figure 4.18c). Tower 0819 had the strongest winds from a coast-parallel direction, either north-northwest or south-southeast, but with maximum mean speeds of only around 8 kt (Figure 4.18d).

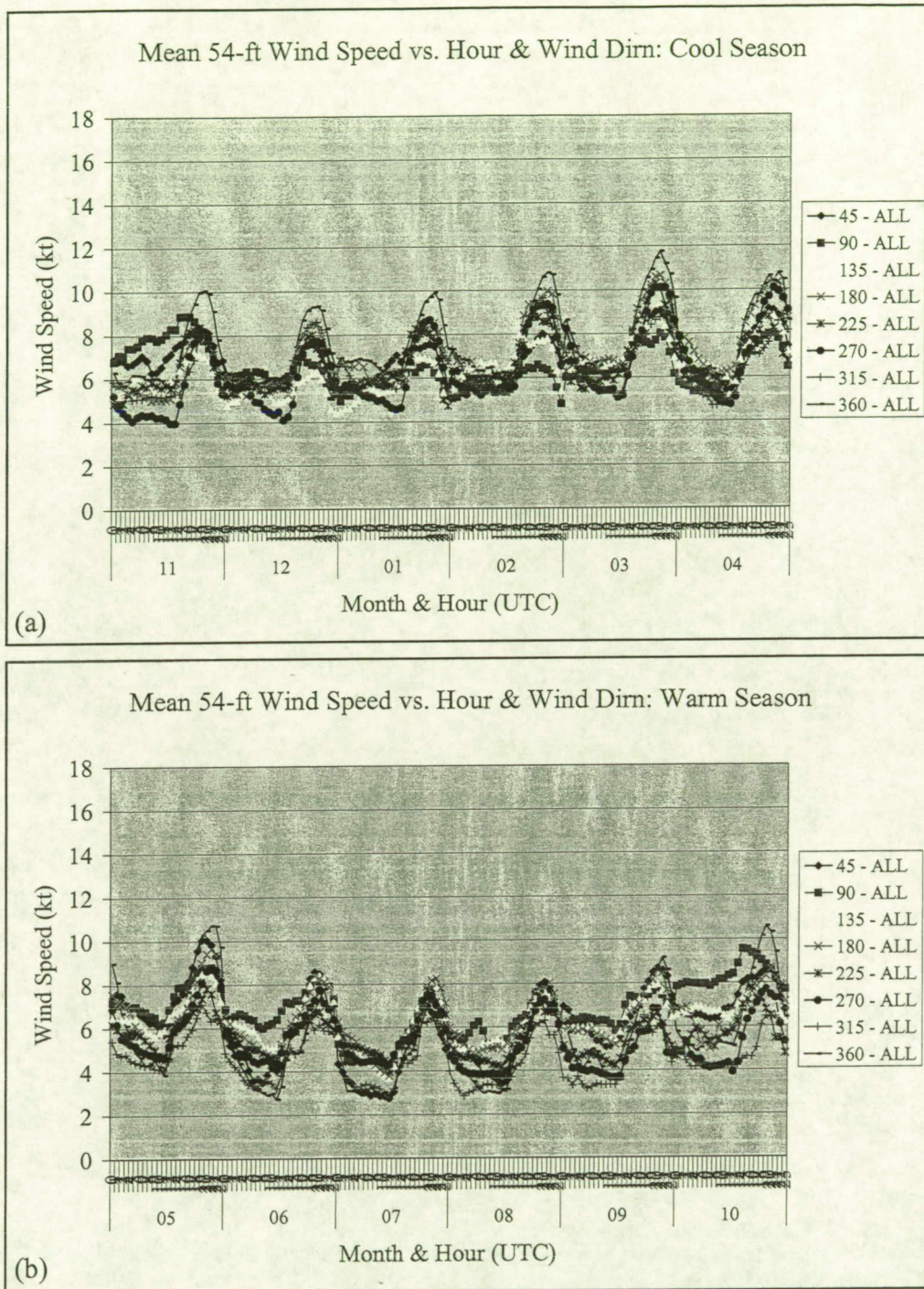


Figure 4.17. Hourly mean wind speeds stratified by wind direction bin for all towers used in the climatology averaged together during (a) the cool-season months, and (b) the warm-season months.

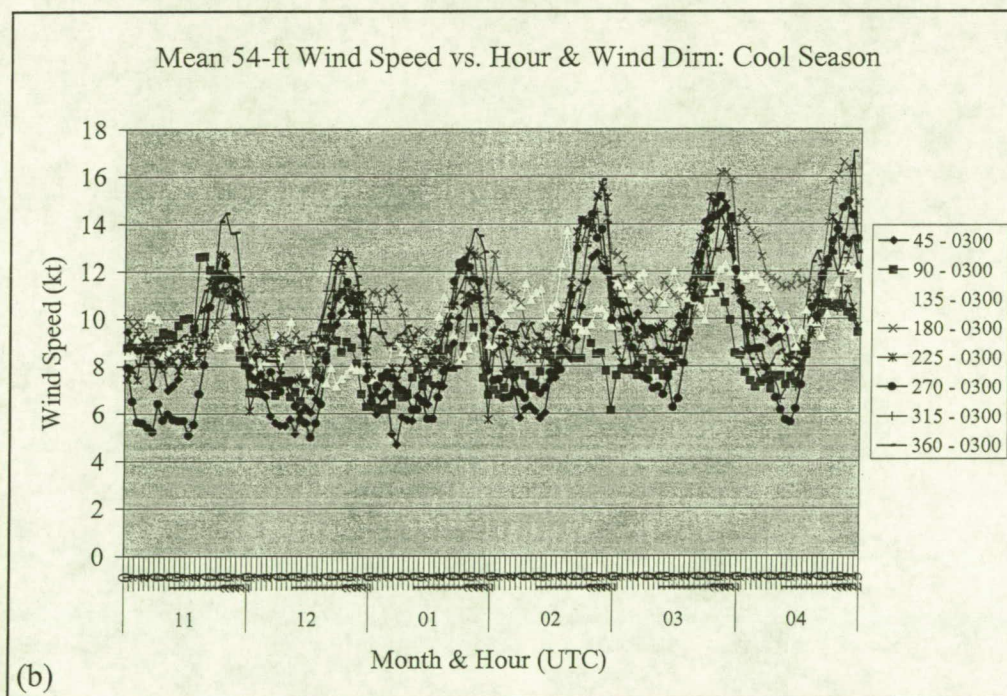
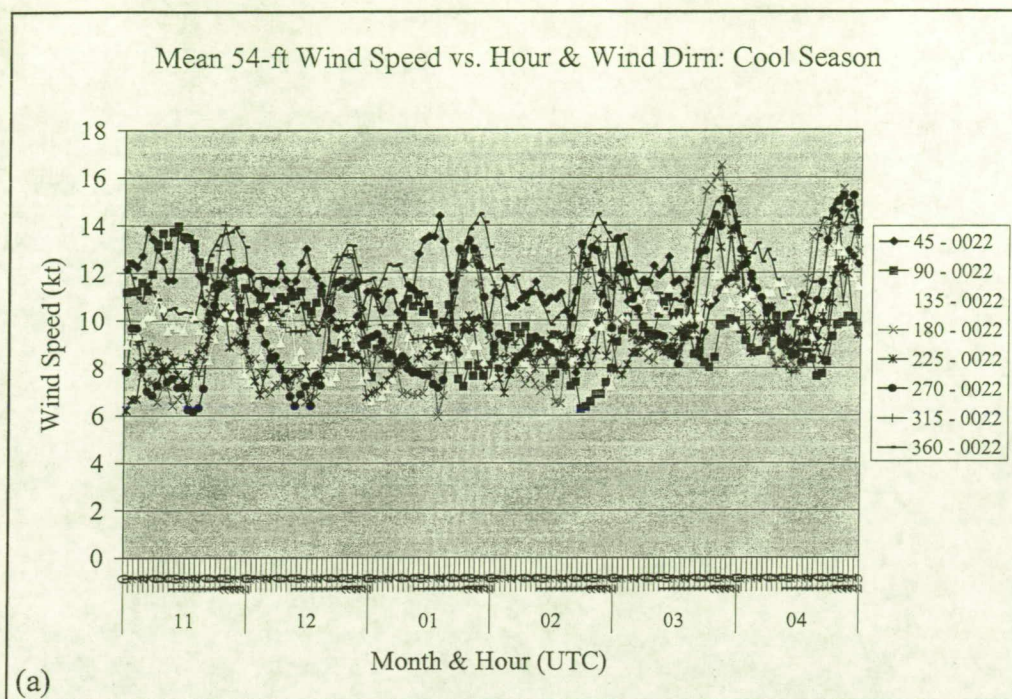


Figure 4.18. Hourly mean wind speeds stratified by wind direction bin during the cool-season months at (a) coastal tower 0022, (b) causeway tower 0300, (c) Merritt Island tower 0509, and (d) mainland tower 0819.

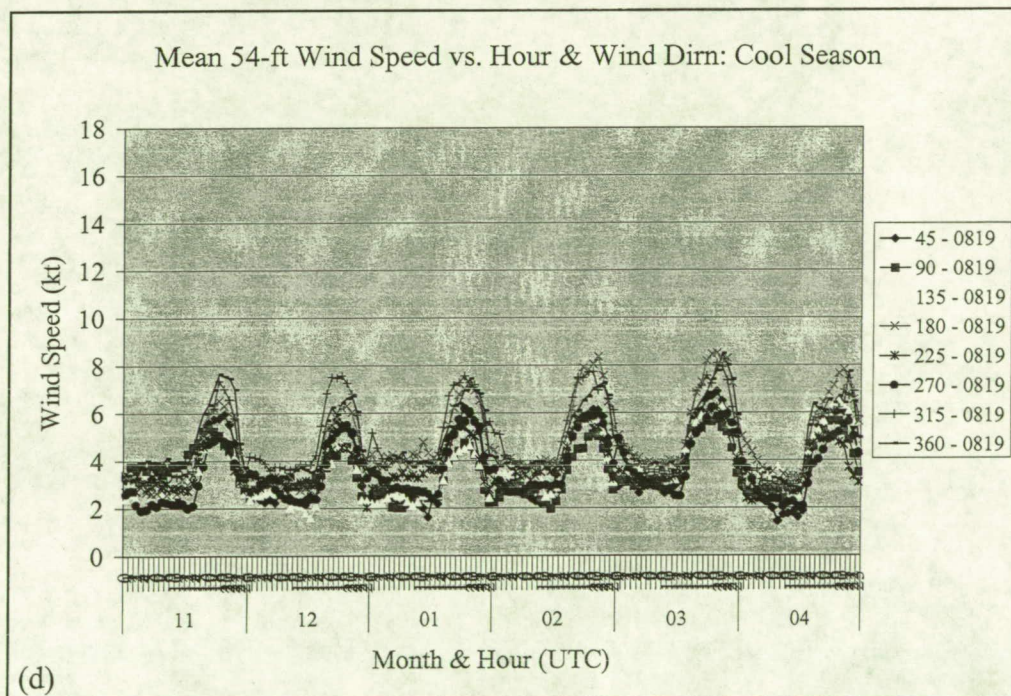
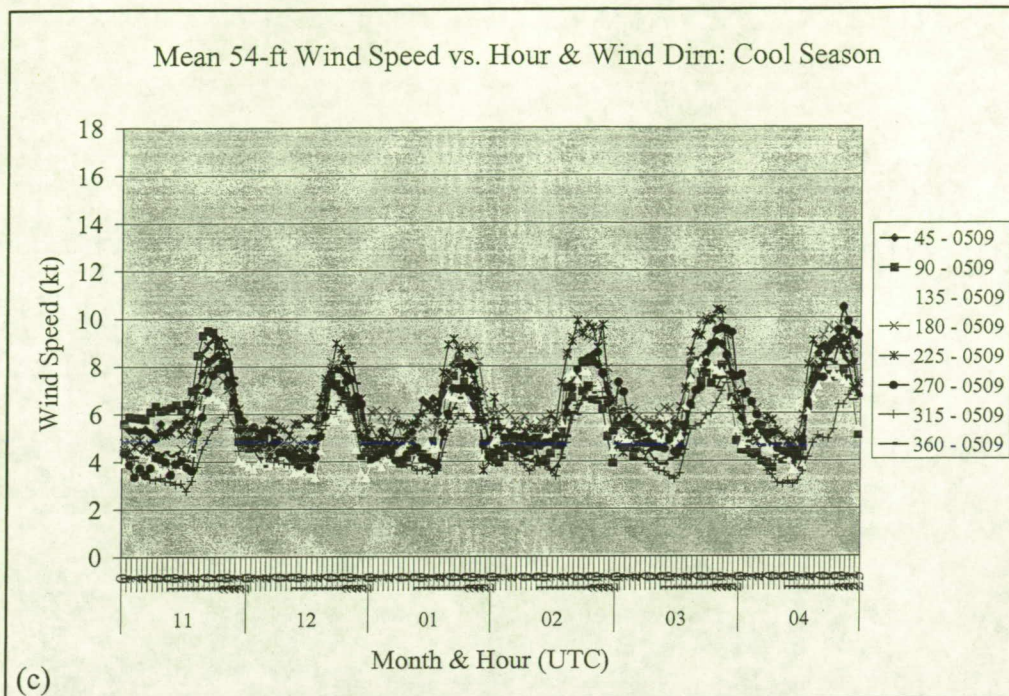


Figure 4.18, cont.

4.5.3 Notable wind speed biases

4.5.3.1 Land-water variations

As described frequently within the climatology results, most wind speed characteristics across KSC/CCAFS are governed by a station's proximity to water bodies. In general, mainland towers had the most negative biases, while coastal and causeway towers had the largest positive biases. Figure 4.19 compares the hourly biases at coastal /

causeway towers 0022 and 0300 to Merritt Island tower 0509 and mainland tower 0819. The coastal/causeway towers consistently had positive biases of 2–4 kt, with biases as large as 5 kt in October. Tower 0819 on the mainland exhibited a low wind speed bias year-round at near -3 kt. Meanwhile, tower 0509 behaved much like other Merritt Island towers (not shown) with near neutral or slight weak wind speed biases. Based on these results, it appears that the frictional effects of the land masses increases steadily from the coast to the mainland Florida.

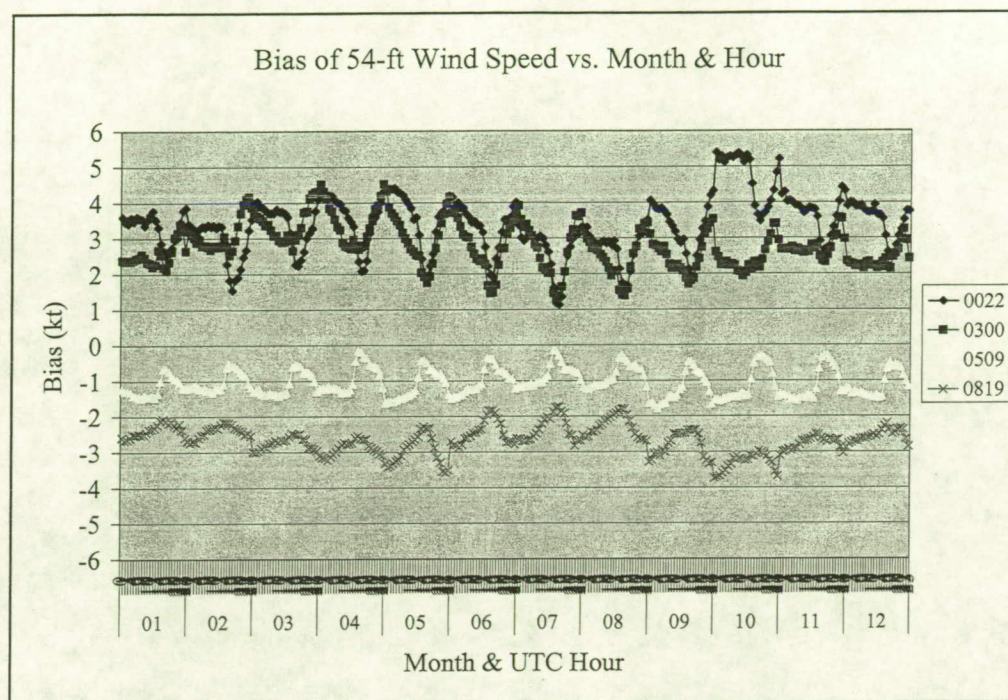


Figure 4.19. Hourly and monthly biases of 54-ft wind speeds at coastal tower 0022, causeway tower 0300, Merritt Island tower 0509, and mainland tower 0819.

4.5.3.2 Biases under specific wind directions

The bias of wind speed under specific wind directions is nearly invariant with the season or time of year, based on the plots of selected towers in Figure 4.20. During both the cool season (Figure 4.20a) and warm season (Figure 4.20b), coastal tower 0022 had the highest positive bias with northeast to east winds, and also for westerly to northwesterly winds. The causeway towers 0300 and 1007 exhibited the largest positive wind speed bias for south-southeast winds (180° bin) during both seasons, as these directions create the largest fetch over water upstream of these towers (see Figure 2.1a).

Conversely at mainland tower 0819, a negative bias between -2 and -4 kt prevailed year-round for all wind directions except for the west/northwest direction (315° bin), which yielded less negative biases. The CCAFS tower 0303 and Merritt Island towers 3131 and 0509 fell between the coastal/causeway and mainland biases. Since the wind speed variations by wind direction across KSC/CCAFS are independent of the time of year, it appears that the geographical features of KSC/CCAFS are the primary drivers for the observed patterns of wind speed variations.

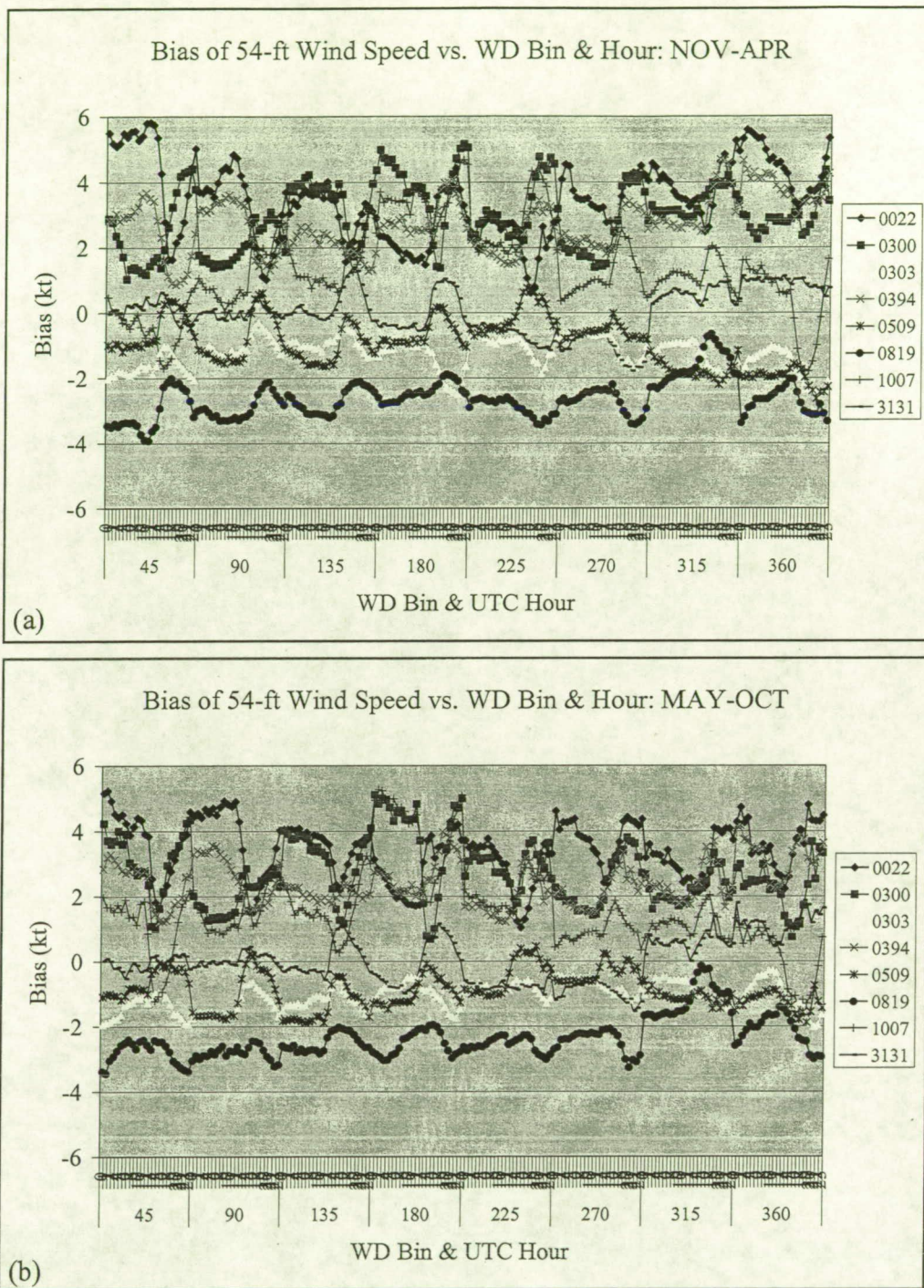


Figure 4.20. The hourly bias of 54-ft wind speeds as a function of wind direction bin at coastal towers 0022 and 0394 (SLC 39A), causeway towers 0300 and 1007, CCAFS tower 0303, Merritt Island towers 0509 and 3131, and mainland tower 0819, valid for (a) the cool-season months, and (b) the warm season months.

4.6 Monthly and Diurnal Variations in Wind Direction Deviation

The standard deviation of wind direction, or direction deviation, is used by Range Safety for dispersion modeling purposes. The direction deviation is calculated over a 30-minute period and reported every 5 minutes. In general, high direction deviations occur with lighter wind speeds and/or highly varying wind directions.

The mean hourly direction deviations at three coastal (0022, 0300, and 0394), two Merritt Island (0509 and 3131), and one mainland tower (0819) are shown in Figure 4.21. As expected, the highest direction deviations occurred over the mainland tower, which had the lightest overall mean wind speeds, whereas the smallest direction deviations tended to occur at the coastal site 0022. Due to convective processes and turbulence in the daytime boundary layer, direction deviations were highest during the afternoon hours compared to the nocturnal hours. Furthermore, afternoon direction deviations were highest during the warm-season months, particularly from June to August (~15–30°, compared to ~10–25° during the remainder of the year). These relatively larger direction deviations during the summer probably resulted from frequent sea-breeze transitions and afternoon convective outflow boundaries.

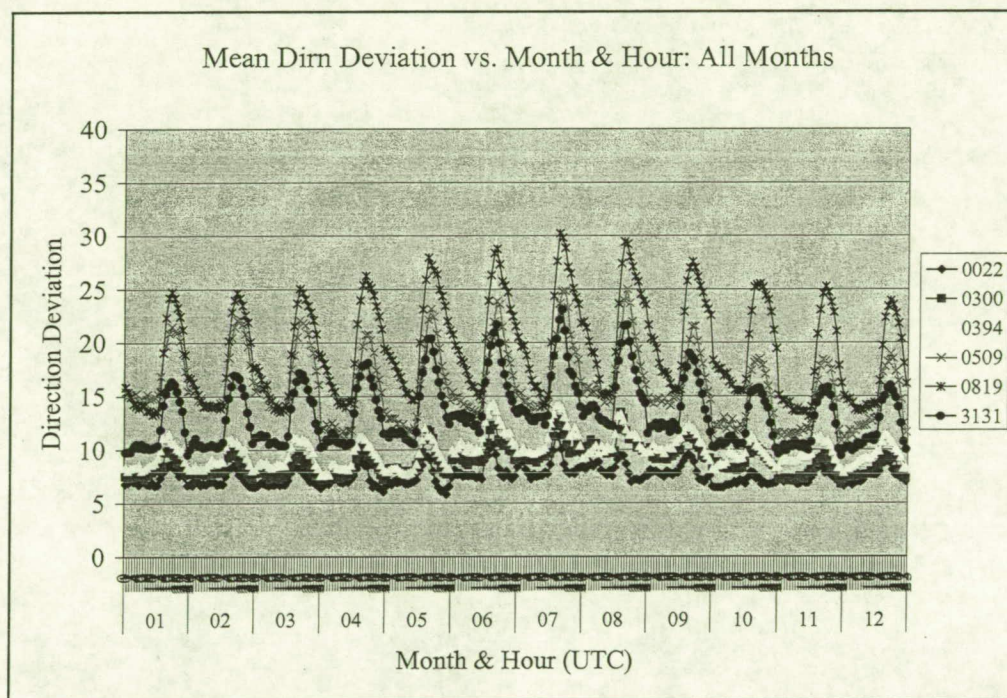


Figure 4.21. The mean hourly and monthly standard deviation of wind direction at coastal towers 0022 and 0394 (SLC 39A), causeway tower 0300, Merritt Island towers 0509 and 3131, and mainland tower 0819.

5. Training for Interactive Analysis and Display Tool

This section provides a stand-alone training and reference guide for using the AMU-developed HyperText Markup Language (HTML) interface for displaying and analyzing the results of the nine-year tower climatology. The HTML interface includes graphical displays of mean, standard deviation, bias, and data availability for any combination of towers, variables, months, hours, and wind direction bins. These graphical displays employ the Microsoft® Excel® (hereafter Excel) pivot chart capability to provide the user with this flexibility. In addition, geographical plots and contours of the various statistical quantities can provide the user with an understanding of the mesoclimate across the KSC/CCAFS tower network. Section 5.1 describes the overview and layout of the AMU-developed interactive HTML tool, and Section 5.2 provides a tutorial and reference guide for using the capabilities of Excel pivot charts.

5.1 Overview and Layout of Interactive Web Tool

A web-based GUI was chosen for portability among various computer platforms. The Mesonet Wind and Temperature Climatology Tool was written using HTML and can be viewed on computers running various operating systems. Since the pivot charts were created using Excel, the web browser required to view and interact with the pivot charts is Microsoft® Internet Explorer® 5.01 Service Pack 2 or later.

The GUI tool uses a navigation style that allows users to jump between data types and parameters with minimal mouse clicks. When the user starts the GUI they are presented with the main page which contains the main menu as shown in Figure 5.1. From here, the user can choose to view the pivot charts, maps, or help files.

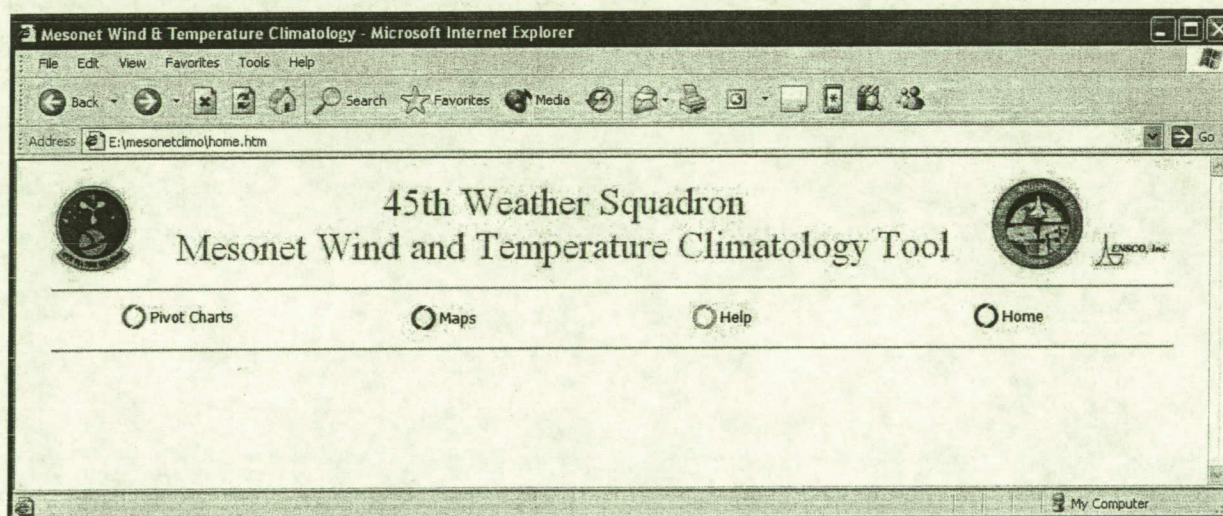


Figure 5.1. Main menu of the GUI provides navigation to the pivot charts, maps, or help files.

5.1.1 Pivot charts and tables link

When the user selects 'Pivot Charts' from the main menu, they are presented with two navigation choices on the pivot chart selection page. They can select a button to display all months and all wind directions or view the data stratified by season and wind direction (Figure 5.2).

Once the time of year/season and wind direction is chosen, the selection button becomes green. This selection scheme continues within all submenus so the user can easily identify their location within the navigation menus. The user can navigate to any data set type, parameter, or time of year/wind direction at any time regardless of the current navigation page. All navigation buttons are active and will take the user to the desired file. Depending on the user's selection they will then be presented with a choice of parameters. If they have chosen all months and all wind directions, they will have four parameters to choose from: temperature by height, 54-ft temperature minus 6-ft temperature, 54-ft wind speed, or 54-ft wind direction deviation (Figure 5.3).

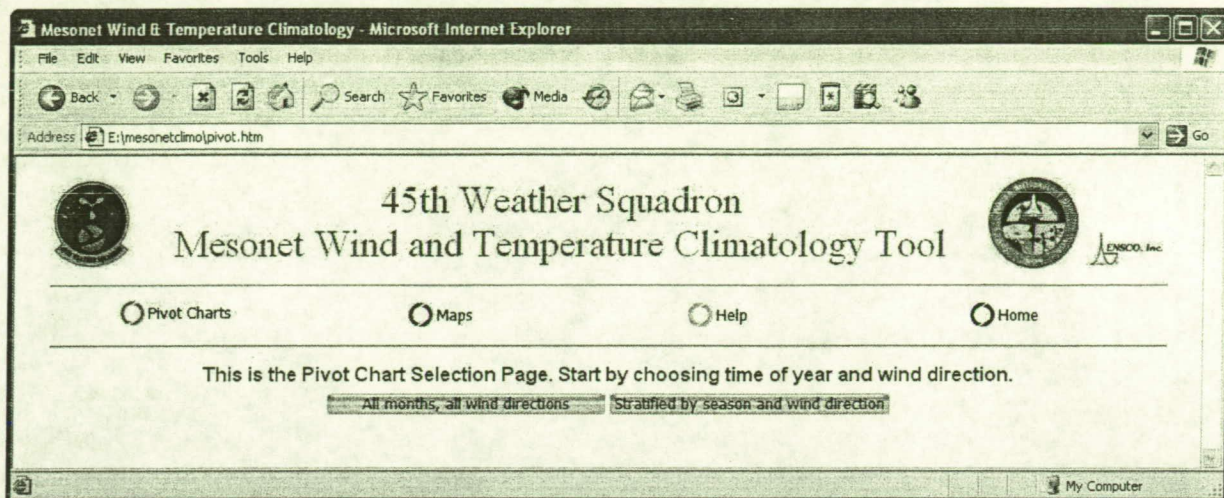


Figure 5.2. The pivot chart selection page provides two navigation choices.

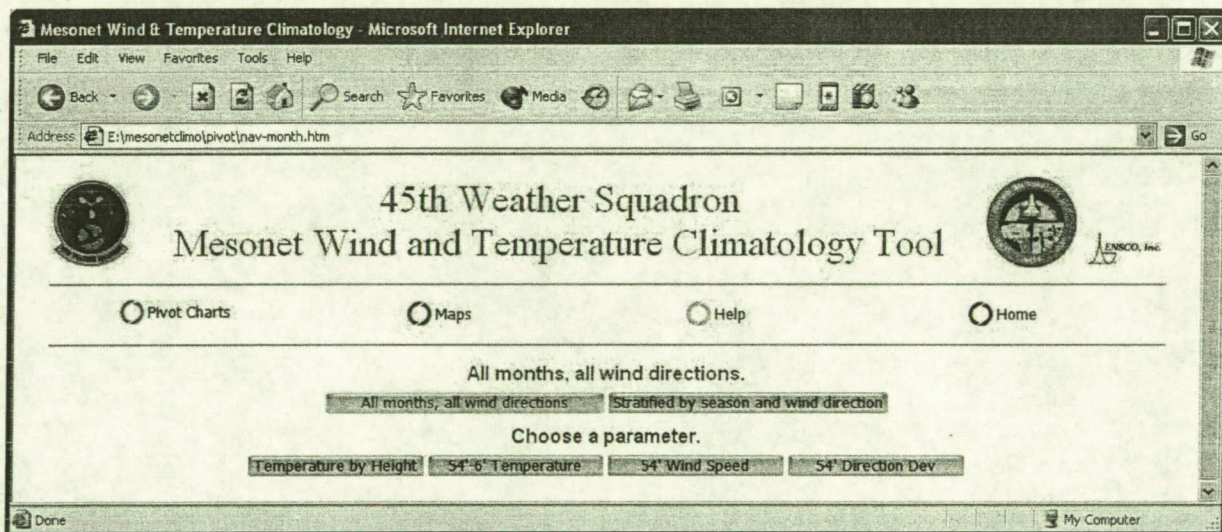


Figure 5.3. Pivot chart parameter selection page for pivot charts displaying all months and all wind directions.

Once the user selects a parameter, they can choose from four data set types: mean, standard deviation, bias, or percent of observations available. For the parameters 54-ft temperature minus 6-ft temperature and 54-ft wind direction deviation, the mean and standard deviation are displayed via the same pivot chart. Figure 5.4 shows the pivot chart data types available for the 54-ft temperature minus 6-ft temperature parameter.

The pivot chart is displayed once the user selects the data type. Figure 5.5 shows the interactive pivot chart for all months and all wind directions for the parameter 54-ft temperature minus 6-ft temperature using the data set of percent of available observations. The options within the pivot chart are fully interactive in the same manner as in the native Excel software that created the chart. The user can manipulate the chart to change the month, tower, and time. In addition to the pivot chart, the corresponding data table is also displayed below the pivot chart as shown in Figure 5.6. Details on how to use and manipulate pivot charts and tables can be found in the tutorial in Section 5.2.

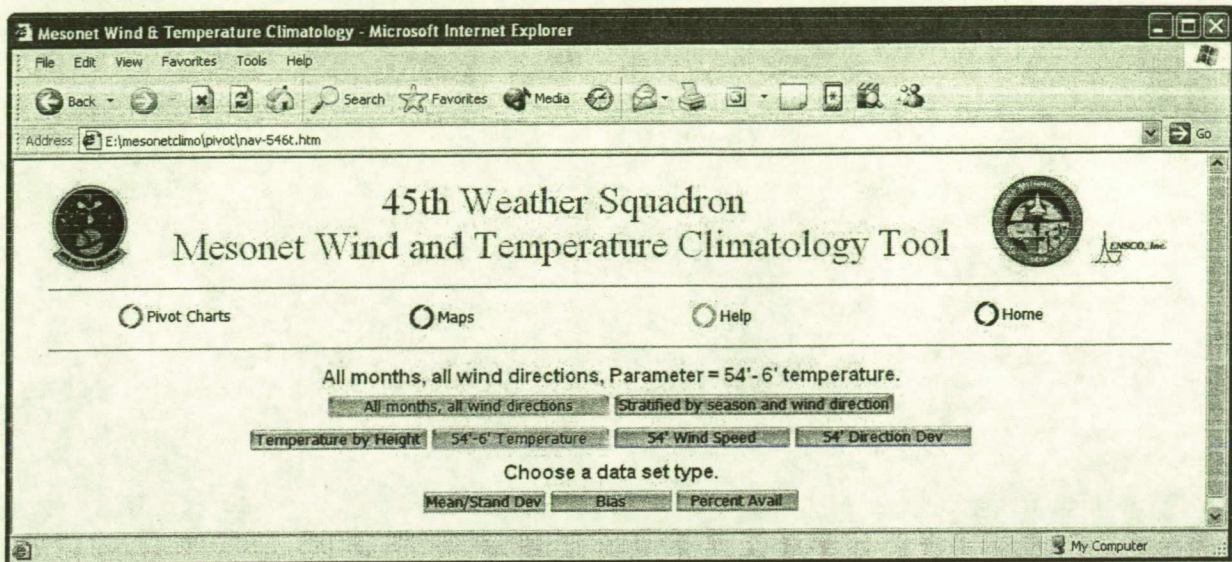


Figure 5.4. Pivot chart data set type selection page for pivot charts displaying all months and all wind directions using a parameter of 54-ft temperature minus 6-ft temperature.

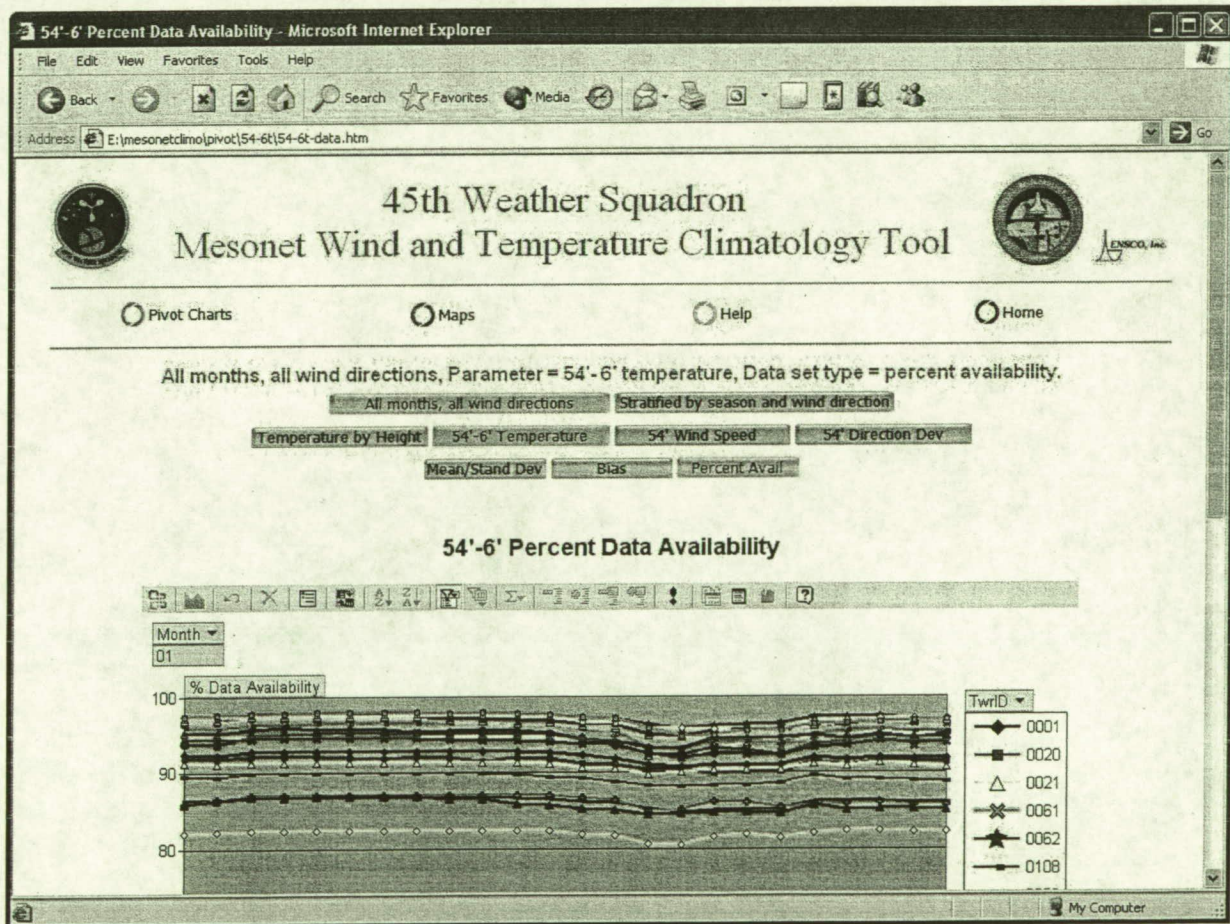


Figure 5.5. Display of a sample pivot chart showing the parameters and data sets chosen by the user.

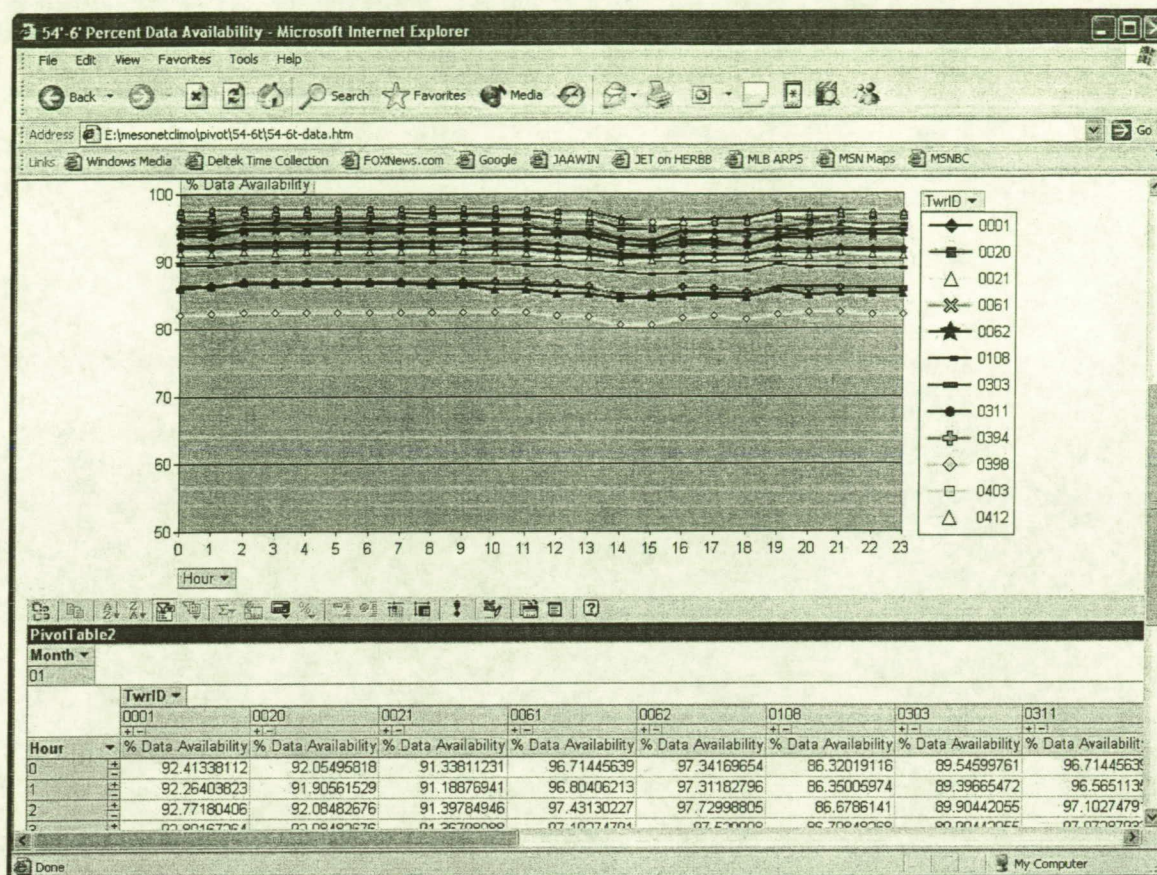


Figure 5.6. Display of a pivot chart with corresponding pivot table.

When the user selects pivot charts stratified by season and wind direction, there are five parameters to choose from: 6-ft temperature, 54-ft temperature, 54-ft temperature minus 6-ft temperature, 54-ft wind speed, or 54-ft wind direction deviation (Figure 5.7). Once the user selects a parameter, they can choose either the cool season data (November to April) or warm season data (May to October) as shown in Figure 5.8. After the user selects the season, they can choose from four data set types: mean, standard deviation, bias, or number of observations available. Figure 5.9 shows the pivot chart data types available for the 6-ft temperature parameter during the cool season.

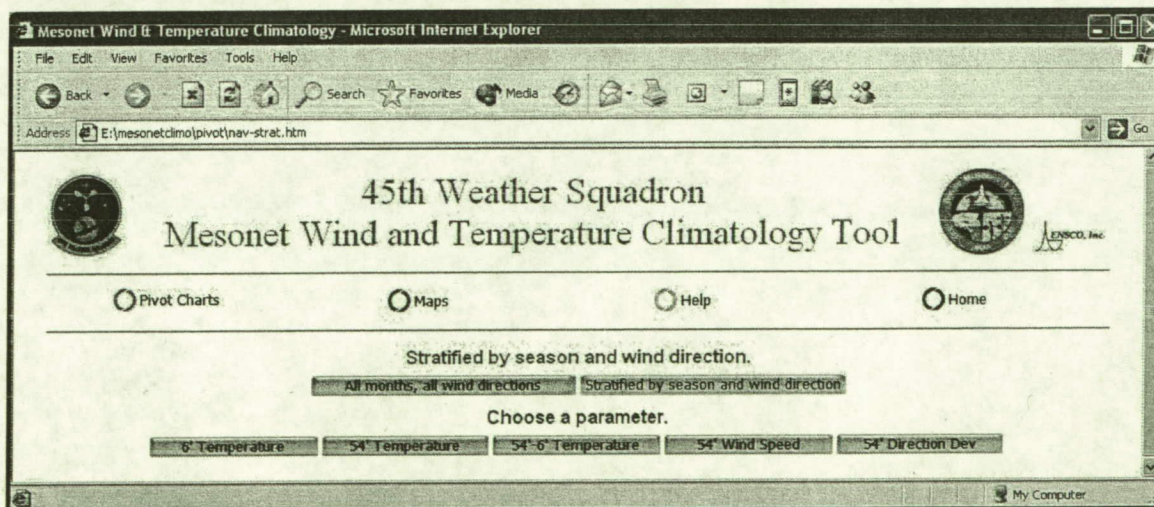


Figure 5.7. Pivot chart parameter selection page for pivot charts stratified by season and wind direction.

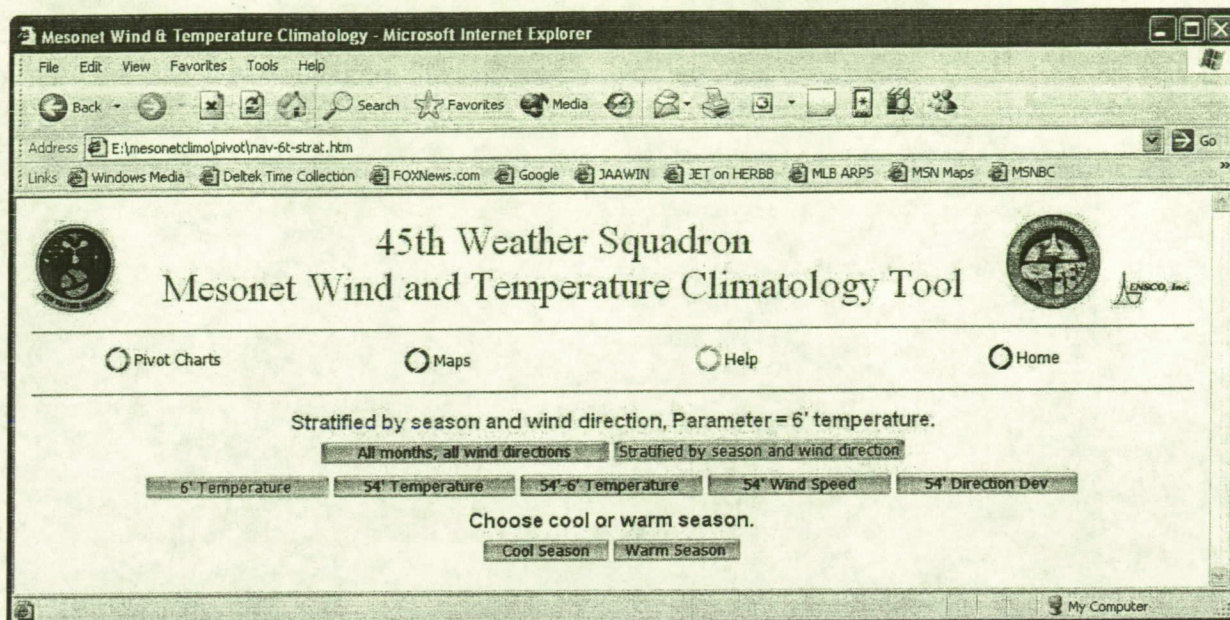


Figure 5.8. Pivot chart season selection page for pivot charts displaying data stratified by season and wind direction using the 6-ft temperature parameter.

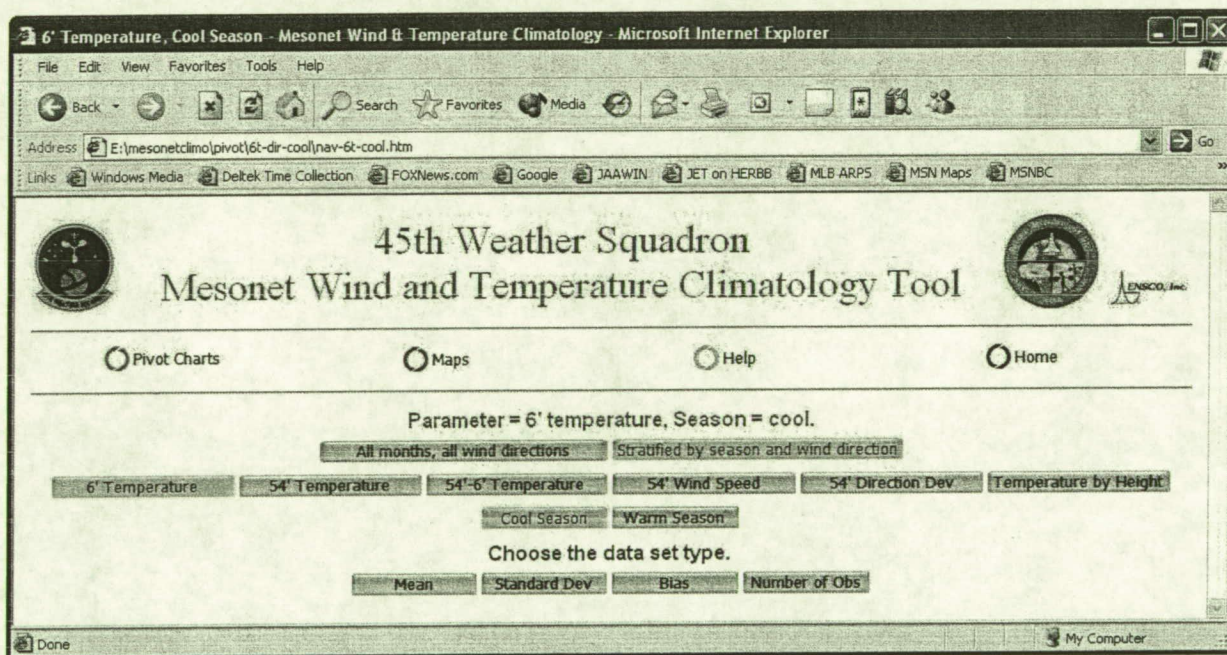


Figure 5.9. Pivot chart data set type selection page for pivot charts displaying data stratified by season and wind direction using the 6-ft temperature parameter during the cool season.

The pivot chart is displayed after the user selects the data type. Figure 5.10 shows the interactive pivot chart for data stratified by season and wind direction for the parameter 6-ft temperature during the cool season using the bias data set. The options within the pivot chart are fully interactive in the same manner as in the native Excel software that created the chart. As with all parameters and data sets, the corresponding pivot table is displayed below the chart.

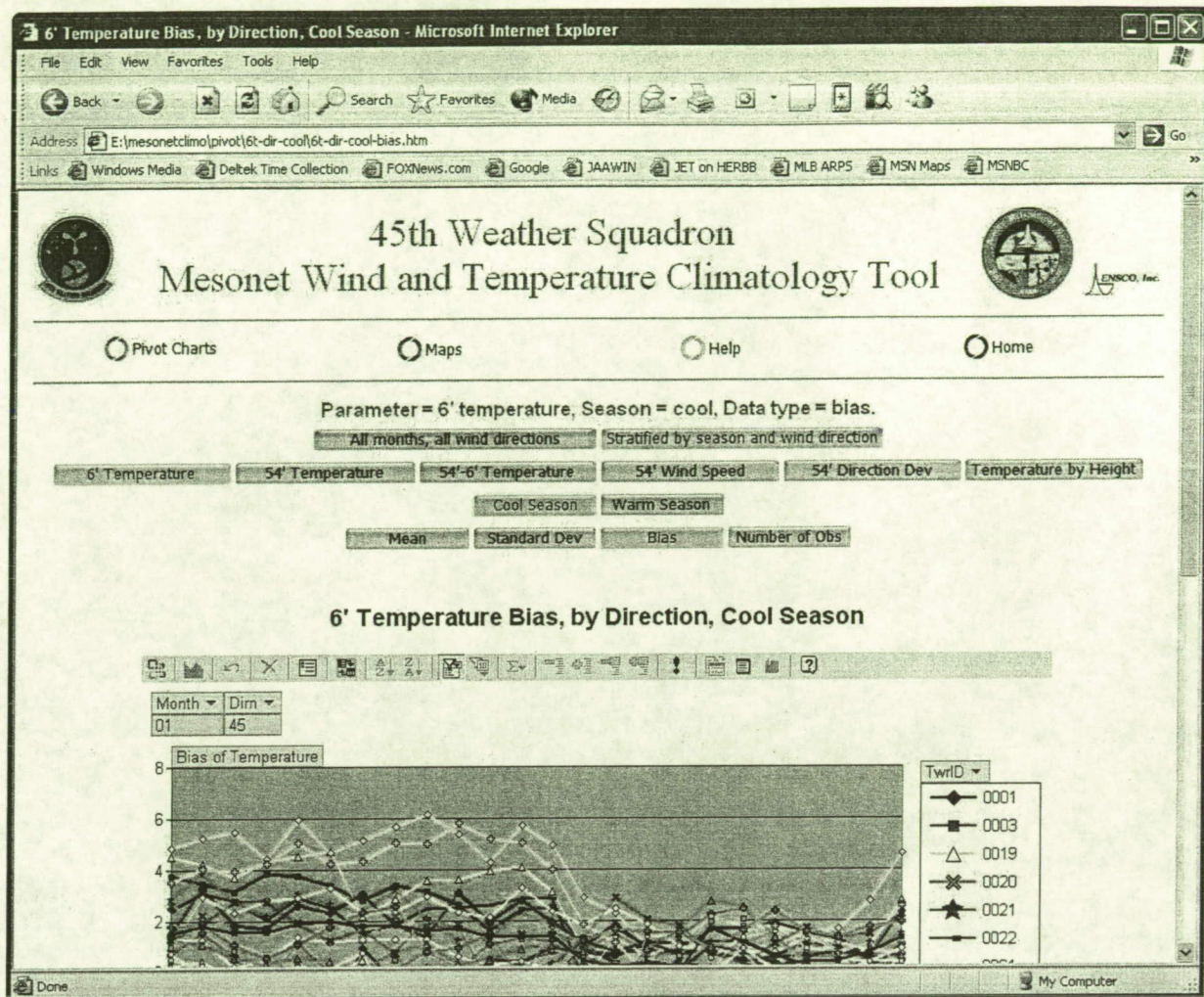


Figure 5.10. Display of a pivot chart stratified by season and wind direction, showing the parameters and data sets selected by the user.

5.1.2 Maps link

When the user selects "Maps" from the main menu, they are presented with all 12 months on the main maps selection page (Figure 5.11). Once a month is chosen, the selected month's button becomes green. This selection scheme continues within all submenus so the user can easily identify their location within the navigation menus. The user can navigate to any data set type, parameter, or time of year/wind direction bin at any time regardless of the current navigation page. All navigation buttons are active and will take the user to the desired file. The user can then choose the hour of day to display, or a loop of all 24 hours (Figure 5.12).

Once the user selects an hour, they can choose a level and parameter as shown in Figure 5.13 and then a wind direction bin as shown in Figure 5.14. After the user selects a wind direction bin, the corresponding map is displayed as shown in Figure 5.15.

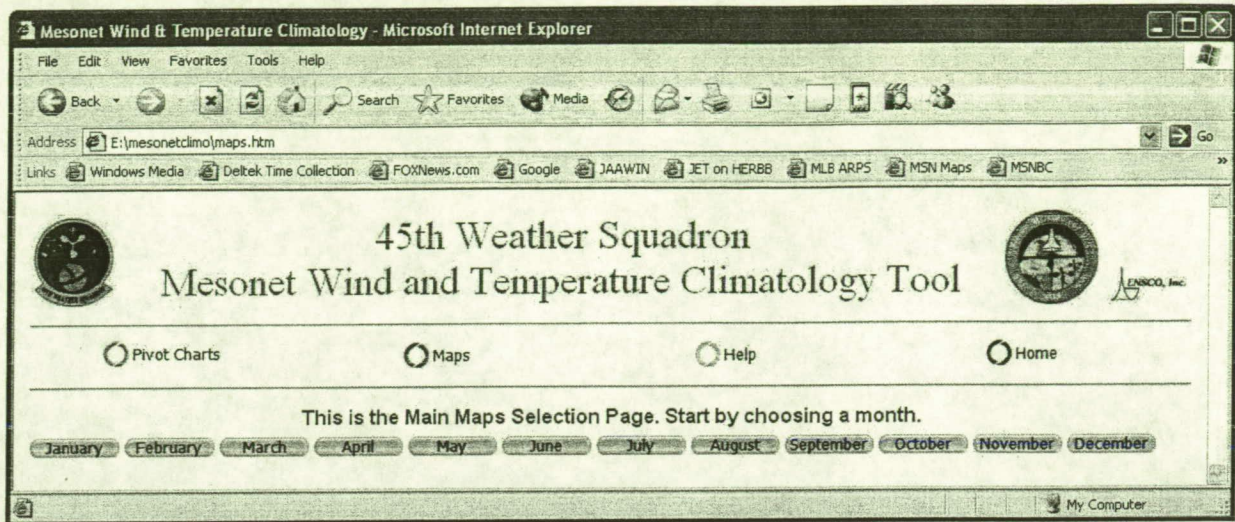


Figure 5.11. The main maps selection page provides navigation to all 12 months.

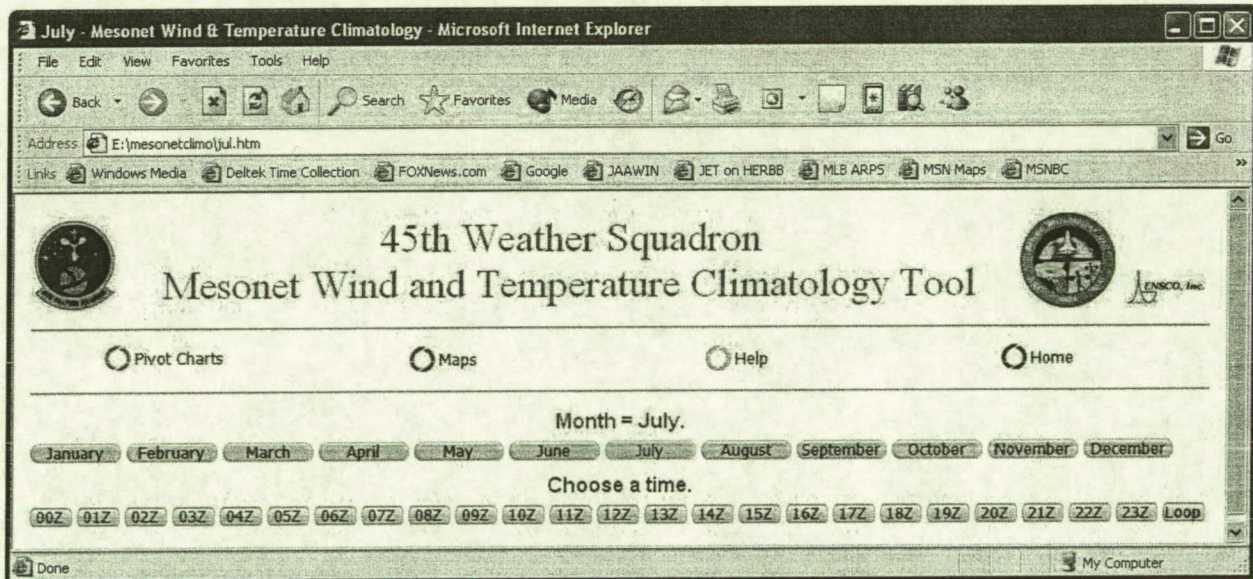


Figure 5.12. Maps hour selection page for maps displaying data from July.

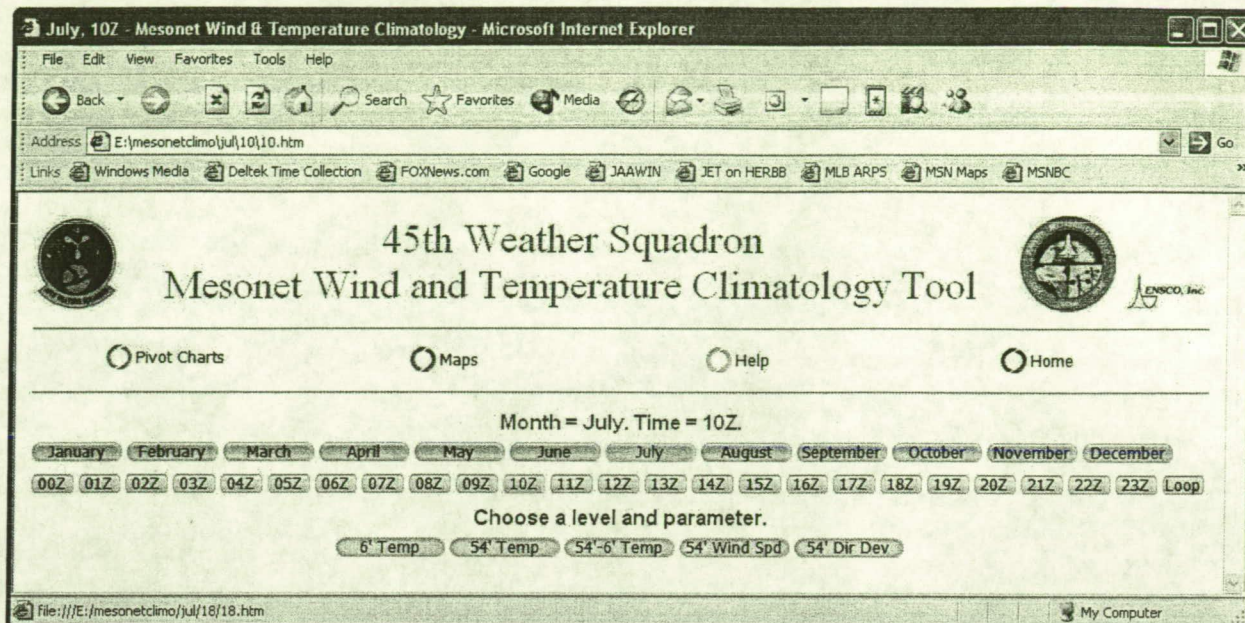


Figure 5.13. Maps level and parameter selection page for maps displaying data from July at 10Z.

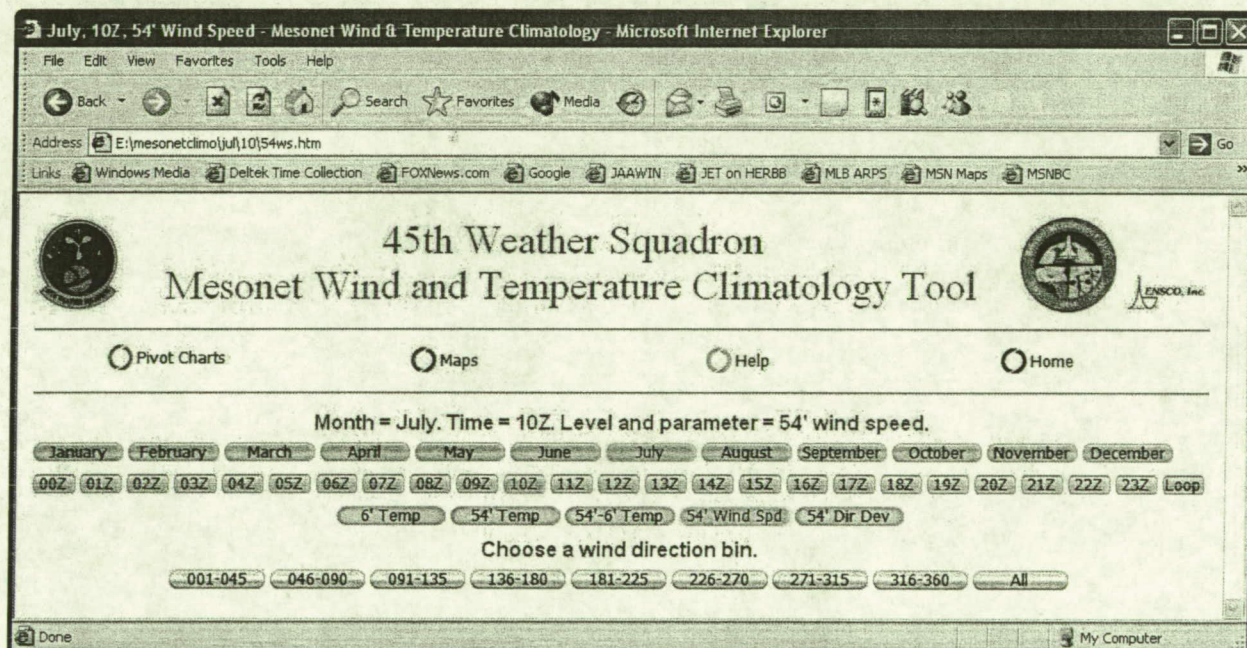


Figure 5.14. Maps wind direction bin selection page for maps displaying data from July at 10Z for 54-ft wind speed.

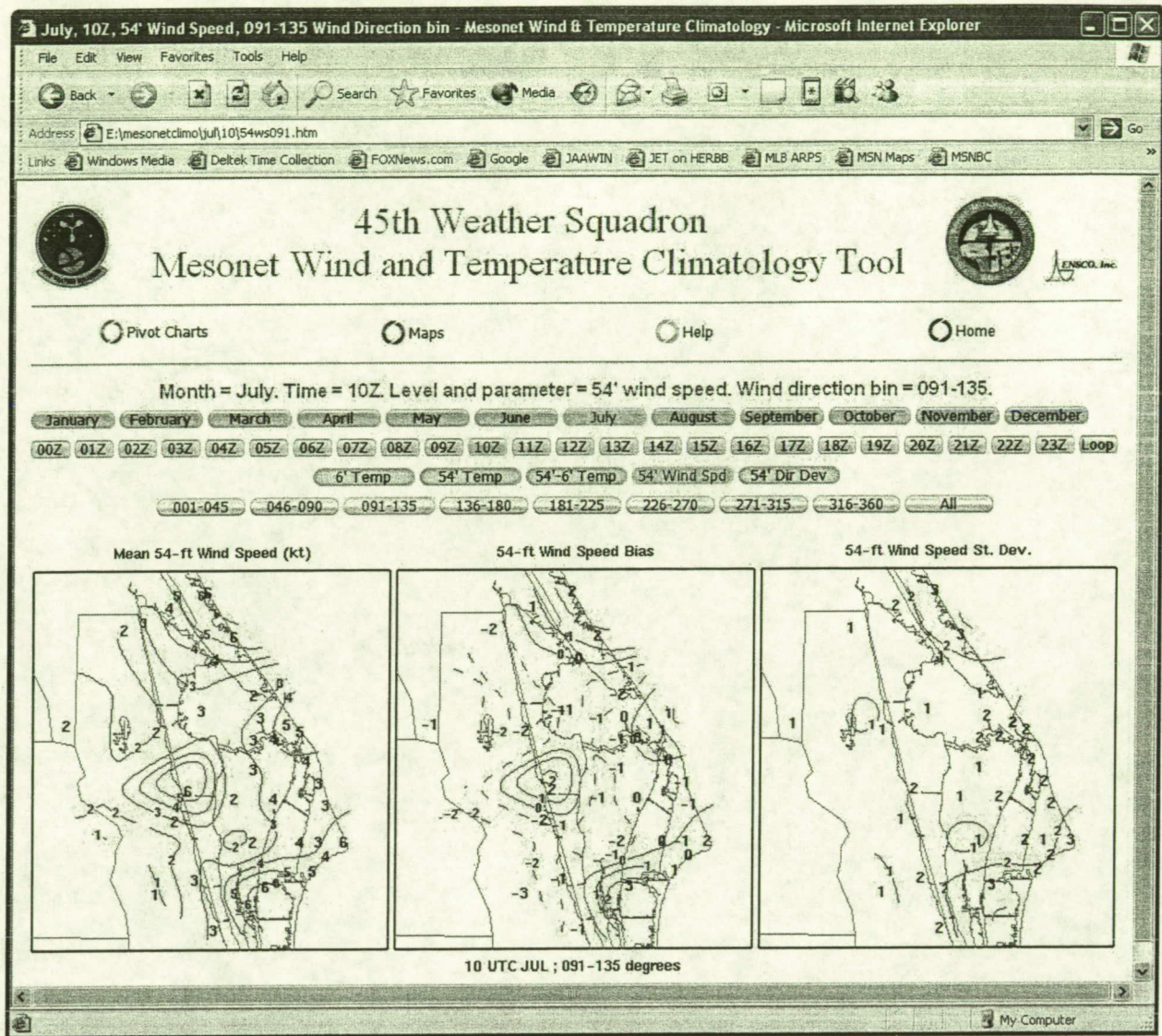


Figure 5.15. Maps page showing data from July at 10Z for 54-ft wind speed with a wind direction bin of 091°-135°.

In addition to the individual hourly maps, users can choose to loop through all hours for any given month, parameter, and wind direction bin. As shown in Figure 5.16, animation control is achieved through an interactive JavaScript tool with the capability to loop continuously through all 24 hours of data, “rock” forward and backward through the data, adjust the animation speed, start/stop the animation, move forward or backward one hour at a time, move to the first or last map, and zoom.

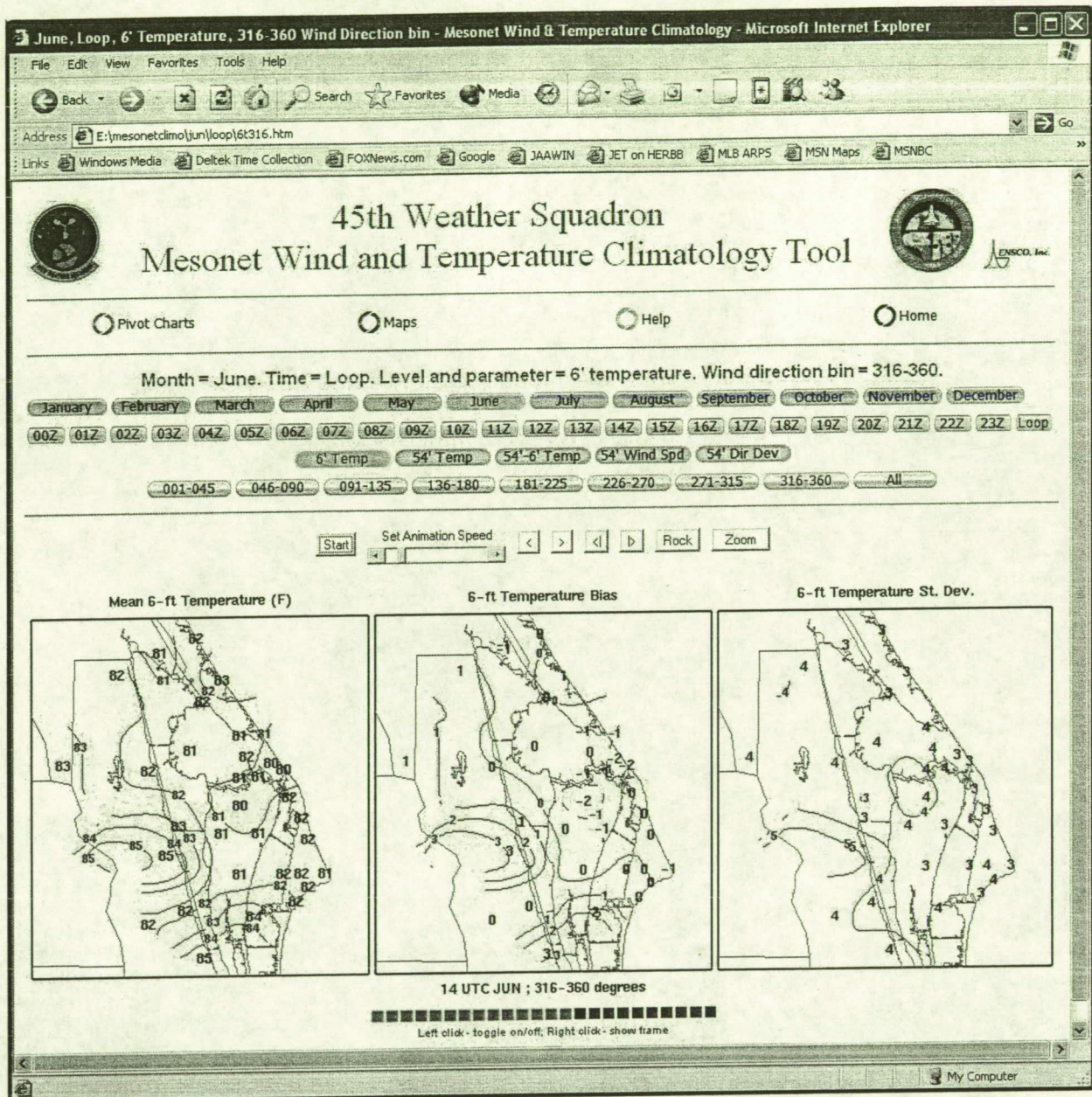


Figure 5.16. Maps page displaying hourly data from June with the JavaScript animation tool, looping through all hours for 6-ft temperature with a wind direction bin of 316°-360°.

5.1.3 Help link

The help link will direct the user to an interactive help page, which contains the same information as provided in Section 5 of this report.

5.1.4 Home link

When the user selects "Home" from the main menu, they return to the home menu as shown in Figure 5.1. At any point in the GUI navigation the user can select "Home" to return to the main menu.

5.2 Excel Pivot Chart Tutorial

All of the graphical climatological statistics developed for the Mesonet Wind and Temperature Climatology Tool are displayed using Excel pivot chart and table capabilities. The values in the charts were calculated using wind tower data from February 1995 through January 2004. This section provides an overview of Excel pivot chart elements, and gives examples of how the charts can be manipulated.

5.2.1 Pivot chart/table overview

Pivot charts and tables are parts of a feature that is exclusive to Excel, created as a means to summarize information in a large database quickly and in a way that is understandable to the user. An individual pivot chart (see Figure 5.17) is linked directly to the rows and columns of a multi-dimensional pivot table (see Figure 5.18). These charts and tables are very flexible, allowing the user to make changes with point-click-drag-drop techniques. Axes can be switched, multiple variables can be represented on one axis, and specific plots can be temporarily removed from the display to facilitate closer examination of other plots.

There are four fields indicated by gray 'buttons' in a pivot chart that can be manipulated, each of which is identified by a label and arrow in Figure 5.17:

- 1) The *Filter* field button(s) in the upper left corner of the chart area represents the multi-dimensionality of the table.
- 2) The *Data* field button is above the left edge of the plot area and its values, whose range is shown along the y-axis, are the data that make up the plots in the charts.
- 3) The *Series* field is equivalent to the chart legend and appears to the right of the plot area with its button at the top of the legend. The items in the *Series* field correspond to the columns in the pivot table.
- 4) The *Category* field button is below the plot area and its values are along the x-axis, which correspond to the rows in the pivot table.

These fields are also found in the pivot table associated with the chart, shown in Figure 5.18.

The *Filter*, *Series*, and *Category* buttons in these charts all have drop-down lists showing the range of values associated with each field, and each value is called an *Item*. Each *Item* in the *Series* and *Category* drop-down lists has a box next to it that can be checked on or off (with a mouse click) to add or remove a particular *Item* from the display (Figure 5.19). This feature allows the user to change the display to focus on field *Items* of interest such as specific tower locations (TwriD), hours, months, or wind direction bins (Dirn). In addition, the '(All)' *Item* at the top of the drop-down list can be checked on or off to turn on or off all *Items* in the list. Using the '(All)' list feature saves much time in clicking many individual *Item* boxes for large drop-down lists. It is important to note, however, that the '(All)' drop-down list feature is only available with software releases newer than Excel 2000.

Moving the field buttons allows the user to change the way the data are displayed. The *Filter*, *Series*, and *Category* buttons can all be interchanged to each other's locations. **The *Data* field button should not be moved since that eliminates the data from the chart. Also, the *Filter*, *Series*, and *Category* buttons should not be moved to the *Data* field location as this move creates a display that is difficult to interpret.** A move is accomplished by clicking and holding on a gray field button of choice and dragging it to the new desired location, holding down the left mouse button until the red 'X' disappears and a blue line is visible. If a move is made in the pivot chart, the same move is automatically made in the pivot table, and vice versa. Field button moves will be described and demonstrated in the following examples.

NOTE: All *Items* in a field drop-down list must be checked before moving the button to another position. Not doing so results in removal of the unchecked *Items* from the drop-down list when the field button is in the new position. Click the '(All)' *Item* box to check all individual *Items* prior to moving a field button.

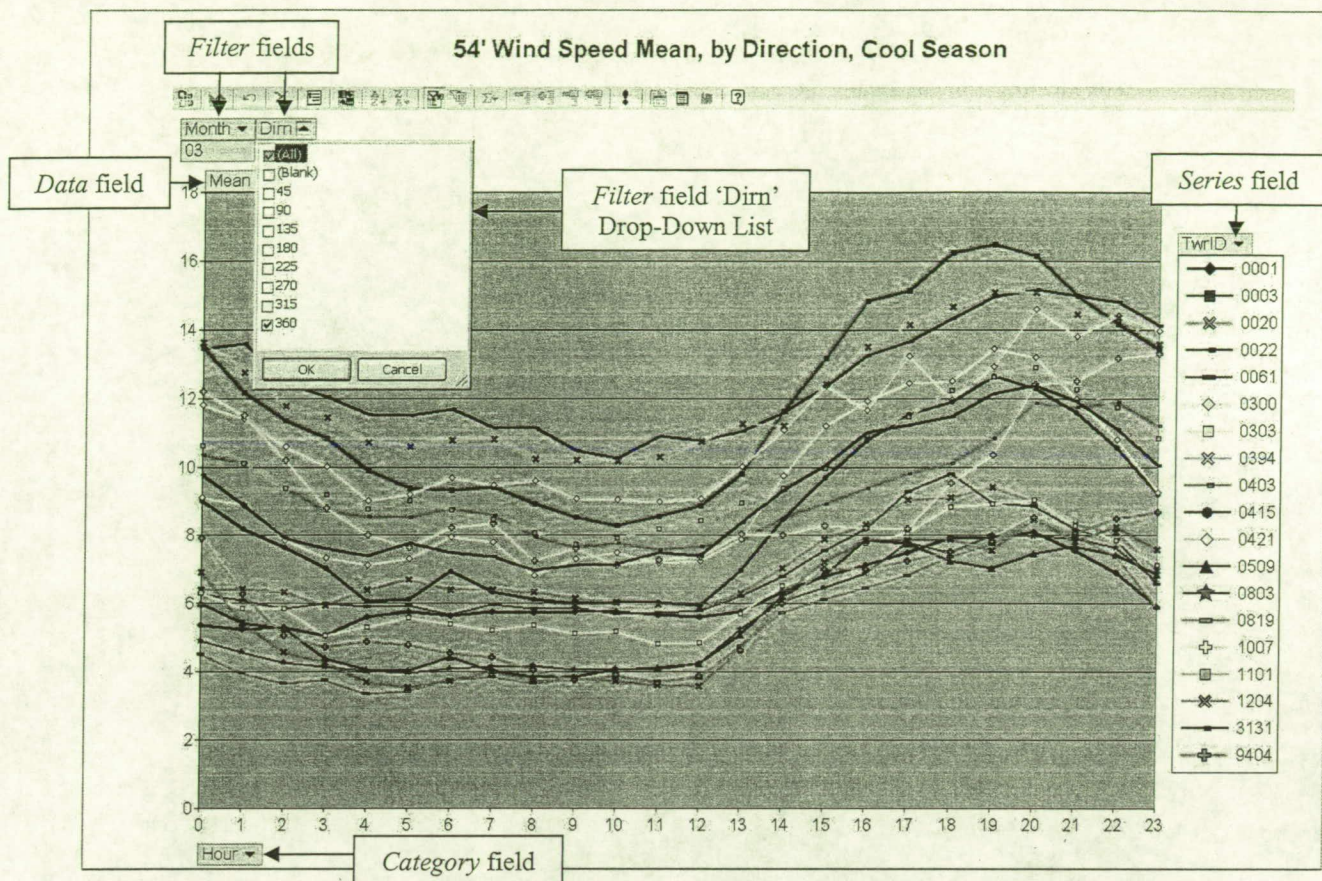


Figure 5.17. Pivot chart demonstrating the locations of the *Filter*, *Series*, *Category*, and *Data* fields as described in the text. The drop-down list for the *Filter* field 'Dirn' is also shown.

PivotTable1										
Month - Dirn -										
03 360										
TwirID -										
	0001	0003	0020	0022	0061	0300	0303	0394	0403	
Hour	Mean Wind Speed	Mean Wind Speed	Mean Wind Speed	Mean Wind Speed	Mean Wind Speed	Mean Wind Speed	Mean Wind Speed	Mean Wind Speed	Mean Wind Speed	
0	5.365979381	13.48765432	6.418502203	13.45783133	6.278287462	11.81412639	6.326018809	13.6402439	10.33777778	
1	5.23902439	12.17582418	6.424489796	13.60064935	6.105263158	11.42140468	5.843657817	12.74516129	10.11666667	
2	5.313984169	11.34267913	6.346153846	12.45289855	5.85488959	10.58171745	5.866261398	11.77160494	9.372469636	
3	5.066974596	10.83544304	5.937086093	12.05384615	5.997214485	10.0025641	5.068010078	11.43108504	8.72	
4	5.615879828	9.898630137	6.393586006	11.52264808	5.916666667	9.019753086	5.320930233	10.70984456	8.547752809	
5	5.757352941	9.372340426	6.695906433	11.49511401	5.94235589	9.196801942	5.582716049	10.58583106	8.533519553	
6	5.648373984	9.316195373	6.419426049	11.67405083	5.671023965	9.679156909	5.408888889	10.76164384	8.780092593	
7	5.760831889	9.398034398	6.395582329	11.13467049	5.985517241	9.466814159	5.217557252	10.81622912	8.581854043	
8	5.743119266	8.936218679	6.330783939	11.14246575	5.855445545	9.585774059	5.37037037	10.21479714	7.961414791	
9	5.754358162	8.514672686	6.173451327	10.47584541	5.873840445	9.072210066	5.133333333	10.21136364	7.854442877	
10	5.760432767	8.283870668	6.02800659	10.26335878	5.703770197	9.036398467	5.185970636	10.174946	7.759837178	
11	5.885670262	8.574338086	5.977777778	10.89178357	5.751295337	8.981282517	4.835725678	10.30257511	7.599486521	
12	5.805143722	8.86583162	5.893175074	10.78853755	5.785016287	9.088888889	4.858678955	10.75362319	7.682481752	
13	5.768545994	9.795532646	6.309968847	11.04051585	6.227124183	10.02590674	5.709375	11.25454545	7.866416979	
14	6.346905537	11.6265625	7.05956679	11.58385093	6.813559322	11.0746888	6.532012195	11.19098143	8.511082138	
15	6.799621928	13.15897436	7.890350877	12.35151515	7.569844789	12.37699681	6.921465969	12.42657343	8.925561798	
16	7.122685185	14.85714286	8.306493506	13.26711185	8.209677419	11.64423077	7.779168667	13.52054795	9.382352941	
17	7.505235602	15.13292434	9.054794521	13.66545455	9.296296296	13.23125	8.081447064	14.14890017	9.788804781	
18	7.934383202	16.25	9.116731518	14.32098785	9.8125	11.96153846	8.841836735	14.66347992	10.11380145	
19	7.912536443	16.47619048	9.4	14.97447796	8.954285714	12.93333333	8.935779817	15.09375	10.84539474	
20	8.109489051	16.1483376	8.993902439	15.18041237	8.861271676	14.60330579	9.053435115	15.07674944	11.86254298	
21	7.554744526	15.00265252	8.331125828	15	8.180904523	13.82608696	8.273722628	14.45535714	11.74881517	
22	6.929577465	14.16883117	8.09202454	14.80285714	7.901515152	14.41450777	7.872791519	14.35224586	11.90586038	
23	5.923529412	13.42288557	6.995575221	14.1143695	6.582317073	13.95154185	7.127035831	13.55501222	11.20192308	
Grand Total	6.259349154	11.87685494	7.124202143	12.55230218	6.879578434	11.12458708	6.464424539	12.24404549	9.325423025	

Figure 5.18. Pivot table associated with the pivot chart in Figure 5.17.

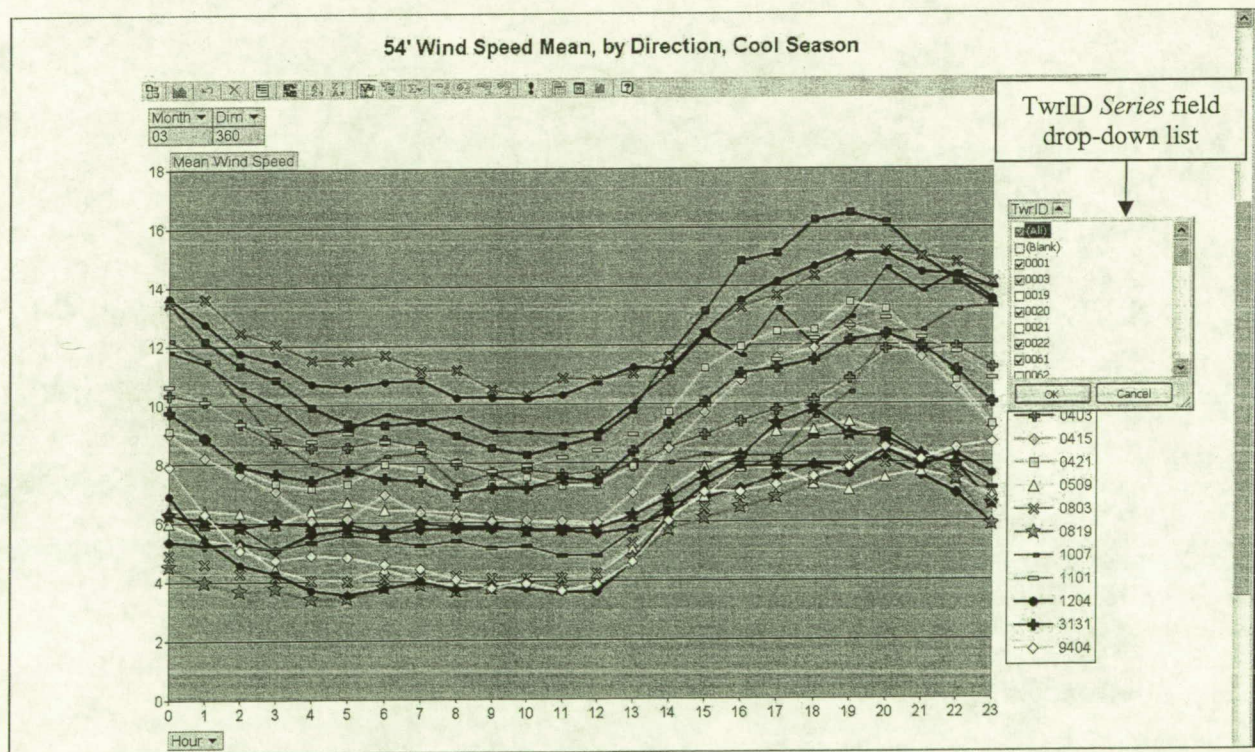


Figure 5.19. Pivot chart as in Figure 5.17, but with the drop-down list for the *Series* field 'TwirID' shown with check boxes next to each *Item*.

5.2.2 Examples of pivot chart/table operations

The examples given here are certainly not exhaustive of all possible charts, tables, and procedures, but contain enough information to get the user started. The user is encouraged to practice with all the charts to become familiar with them. The examples are given in a step-by-step format. Read each step and complete the associated exercises before proceeding to the next step. Figures are provided so the user will have a reference to what the results of the practice session should look like.

5.2.2.1 Example 1: Temperature climatology at tower 303

This example will step the user through the Mesonet Wind and Temperature Climatology Tool to access temperature climatological data and manipulate the display interactively. The first exercise will create a display that overlays all monthly mean 6-ft temperatures at tower 0303.

1. Beginning with the home portion of the Mesonet Wind and Temperature Climatology Tool, click on 'Pivot Charts' in the upper left.
2. Next, click on 'All months, all wind directions' followed by 'Temperature by Height', then 'Mean'. Prior to displaying the pivot chart, a Microsoft Office web components window will pop up if the GUI tool is run across a server rather than a local disk (Figure 5.20). Simply click 'OK' to continue to the pivot chart.
3. The default pivot chart shown in Figure 5.21 displays 6-ft temperatures for January at all towers (*Filter* fields Height = 6 and Month = 01, *Series* field TwrID displaying all towers, and *Category* field Hour showing all hours along the x-axis). Note that due to space limitations in the display, only the first 22 tower identifiers are shown in the legend beneath the *Series* field button; however, all data are plotted in the graph.
4. Click the arrow on the 'TwrID' *Series* field button to access the drop-down list of all tower IDs. Click the checked box next to '(All)' to uncheck all tower IDs. Using the windows scroll bar, move down to *Item* '0303' and check the box to display data only at tower 0303. Click 'OK' at the bottom of the drop-down list.
5. Select all months by clicking the arrow on the 'Month' *Filter* field button (upper left) to access the drop-down list. Next, click on the box next to the *Item* '(All)' to select all months and click 'OK'.
6. Left-click the 'Month' field button and drag it onto the 'TwrID' button. Release the mouse button once a blue line appears on the edge of the 'TwrID' *Series* button and a small display window reads "Drop Series Fields Here". **Caution: If you release the left mouse click while a red 'X' appears next to the mouse icon, the field button will disappear from the pivot chart. If this occurs, the best fix is to close the GUI tool, re-open the application, and start over with step (1) above. No data will be lost.**
7. The resulting display consists of 12 separate curves of mean 6-ft temperatures at tower 303 for each month of the year (Figure 5.22). To examine any individual value within the pivot chart, simply move the mouse pointer over any of the individual labels and a small pop-up window will display the data from the accompanying pivot table. In this example, the mouse pointer was moved over the April curve at UTC hour 16 (04 - 0303 - 16, Mean Temperature = 77.07°F in Figure 5.22).
8. Finally, left-click the 'Month' field and drag it down to the left side of the 'Hour' *Category* field button. Release the mouse button once a blue line appears on the left edge of the 'Hour' button and a small display window reads "Drop Category Fields Here". The resulting plot shows the annual march of the hourly mean 6-ft temperatures from January to December (Figure 5.23). Each month contains 24 hourly mean temperatures ranging from 00 to 23 UTC, thus depicting the mean diurnal range of 6-ft temperatures for all months.

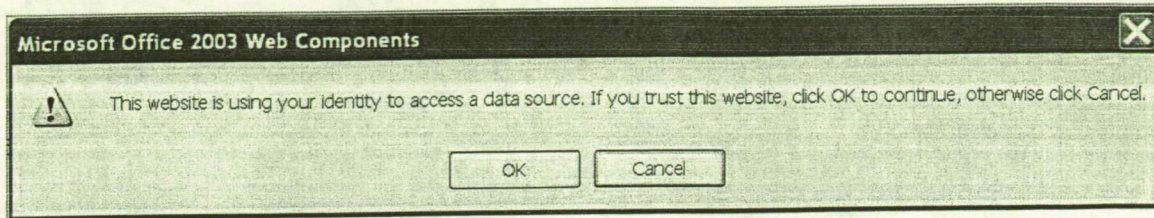


Figure 5.20. Warning pop-up window when first accessing pivot chart data if the GUI tool is run from a server.

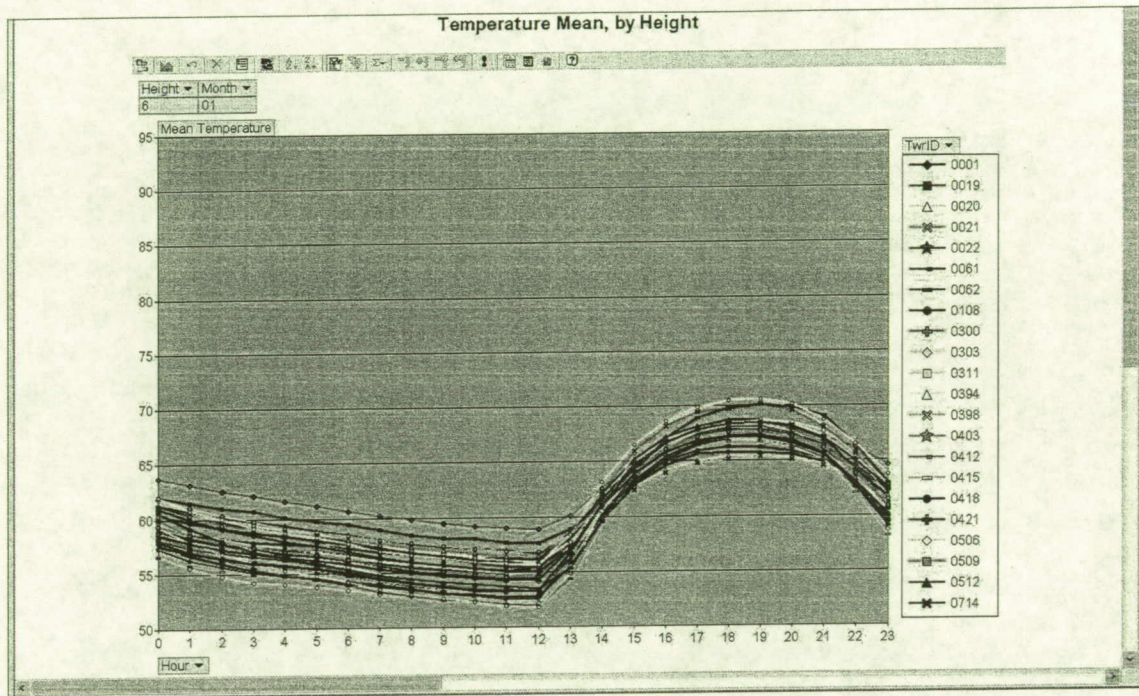


Figure 5.21. Default pivot chart displayed when selecting all months and all wind direction, temperature by height, and mean from the Mesonet Wind and Temperature Climatology Tool.

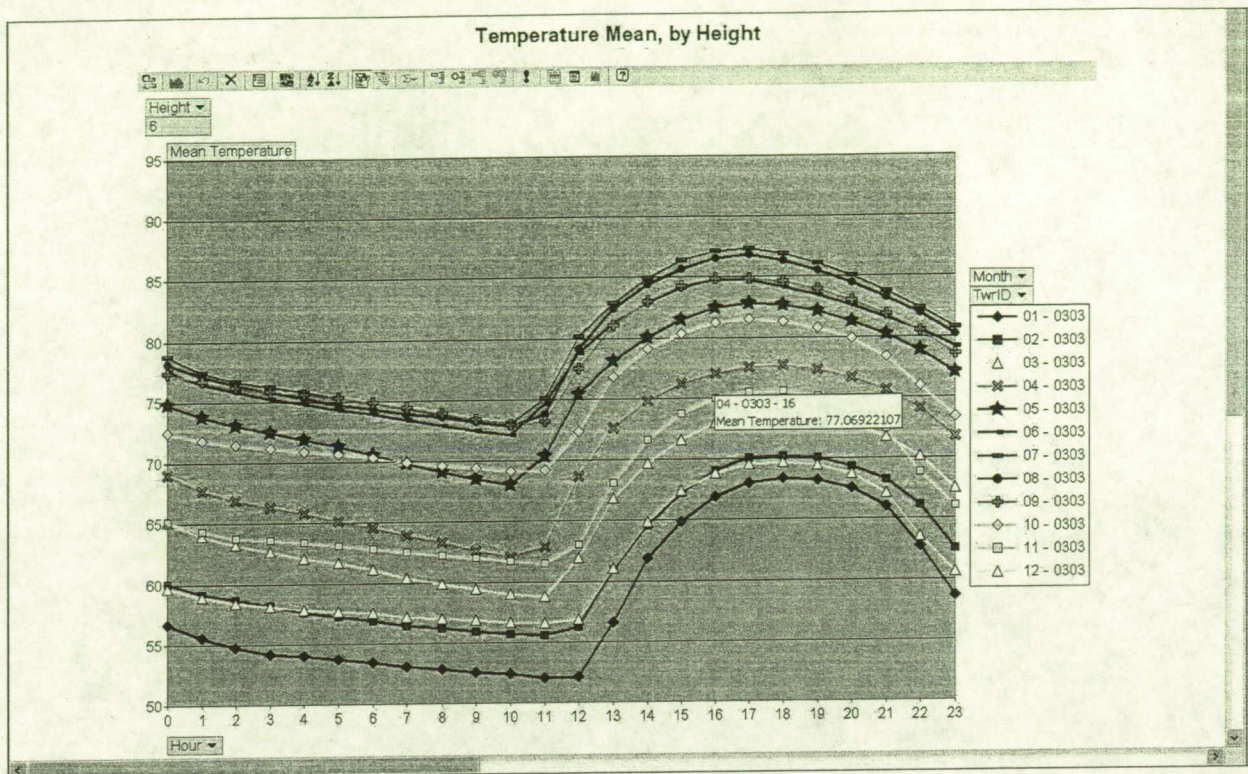


Figure 5.22. Display of all monthly mean 6-ft temperatures at tower 0303 as a function of UTC hour. The value from the corresponding pivot table shows up in a small pop-up window if the mouse is moved over any individual plotted element.

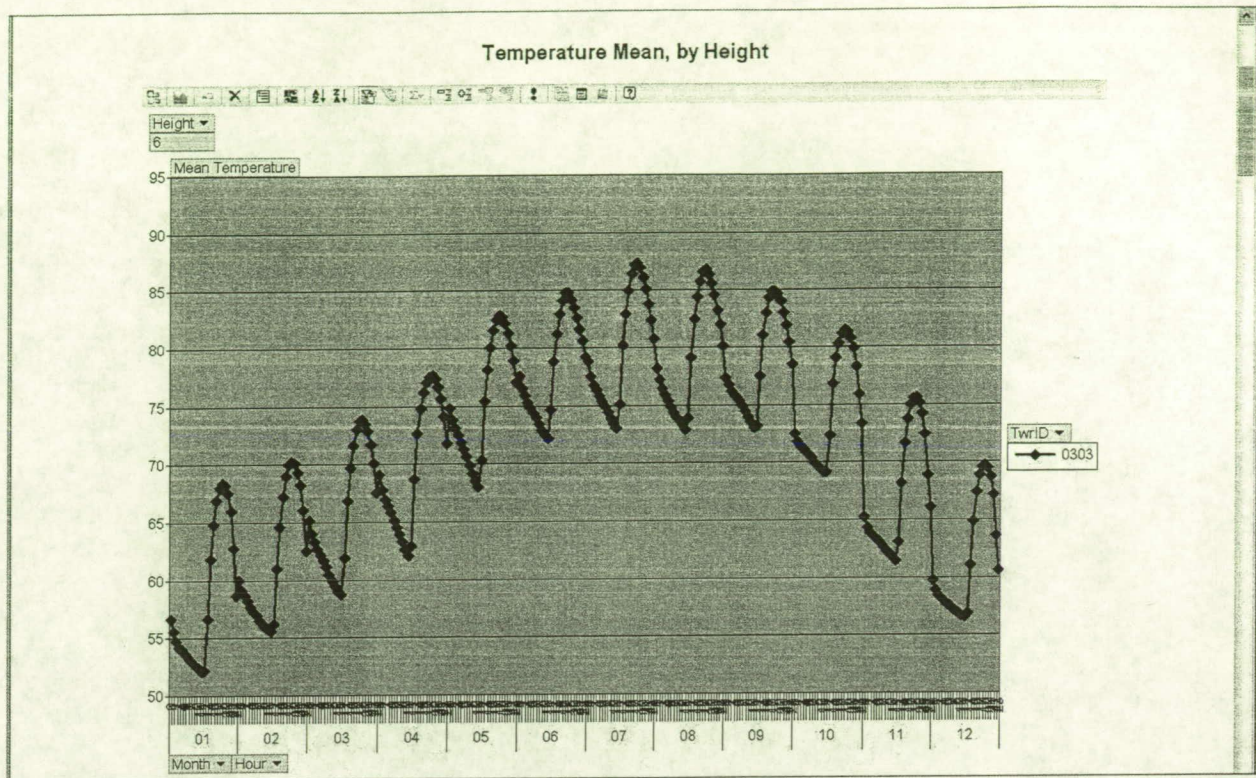


Figure 5.23. Display of hourly mean 6-ft temperatures at tower 0303 for all months, with the x-axis containing both 'Month' and 'Hour' as the *Category* fields.

5.2.2.2 Example 2: Temperature bias climatology for multiple heights and towers

This example will step the user through the GUI tool to access temperature bias climatological data and manipulate the display interactively. This exercise will create displays that overlay data for multiple towers and heights, embellishing on the ideas from Example 1.

1. Complete steps (1)–(3) from Example 1, except click on 'Bias' instead of 'Mean' to bring up the default graph of 6-ft temperature biases during January at all towers (Figure 5.24).
2. Click the arrow on the 'TwrID' *Series* field button to access the drop-down list of all tower IDs. Click the checked box next to '(All)' to uncheck all tower IDs. Click the boxes next to IDs 0061, 0300, 0303, 1101, and 3131, using the windows scroll bar on the right side of the drop-down list. Click 'OK' at the bottom of the drop-down list.
3. Click the arrow on the 'Height' *Filter* field button to bring up its drop-down list. Check the box next to '(All)' and click 'OK'.
4. Drag the 'Height' button down to the left side of the 'Hour' *Category* field button. Release the mouse button once a blue line appears on the left edge of the 'Hour' button and a small display window reads "Drop Category Fields Here". The resulting display (Figure 5.25) shows the January temperature biases at both 6 ft and 54 ft for the tower IDs selected in step (2). Note that since 54-ft temperatures are not measured at tower 0300, the curve does not display any data on that portion of the graph.
5. Next, drag the 'Height' button back up to the *Filter* field location to the left side of the 'Month' field button. Release the mouse button once a blue line appears on the left edge of the 'Month' button and a

small display reads “Drop Filter Fields Here”. Access the drop-down list for ‘Height’ and check only the box by 6.

6. Click on the arrow on the ‘Month’ *Filter* field button to access the drop-down list, select ‘(All)’, and click ‘OK’. Then drag the ‘Month’ button on top of the ‘TwrID’ *Series* field button, releasing the mouse button once a small display reads “Drop Series Fields Here”.
7. Finally, drag the ‘TwrID’ *Series* button to the left side of the ‘Hour’ *Category* button, releasing the mouse once a blue line appears on the left edge of the ‘Hour’ button and a small display reads “Drop Category Fields Here”. The final graph in Figure 5.26 shows the hourly 6-ft temperature biases for all 12 months at towers 0061, 0300, 0303, 1101, and 3131.

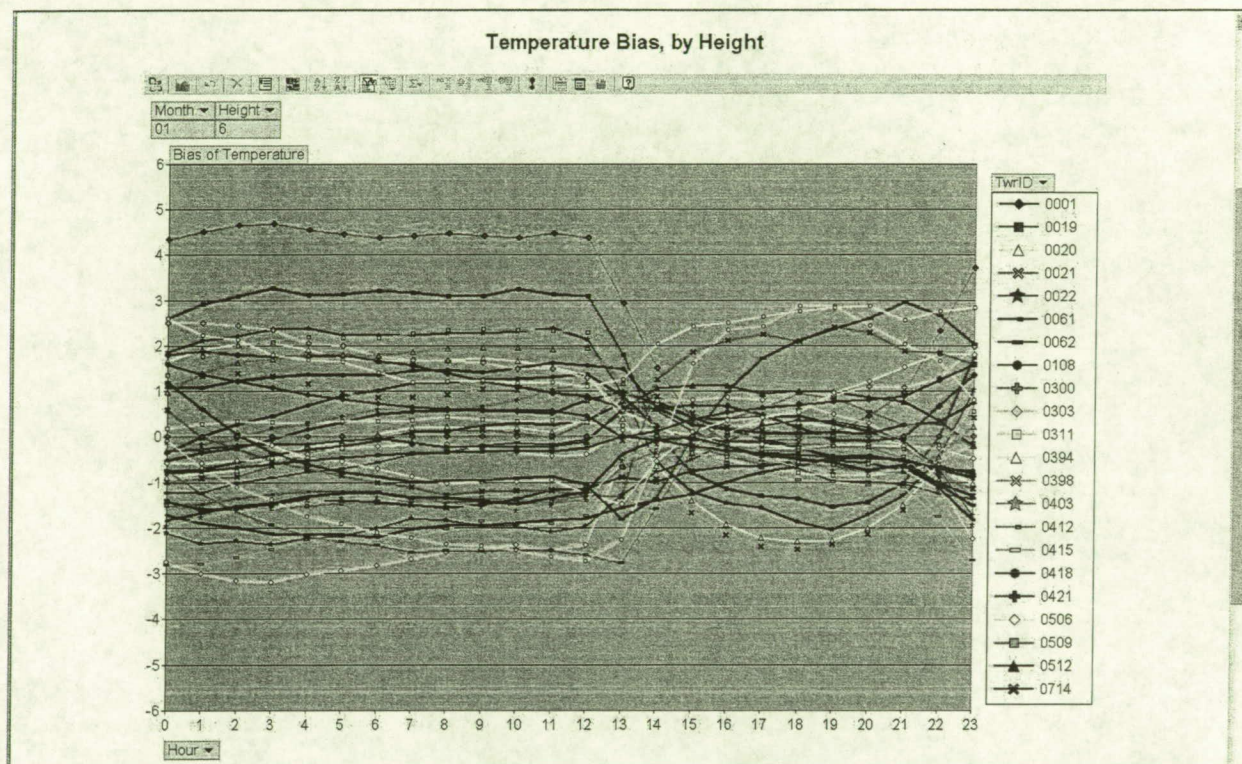


Figure 5.24. Default pivot chart displayed when selecting all months and all wind directions, temperature by height, and bias from the Mesonet Wind and Temperature Climatology Tool.

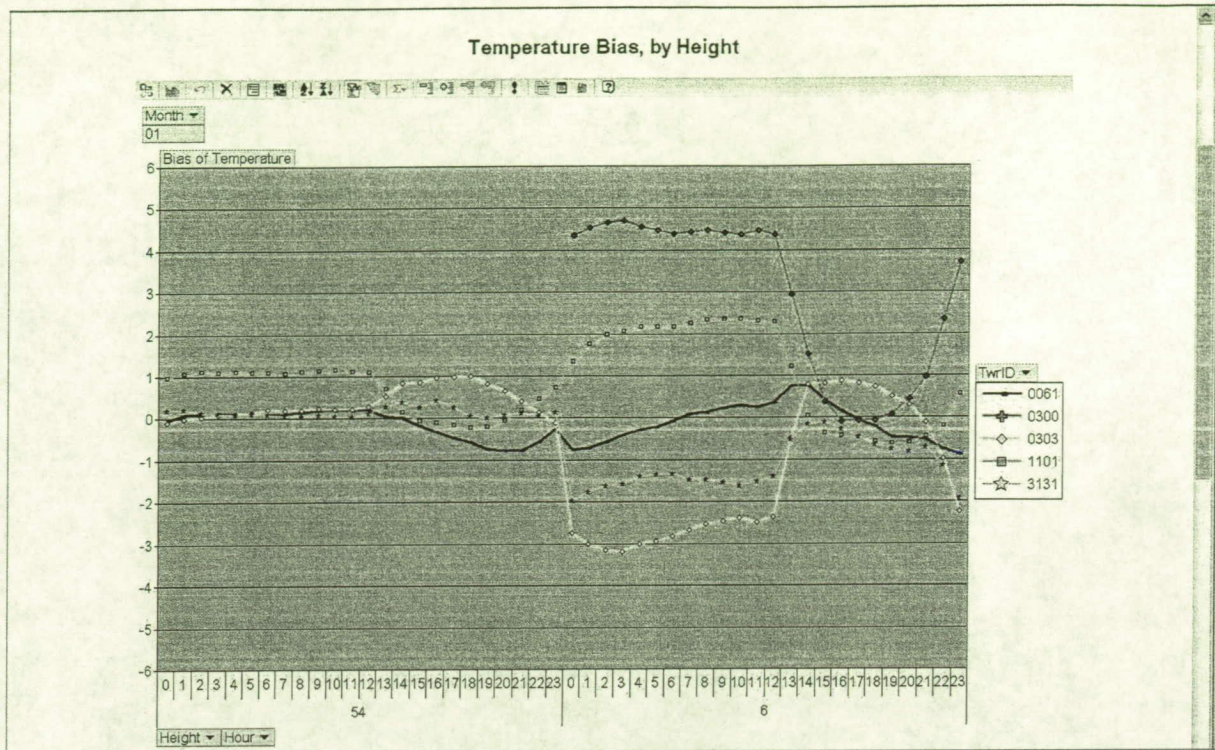


Figure 5.25. Display of the 54-ft and 6-ft hourly temperature biases during January for towers 0061, 0300, 0303, 1101, and 3131.

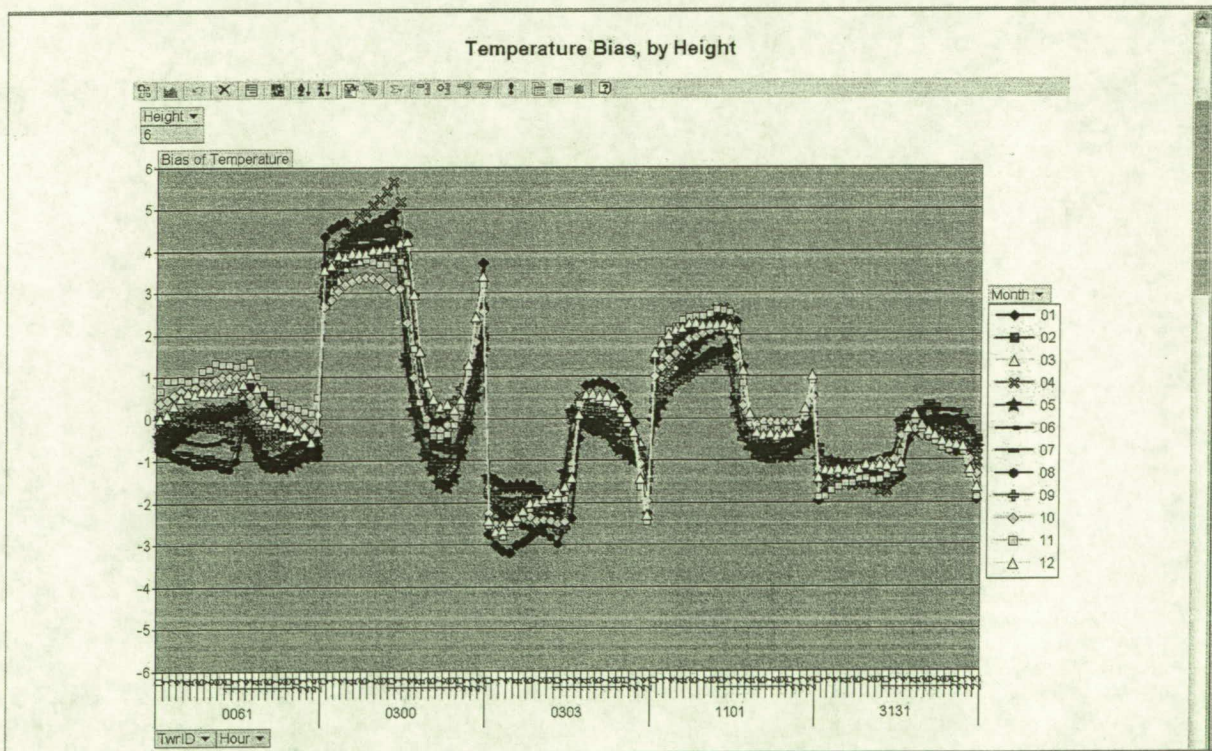


Figure 5.26. Display of the 6-ft hourly temperature biases for all months at towers 0061, 0300, 0303, 1101, and 3131.

5.2.2.3 Example 3: Wind speed climatology by wind direction bin

The third example will lead the user through the Mesonet Wind and Temperature Climatology tool to examine wind speed climatological data arranged by wind direction bins during the cool-season months. Again, this example embellishes on the concepts learned from the previous two examples.

1. From the Home location in the Mesonet Wind and Temperature Climatology Tool, click on 'Pivot Charts', then 'Stratified by season and wind direction', '54-ft Wind Speed', 'Cool Season', and finally 'Mean'. Again, click 'OK' if the application is being run from a server. The default plot will show hourly mean wind speeds during January for all wind direction bins (not shown).
2. Ensuring that all wind direction bins are selected, drag the 'Dirn' *Filter* field button down to the left side of the 'Hour' *Category* field button. Release the mouse button only after a blue line shows on the left edge of 'Hour' and a small display indicates "Drop Category Fields Here". The resulting cluttered graph displays hourly mean wind speeds at all towers during January for 8 different wind direction bins ranging from 45° to 360° (Figure 5.27). The wind direction bin labeling convention is based on the ending value in the bin range, as summarized in Table 4.1 (e.g. 45° bin contains wind directions ranging from 1° to 45°).
3. To simplify the display, change the number of towers displayed to only three: 0398, 0412, and 1012 (one tower each from the coast, Merritt Island, and mainland Florida). Select the arrow to access the drop-down list under 'TwrID', deselect all towers, and then click on only these three tower IDs. As seen in Figure 5.28, the coastal tower 0398 (SLC 39B) has the highest average wind speeds during January for all wind direction bins, whereas the mainland tower 1012 has the weakest mean wind speeds.
4. Finally, examine the monthly variations of the hourly mean wind speeds at only tower 0398 during the cool season. First, deselect towers 0412 and 1012 from the 'TwrID' drop-down list. Since the daytime hours appear to have the strongest wind speeds, access the drop-down list of the 'Hour' *Category* field, and uncheck UTC hours 00 through 11, leaving only the daytime hours 12 through 23. Select '(All)' from the 'Month' *Filter* field drop-down list. Drag the 'Month' button to the top portion of the 'TwrID' button. The final graph shows the mean monthly wind speeds during hours 1200 UTC to 2300 UTC at tower 0398, stratified by wind direction (Figure 5.29). For south to northwest winds (180°–360° bins), February, March, and April tend to have the strongest mean wind speeds, whereas November has the highest mean wind speeds for east-northeast directions (90° bin).

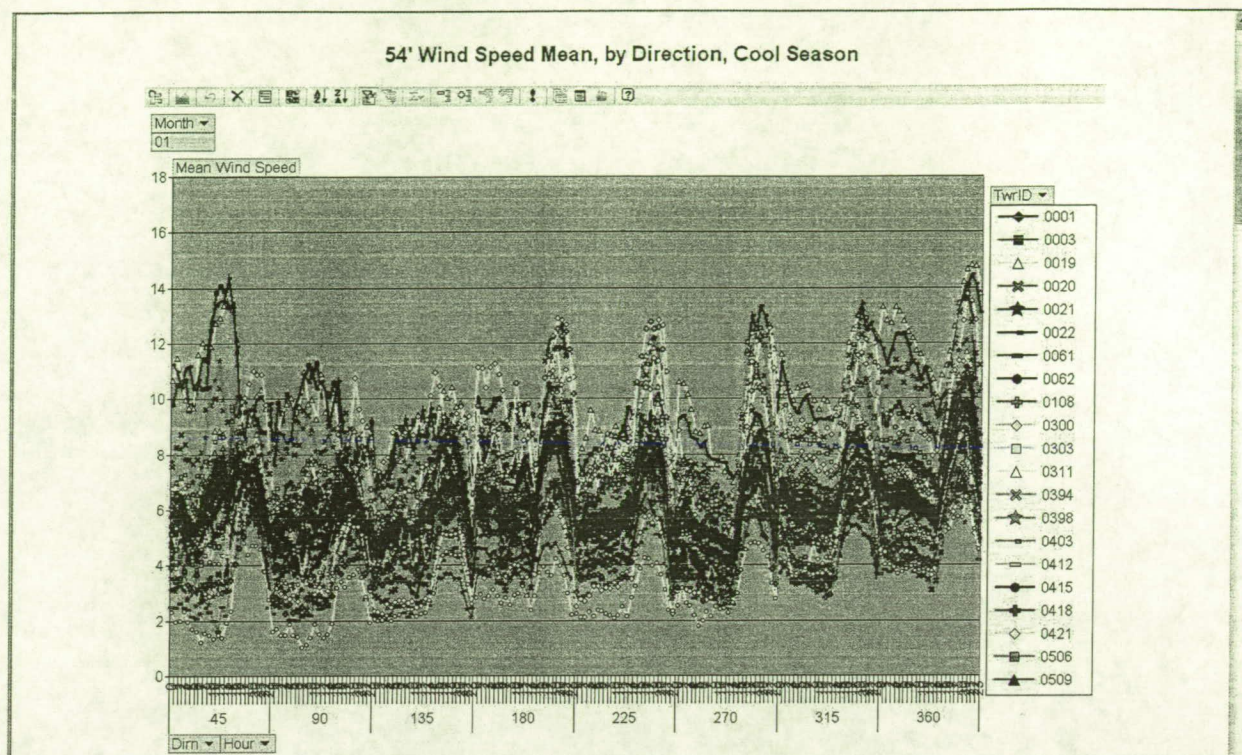


Figure 5.27. Display of hourly mean 54-ft wind speeds at all towers during the month of January, stratified by wind direction bin.

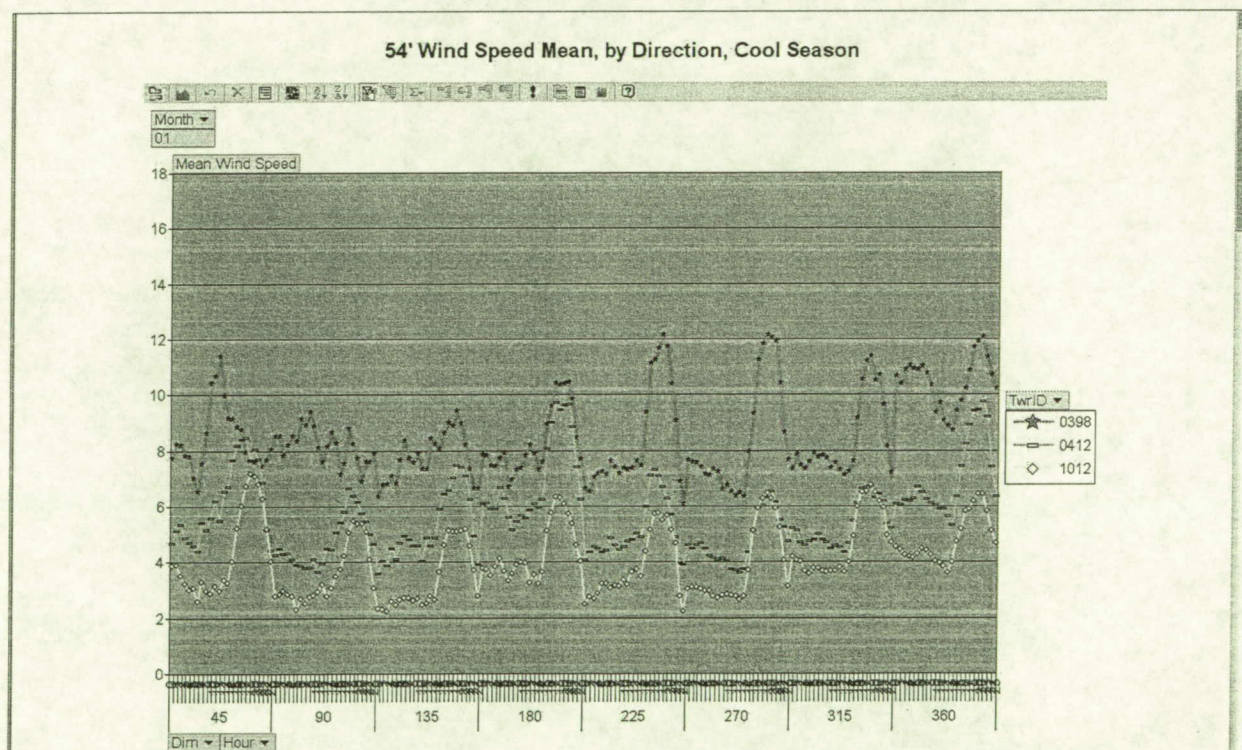


Figure 5.28. Display of hourly mean 54-ft wind speeds at towers 0398 (SLC 39B), 0412, and 1012 during January, stratified by wind direction bin.

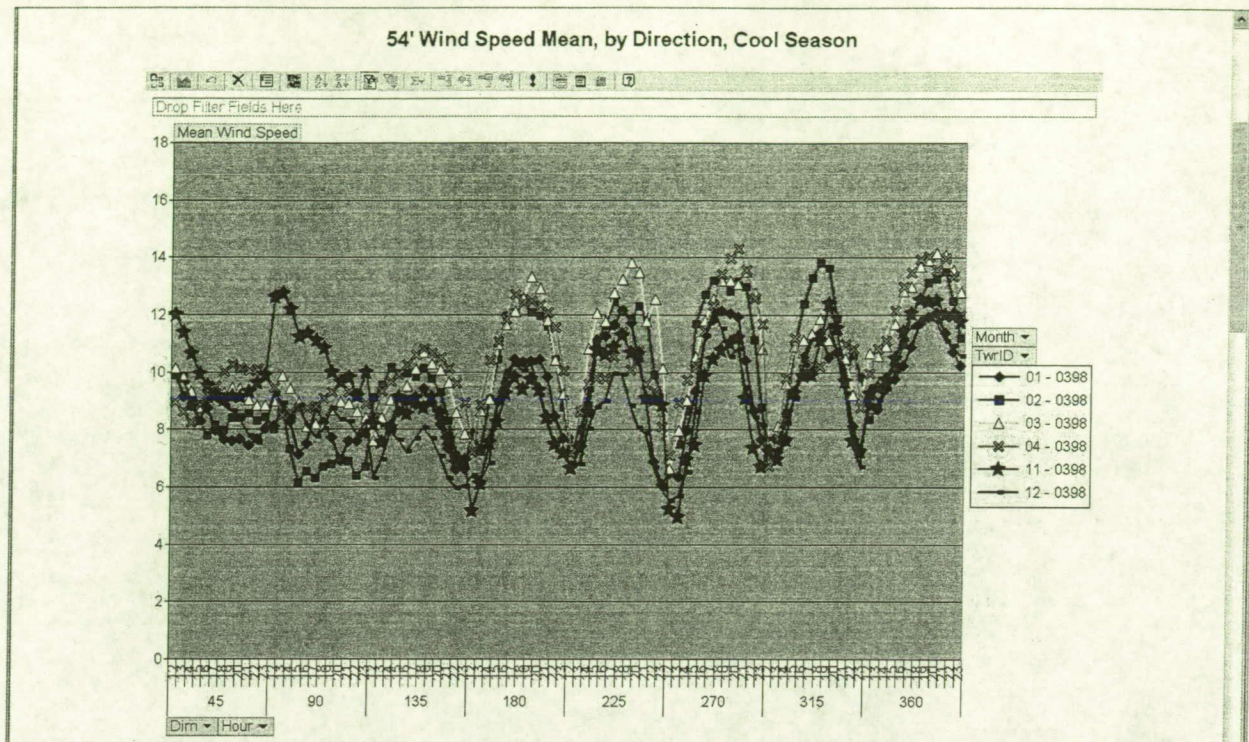


Figure 5.29. Display of hourly mean 54-ft wind speeds at tower 0398 (SLC 39B) for all cool-season months, stratified by wind-direction bin.

6. Summary

This report presented a nine-year, monthly mesoclimatology of temperatures and winds at 6 ft and 54 ft for the KSC/CCAFS tower network. Data were analyzed at 33 separate tower locations, four of which were located near launch complexes and had two sensors on opposite sides of the towers. The 33 selected towers provided 6-ft temperature and 54-ft wind data archived at 5 minute intervals, while 19 towers also provided 54-ft temperature readings every 5 minutes. The period of record for the analysis was February 1995 to January 2004. Variables analyzed for the climatology included the 6-ft and 54-ft temperature, the difference between the 54-ft and 6-ft temperature (i.e. near-surface stability), 54-ft wind speed, and 54-ft wind direction deviation.

The monthly mesoclimatology was developed by computing hourly means, standard deviations, biases, and data availability counts of temperatures and winds at all towers and sensors. Only towers with at least 70% data availability were used in any given month in order to obtain meaningful results. The forecast critical towers outside of KSC/CCAFS typically had the lowest data availability because of their remote, occasionally inaccessible locations, battery power recharged by solar panels, problems associated with the repeater tower being overhauled, and periodic radio frequency interference. The launch/safety towers within KSC/CCAFS have ac power with battery backup so their reliability was much higher.

Prior to making calculations, several automated QC algorithms were applied to the data, as well as a manual QC process for temperatures. In addition to standard hourly calculations, data were also categorized into separate wind direction bins every 45°, and statistics were computed to determine the climatological variations across KSC/CCAFS under different wind directions. The S-PLUS statistics software was used to manage and stratify data, and perform all calculations. Data were displayed and analyzed using pivot charts from the Microsoft Excel software and GEMPAK contoured station plots with map backgrounds.

The mesoclimate of KSC/CCAFS is largely driven by the complex land-water interfaces of KSC/CCAFS. Towers with close proximity to water typically exhibited much warmer nocturnal temperatures and substantially higher wind speeds throughout the year. A 7–10°F difference occurred in the mean 6-ft temperature across the tower network throughout the year, most notable in the pre-dawn hours. Even larger 6-ft temperature variations occurred within specific wind direction ranges. The variations in 54-ft temperatures were much smaller across KSC/CCAFS, so the near-surface stability (54-ft minus 6-ft temperature) was primarily a function of the 6-ft temperatures.

Mean domain-wide wind speeds were generally 4–6 kt during the nocturnal hours and 7–9 kt during the day. The strongest mean nocturnal wind speeds of 6–7 kt occurred from October to March (the synoptic season). Meanwhile, the strongest mean daytime wind speeds of 8.5–9.5 kt occurred from February to May, probably due to a combination of synoptic systems and strengthening sea-breeze circulations during this latter portion of the Florida dry season.

Coastal and causeway towers tended to have mean wind speeds 2–4 kt stronger than the overall network mean. Meanwhile, mainland towers had mean speeds weaker than the network mean by about the same magnitude. The resulting gradient in the mean wind speed across the network was typically 5–8 kt over a distance of 15–20 nm (20–30 km), with the strongest speeds occurring at the Atlantic coastal towers.

The standard deviation of the wind direction followed the diurnal variation in wind speeds. Higher direction deviations and wind speeds occurred during the day compared to night due to turbulent and convective processes. The direction deviation was highest over inland stations and Merritt Island/CCAFS towers not adjacent to any water body. Direction deviation tended to be highest during the afternoon hours of the summer months when sea-breeze fronts and convective outflows led to large variations in wind direction.

Most biases in the climatology were largely a result of the geographical variability, which tended to mask any smaller instrument, processing, and exposure errors. The coastal and causeway towers had cool (warm) biases during the day (night) compared to Merritt Island and mainland towers. The towers located near water bodies also had high wind speed biases, whereas the mainland towers experienced low wind speed biases relative to the overall network average. Tower 1204 exhibited the most noticeable exposure and sheltering bias in the 6-ft temperatures. This sensor

relies on natural aspiration and is often sheltered from the wind by surrounding pine trees, resulting in a substantial warm temperature bias when the sun shines on the instrument in the mid-late morning hours during the spring and summer months. However, tower 1204 will be replaced under RSA.

The AMU developed an HTML-based GUI for displaying and analyzing the results of the nine-year tower climatology. The GUI tool includes graphical displays of mean, standard deviation, bias, and data availability for any combination of towers, variables, months, hours, and wind direction bins. These graphical displays employ the Excel pivot chart capability to provide the user with this flexibility. In addition, geographical plots and contours of the various statistical quantities can provide the user with an understanding of the meteorological variations across the tower network. The geographical three-panel plots consist of mean, bias, and standard deviation of each variable, month, hour, and wind direction bin, and can be animated on an hourly basis by the user. The web browser required to view and interact with the pivot charts is Microsoft Internet Explorer 5.01 Service Pack 2 or newer. All AMU customers will receive a copy of the complete GUI tool as part of the task deliverable.

7. References

- Barnes, S. L., 1973: Mesoscale objective analysis using weighted time-series observations. NOAA Tech. Memo. ERL NSSL-62, National Severe Storms Laboratory, Norman, OK, 73069, 60 pp. [NTIS COM-73-10781].
- Case, J. L., and M. M. Wheeler, 2002: Final report on land-breeze forecasting. NASA Contractor Report CR-2002-211181, Kennedy Space Center, FL, 66 pp. [Available from ENSCO, Inc., 1980 N. Atlantic Ave., Suite 230, Cocoa Beach, FL 32931.]
- Case, J. L., J. Manobianco, T. D. Oram, T. Garner, P. F. Blottman, and S. M. Spratt, 2002: Local data integration over east-central Florida using the ARPS Data Analysis System. *Wea. Forecasting*, **17**, 3-26.
- Computer Sciences Raytheon (CSR), 2000: *45th Space Wing Eastern Range Instrumentation Handbook*, Computer Sciences Raytheon Inc., 758 pp.
- Harms, D. E., B. F. Boyd, M. S. Gremillion, M. E. Fitzpatrick, and T. D. Hollis, 2001: Weather support to space launch: A quarter-century look at weather instrumentation improvements. Preprints, *11th Symp. on Meteorological Observations and Instrumentation*, Albuquerque, NM, Amer. Meteor. Soc., 259-264.
- Haugen, D. A., and J. J. Fuquay, 1963: The ocean breeze and dry gulch diffusion programs Volume I. U. S. Air Force Project Order No. 61-577, Air Force Cambridge Research Laboratories, Hanscom Field, MA, 252 pp.
- Haugen, D. A., and J. H. Taylor, 1963: The ocean breeze and dry gulch diffusion programs Volume II. U. S. Air Force Project Order No. 61-577, Air Force Cambridge Research Laboratories, Hanscom Field, MA, 112 pp.
- Insightful Corporation, 2000: *S-PLUS® 6 User's Guide*, Insightful Corp., Seattle, WA, 470 pp.
- Koch, S. E., M. DesJardins, and P. J. Kocin, 1983: An interactive Barnes objective map analysis scheme for use with satellite and conventional data. *J. Appl. Meteor.*, **22**, 1487-1503.
- Lambert, W. C., 2002: Statistical short-range guidance for peak wind speed forecasts on Kennedy Space Center/Cape Canaveral Air Force Station: Phase I results. NASA Contractor Report CR-2002-211180, Kennedy Space Center, FL, 39 pp. [Available from ENSCO, Inc., 1980 N. Atlantic Ave., Suite 230, Cocoa Beach, FL 32931.]
- Watson, A. I., R. E. Lopez, R. L. Holle, J. R. Daugherty, and R. Ortiz, 1989: Short-term forecasting of thunderstorms at Kennedy Space Center, based on the surface wind field. Preprints, *Third Conference on Aviation Systems*, Anaheim, CA, Amer. Meteor. Soc., 222-227.

List of Abbreviations and Acronyms

Term	Description
2D	two-dimensional
45 WS	45th Weather Squadron
AMU	Applied Meteorology Unit
CCAFS	Cape Canaveral Air Force Station
Dirn	Wind Direction
ft	feet
GIF	Graphical Interchange Format
GUI	Graphical User Interface
HTML	HyperText Markup Language
ID	Identifier
KSC	Kennedy Space Center
kt	knots
m s^{-1}	meters per second
nm	nautical miles
NWS	National Weather Service
QC	Quality Control
RH	Relative Humidity
RMS	Root Mean Square
UTC	Universal Time Coordinated
V	Volts
WINDS	Weather Information Network Display System

NOTICE

Mention of a copyrighted, trademarked or proprietary product, service, or document does not constitute endorsement thereof by the author, ENSCO Inc., the AMU, the National Aeronautics and Space Administration, or the United States Government. Any such mention is solely for the purpose of fully informing the reader of the resources used to conduct the work reported herein.

REPORT DOCUMENTATION PAGE			Form Approved OMB No. 0704-0188	
<small>Public reporting burden for this collection of information is estimated to average 1 hour per response, including the time for reviewing instructions, searching existing data sources, gathering and maintaining the data needed, and completing and reviewing the collection of information. Send comments regarding this burden estimate or any other aspect of this collection of information, including suggestions for reducing this burden to Washington Headquarters Services, Directorate for Information Operations and Reports, 1215 Jefferson Davis Highway, Suite 1204, Arlington, VA 22202-4302, and to the Office of Management and Budget, Paperwork Reduction Project (0704-0188), Washington, DC 20503.</small>				
1. AGENCY USE ONLY (Leave blank)		2. REPORT DATE August 2004		3. REPORT TYPE AND DATES COVERED Contractor Report
4. TITLE AND SUBTITLE Tower Mesonetnetwork Climatology and Interactive Display Tool			5. FUNDING NUMBERS C-NAS10-01052	
6. AUTHOR(S) Jonathan L. Case and William H. Bauman III				
7. PERFORMING ORGANIZATION NAME(S) AND ADDRESS(ES) ENSCO, Inc., 1980 North Atlantic Avenue, Suite 230, Cocoa Beach, FL 32931			8. PERFORMING ORGANIZATION REPORT NUMBER 04-001	
9. SPONSORING/MONITORING AGENCY NAME(S) AND ADDRESS(ES) NASA, John F. Kennedy Space Center, Code YA-D, Kennedy Space Center, FL 32899			10. SPONSORING/MONITORING AGENCY REPORT NUMBER NASA/CR-2004-211526	
11. SUPPLEMENTARY NOTES Subject Cat.: #47 (Meteorology and Climatology)				
12A. DISTRIBUTION/AVAILABILITY STATEMENT Unclassified - Unlimited			12B. DISTRIBUTION CODE	
13. ABSTRACT (Maximum 200 Words) <p>Forecasters at the 45th Weather Squadron and Spaceflight Meteorology Group use data from the tower network over the Kennedy Space Center (KSC) and Cape Canaveral Air Force Station (CCAFS) to evaluate Launch Commit Criteria, and issue and verify forecasts for ground operations. Systematic biases in these parameters could adversely affect an analysis, forecast, or verification. Also, substantial geographical variations in temperature and wind speed can occur under specific wind directions. To address these concerns, the Applied Meteorology Unit (AMU) developed a climatology of temperatures and winds from the tower network, and identified the geographical variation and significant tower biases.</p> <p>The mesoclimate is largely driven by the complex land-water interfaces across KSC/CCAFS. Towers with close proximity to water typically had much warmer nocturnal temperatures and higher wind speeds throughout the year. The strongest nocturnal wind speeds occurred from October to March whereas the strongest mean daytime wind speeds occurred from February to May.</p> <p>These results of this project can be viewed by forecasters through an interactive graphical user interface developed by the AMU. The web-based interface includes graphical and map displays of mean, standard deviation, bias, and data availability for any combination of towers, variables, months, hours, and wind directions.</p>				
14. SUBJECT TERMS Tower observations, climatology, operational tools			15. NUMBER OF PAGES 88	
			16. PRICE CODE	
17. SECURITY CLASSIFICATION OF REPORT UNCLASSIFIED	18. SECURITY CLASSIFICATION OF THIS PAGE UNCLASSIFIED	19. SECURITY CLASSIFICATION OF ABSTRACT UNCLASSIFIED	20. LIMITATION OF ABSTRACT NONE	